AN APPLICATION OF THE WIENER-HOPF TECHNIQUE TO THE SOLUTION OF H-POLARIZATION INDUCTION OVER A COASTLINE

by

MARTIN ADRIAN NICOLL

B.Sc., University of Victoria, 1973

A THESIS SUBMITTED IN PARTIAL FULFILLMENT

OF THE REQUIREMENTS FOR THE DEGREE OF

MASTER OF SCIENCE

in the Department

of

Physics

We accept this thesis as conforming

to the required standard

[redacted]

UNIVERSITY OF VICTORIA

June 1976

ABSTRACT

Supervisor: Professor J. T. Weaver

The Wiener-Hopf technique uses results from complex analysis to obtain analytic solutions to differential equations with mixed boundary conditions. This type of problem arises frequently in geomagnetic induction models.

In this thesis the technique is applied to two models with magnetic polarized fields over an ocean edge. The earth's properties were assumed to be constant in the direction parallel to the coastline resulting in a two dimensional mathematical problem. In both models the crust was assumed to have a small conductivity to allow current flow. The difference between the models is that the first assumes the depth to the mantle is infinite while the second has a mantle of infinite conductivity at a finite depth.

The solution of the second model demonstrates the existence of current loops flowing from the sea through the crust and returning via the mantle.

ACKNOWLEDGEMENTS

The author would like to thank Dr. J.T. Weaver for his guidance during the progress of this work, and Dan McGregor for his assistance in computing the numerical results.

The University of Victoria and the National Research Council of Canada are to be thanked for their financial support.

TABLE OF CONTENTS

LIST OF TABLES

CHAPTER 1

INTRODUCTION

It is common for observations of geomagnetic variations along a coastline to demonstrate a much stronger correlation between the vertical component and the horizontal component perpendicular to the coastline (Parkinson, 1959, 1962; Everett and Hyndman 1967). The nature of this correlation is that the vector representing a magnetic disturbance at a coastline tends to lie in an inclined plane such that the horizontal projection of the normal to this plane points to the nearest deep water. This projection, which in most cases is normal to the coastline, is referred to as a "Parkinson arrow". (See Fig. 1.1) There are exceptions to this rule but they can generally be accounted for by a complicated continental shelf or by some overpowering geomagnetic effect such as the equatorial electrojet. (Parkinson, 1962)

One suggested explanation of this effect is that a vertical magnetic field induces horizontal current loops in the ocean which are channelled along the coastline by the poorly conducting land. This current will be flowing parallel to the coastline implying that the induced magnetic field will have a horizontal component perpendicular to the coastline. Thus the horizontal field would be correlated with the vertical field which implies the resulting vector will always lie in a prefered plane. This induction system, however, cannot explain the variations in the angle of the preferred plane to the horizontal from one area to another, since the properties of the sea are relatively constant. This is in agreement with model studies by Parkinson (1964), who found the effect of the ocean too small, and by Dosso (1966), who concluded that the magnitude of the induced fields decreased with smaller frequencies and were negligible at .01 c.p.s.

Dosso (1966) also studied the effect of an upwelling of the mantle beneath the coastline and found that the induced fields were important for shorter frequencies than with no mantle. This result is consistent with Lambert and Caner's, (1965), interpretation of the observational

results of Western Canada.

An alternate method of obtaining the required effect is to have the stronger horizontal field induce vertical current loops in the earth which, because of the poorly conducting land, will create a large current disparity across a coastline and hence an induced field with a vertical component proportional to the original horizontal field. This method was not considered originally since it has been shown, Bullard and Parker (1970), that the ocean is not deep enough to allow any currents induced by the horizontal field to be significant. At the 2nd Workshop on Electromagnetic Induction in the Earth, held in Ottawa, Brewitt-Taylor (1974) and Bailey (1974) considered the possibility of vertical current loops involving the crust. This arrangement allows current loops of large vertical extent which implies the currents induced by horizontal fields could be important. The questionable aspect of this hypothesis is whether or not the conductivity of the crust is high enough to permit a significant current flow. One favourable aspect is that the numerous anomalies in the earth's crust could certainly account for any variance in the angle of preferred plane.

In this thesis the vertical current loops are investigated by obtaining an analytic solution of the diffusion equation in a crust which is half covered by a super-conducting ocean. The solution is obtained by the Wiener-Hopf technique which was suggested for this type of problem by R. C. Bailey, (1974). His model, which did not include any mantle, is re-calculated before the more complex model with a super-conducting mantle is discussed. Both models are two dimensional in the sense that nothing in the models change in the third direction. To really analyse the correlation between the horizontal and vertical field components at a coastline one needs to consider the inducing field perpendicular to the coastline in a three dimensional model. This problem would be very difficult to solve, so the easier H-polarization, inducing field parallel to the coast, will be considered here. This mode, however, generates current loops in the wrong direction to create the coast-effect but the analysis will help determine whether or not current loops involving the crust are important. Although numerical methods can solve more complex models,

e. g. Brewitt-Taylor (1975, 1976), an analytic solution provides a valuable check on these methods and can also demonstrate the inter-dependence of the various parameters involved.

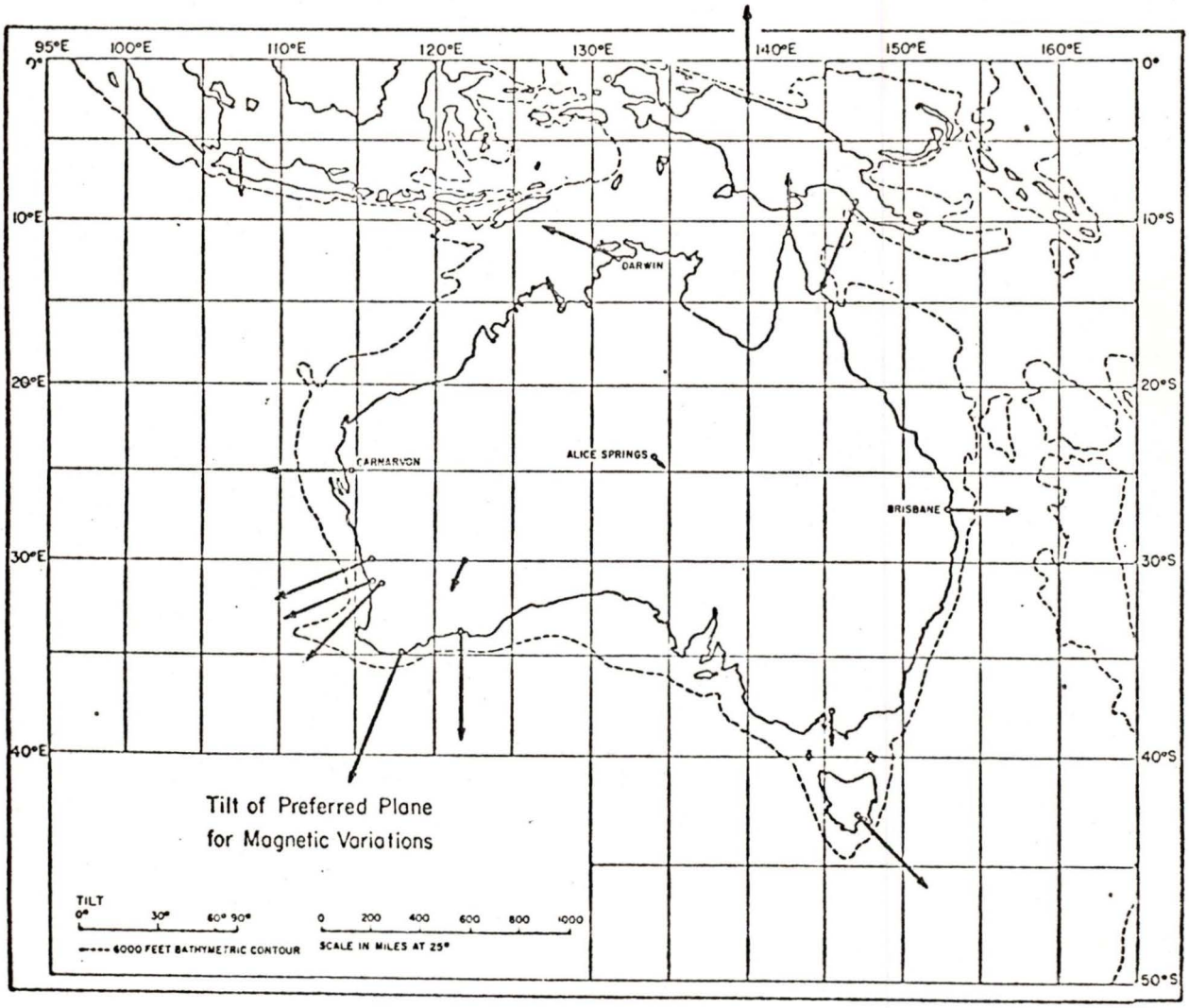

Fig.1.1 "Parkinson vectors", that is the horizontal projection of the normal to the plane in which the disturbance vector lies during a magnetic bay (from Parkinson 1964)

CHAPTER 2

THE EQUATIONS OF ELECTROMAGNETIC INDUCTION

2.1 The Diffusion Equation from Maxwell's Equations

Maxwell's equations in M.K.S. units with permeability μ_0 and relative permittivity κ are,

$$\vec{\nabla} \times \vec{E} = -\partial \vec{B}/\partial t \tag{2.1}$$

$$\vec{\nabla} \times \vec{B} = \mu_0 \sigma \vec{E} + \mu_0 \varepsilon_0 \kappa \partial \vec{E}/\partial t \tag{2.2}$$

$$\vec{\nabla} \cdot \vec{B} = 0 \tag{2.3}$$

$$\vec{\nabla} \cdot \vec{E} = \rho/(\kappa \varepsilon_0) \tag{2.4}$$

By taking the curl of equation (2.2) we obtain

$$\vec{\nabla} \times (\vec{\nabla} \times \vec{B}) = \mu_0 \sigma \vec{\nabla} \times \vec{E} + \mu_0 \varepsilon_0 \kappa \partial (\nabla \times \vec{E})/\partial t \tag{2.5}$$

The combination of this result with equations (2.1) and (2.3) yields

$$\vec{\nabla}^2 \vec{B} = \mu_0 \sigma \partial \vec{B}/\partial t + \kappa \mu_0 \varepsilon_0 \partial^2 \vec{B}/\partial t^2 \tag{2.6}$$

If we consider a typical geomagnetic variation to have a period τ, then the second, displacement current, term will be negligible if

$$\varepsilon_0/\tau \ll \sigma$$

since κ is of order 1. The above is an excellent approximation for geomagnetic studies of the earth. In the atmosphere, however, $\sigma=0$ so for the displacement current term to remain negligible it must be much less than the left hand side of equation (2.6). This will be the case if

$$\mu_0 \varepsilon_0/\tau^2 \ll 1/L^2$$

where L is the characteristic length of the region under investigation. The largest possible characteristic length one could study would be the radius of the earth which implies that the above condition will always be satisfied for $f<10$ *Hz*. Naturally for smaller L higher frequencies would be allowable. Thus we can neglect displacement currents in equation (2.6) to obtain

$$\nabla^2 \vec{B} = 0 \tag{2.7}$$

in the atmosphere, and

$$\nabla^2 \vec{B} = \mu_0 \sigma \partial \vec{B}/\partial t \tag{2.8}$$

in the earth.

If B is assumed to have an $\exp(i\omega t)$ dependence equation (2.8) becomes

$$\nabla^2\vec{B} = i\omega\mu_0\sigma\vec{B} \tag{2.9}$$

2.2 Description of the Models

The first model depicts the earth at an ocean edge as a half space with the other half of the space representing the atmosphere. The ocean is portrayed by an infinitely thin super conducting half plane between the earth and the atmosphere. (See figure 2.1). The geometry of the model does not change in the direction parallel to the edge of the half-plane which is also the direction of the imposed source field. The atmosphere is assigned a zero conductivity, the earth a finite conductivity σ, and the sea an infinite conductivity. The source field is assumed to have an $\exp(i\omega t)$ time-dependence and the permeability of the whole region is taken as μ_0.

The second model is exactly the same as the first except for a super-conducting mantle positioned at a depth D in the earth. (See figure 2.2). By the symmetry of the models in the x-direction we can deduce that B will not be a function of x which reduces the applicable component of equation (2.9) to

$$\frac{\partial^2 B}{\partial y^2} + \frac{\partial^2 B}{\partial z^2} = i\alpha^2 B \qquad (2.10)$$

where we have defined $\omega\mu_0\sigma \equiv \alpha^2$ for convenience .

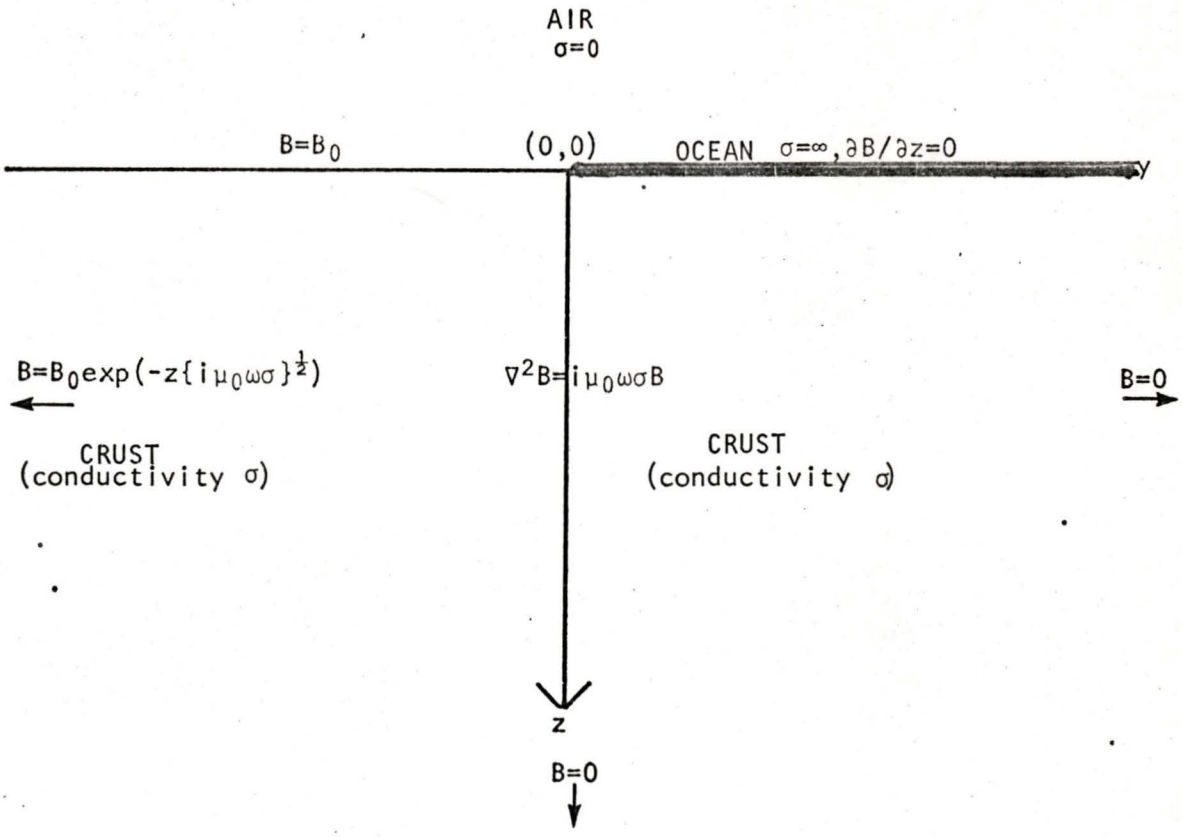

Fig. 2.1 The First Model - an infinite crust

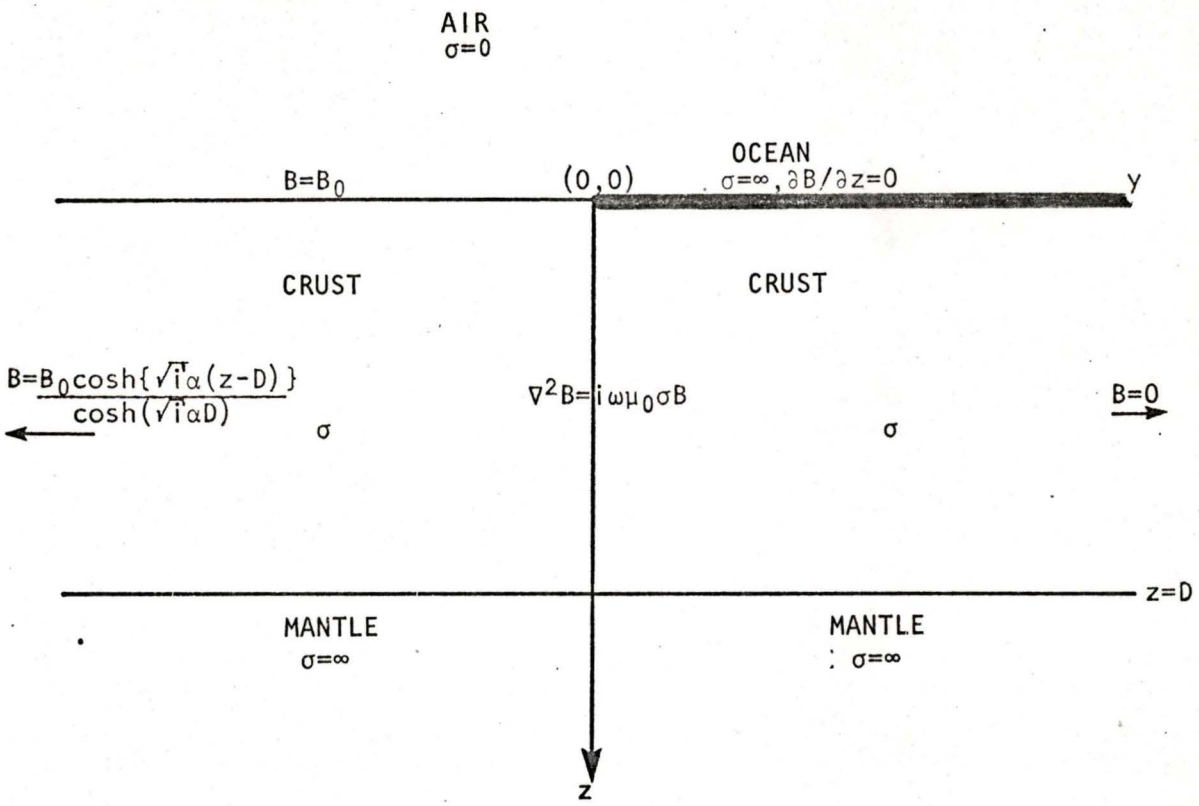

Fig. 2.2 The Second Model - a crust with a good conducting mantle at a depth D

2.3 The Boundary Conditions

The condition $\vec{B}_s = |\vec{B}_s|\,\hat{x}$ along with equation (2.2) implies that

$$\partial B/\partial y = 0$$

and

$$\partial B/\partial z = 0 \qquad (2.11)$$

in the atmosphere, since $\sigma = 0$ and the displacement current term is neglected.

It follows immediately that $B = B_0$, a constant, throughout the atmosphere. This gives the boundary condition $B = B_0$ along the surface $z = +0$, $y < 0$ since the tangential component of the field must be continuous across the surface of a conductor. (This condition does not apply to a superconductor). For $y > 0$ we apply the condition that the tangential electric field at the surface of a superconductor must vanish to the x-component of equation (2.2) to obtain $\partial B/\partial z = 0$ for $z = +0$. Owing to the shielding effect supplied by the superconductor we can expect that $B \to 0$ as $y \to +\infty$. At $y = -\infty$ the effect of the superconductor will be negligible so the boundary condition can be obtained by solving the model with no sea. With no sea the symmetry of the problem will imply that B will have no y dependence reducing equation (2.10) to

$$\partial^2 B/\partial z^2 = i\alpha^2 B \qquad (2.12)$$

This equation has the solution $B = B_0 \exp(-\sqrt{i}\alpha z)$. (The positive exponential argument is ruled out since B must be finite as $z \to \infty$.) The second model differs from the first by having a $\partial B/\partial z = 0$ boundary condition at $z = D$ so the boundary condition as $y \to -\infty$ can be obtained by solving equation (2.13) with this additional condition to obtain

$$B = \frac{B_0 \cosh\{\sqrt{i}\alpha(z-D)\}}{\cosh(\sqrt{i}\alpha D)} \qquad (2.13)$$

CHAPTER 3

THE SOLUTION OF THE FIRST MODEL

We shall use the Fourier transforms as defined in Noble (p.23), namely

$$\hat{f}(\zeta) = (2\pi)^{-\frac{1}{2}} \int_{-\infty}^{\infty} f(y)\exp(i\zeta y)\,dy \qquad (3.1)$$

where $\zeta = \xi + i\eta$. The inverse transform is defined with the condition that if $\hat{f}(\zeta)$ is analytic between $i\tau_-$ and $i\tau_+$ then

$$f(y) = (2\pi)^{-\frac{1}{2}} \int_{-\infty}^{\infty} \hat{f}(\zeta)\exp(-i\zeta y)\,d\zeta \qquad (3.2)$$

providing $\tau_- < \tau < \tau_+$.

By taking the Fourier transform of equation (2.10) we obtain

$$-\zeta^2\hat{B} + \partial^2\hat{B}/\partial z^2 = i\alpha^2\hat{B} \qquad (3.3)$$

which is a standard differential equation with the solution

$$\hat{B}(\zeta,z) = A(\zeta)\exp(-z\sqrt{\zeta^2+i\alpha^2}) + C(\zeta)\exp(z\sqrt{\zeta^2+i\alpha^2}) \qquad (3.4)$$

Owing to the ambiguity in the square root function it is more explicit to write

$$\sqrt{\zeta^2+i\alpha^2} = |\zeta-\exp(-i\pi/4|^{\frac{1}{2}}\exp(i\phi/2)\,|\zeta-\alpha\exp(i3\pi/4)|^{\frac{1}{2}}\exp(i\theta/2). \qquad (3.5)$$

where θ and ϕ are defined in Fig. (3.1) and the square roots are defined positive. The necessity for a finite result as $z\to\infty$ along with equation (3.5) simplifies the solution to the form

$$\hat{B}(\zeta,z) = A(\zeta)\exp\{-z|\zeta-\exp(i\pi/4)\alpha|^{\frac{1}{2}}|\zeta-\exp(i3\pi/4)\alpha|^{\frac{1}{2}}\exp\{i\tfrac{1}{2}(\theta+\phi)\} \qquad (3.6)$$

where $\frac{1}{2}(\theta+\phi)$ is restricted to be between $-\pi/2$ and $\pi/2$ when the argument of the exponential goes to infinity.

Now the z=0 boundary conditions can be applied to obtain

$$\hat{B}(\zeta,0) = A(\zeta) \equiv \hat{B}(\zeta,0)_- + \hat{U}_+(\zeta) \qquad (3.7)$$

where $B(y,0)_-$ is the boundary condition for $y<0$ and $U_+(y)$ is the unknown boundary condition for $y>0$. By simply taking the Fourier transform of the known boundary condition we have

$$\hat{B}(\zeta,0)_- = (2\pi)^{-\frac{1}{2}} \int_{-\infty}^{0} B_0\exp(i\zeta y)\,dy = (2\pi)^{-\frac{1}{2}} B_0/i\zeta \qquad (3.8)$$

which is only defined for $\eta<0$, since a positive value would create a diverging integrand at $y=-\infty$.

By differentiating equation (3.6) with respect to z then

substituting z=0 into the result we obtain

$$\left.\frac{\hat{B}(\zeta,z)}{\partial z}\right|_{z=0} = -\sqrt{\zeta^2+i\alpha^2}A(\zeta) \equiv \hat{F}_{-}+0 \qquad (3.9)$$

where F_- is the unknown boundary value of $\partial B/\partial z$ for $y<0$ and $\partial B/\partial z = 0$ is the value for $y>0$.(Note that $\sqrt{\zeta^2+i\alpha^2}$ is defined as in equation (3.5)but will be used in the shorter form for convenience)The combination of equations (3.7),(3.8) and (3.9)yields

$$-\hat{F}_{-}/\sqrt{\zeta^2+i\alpha^2} = B_0/\{i\sqrt{2\pi}\zeta\}+ \hat{U}_{+} \qquad (3.10)$$

It is now necessary to investigate the regions of analyticity,in the ζ plane,of the various functions defined above.From the definition of the complex square root function and its prevalence in equation(3.6) it follows that $\hat{B}(\zeta,z)$ has branch points at $\alpha\exp(-i\pi/4)$ and $\alpha\exp(i3\pi/4)$ There is also a pole at $\zeta=0$ due to the form of $\hat{B}(\zeta,0)_-$ in equation (3.8) (see Fig.(3.1) By definition $\hat{U}_+$ can be expressed in the form

$$\hat{U}_{+} = (2\pi)^{\frac{1}{2}}\int_{0}^{\infty} B(y_{+},0)\exp(-\eta y + i\xi y)dy \qquad (3.11)$$

For large y it is natural to assume that $B(y_+,0)$ is an exponentially decaying function of y.(ie.$B(y_+,0) \to \exp(-cy)$ for $c>0$ and $y\to\infty$) Thus the integrand of (3.11) will be dependent upon $\exp(-\{\eta+c\}y)$ and hence will only be analytic for $y\to+\infty$ if

$$\eta > -c \qquad (3.12)$$

Similarily we have

$$\hat{F}_{-} = (2\pi)^{\frac{1}{2}}\int_{-\infty}^{0} \frac{\partial B(y_{-},0)}{\partial z}\exp(-\eta y + i\xi y)dy \qquad (3.13)$$

which is analytic for $\eta<0$ (since $\partial B(y_-,0)/\partial z \to B_0\sqrt{i\omega\mu_0\sigma}$ as $y \to -\infty$)Hence for the inversion path to remain completely within regions of analyticity η must satisfy all of the above conditions.A suitable choice is to situate the path ε below the real axis in the ζ plane.(It is now apparent that the '+' in $\hat{U}_+$ and the '-' in $\hat{F}_-$ signifies that these functions are analytic in $\eta>-\alpha/\sqrt{2}$ and $\eta<0$ respectively)

By inspection of equations (3.6) and (3.7) we see that to solve for $\hat{B}(\zeta,z)$ it will be necessary to obtain $\hat{U}_+$ in terms of known quantities. To do this we shall require the separation of equation (3.10) into '+' and '-' terms.If we write $(\zeta^2 + i\alpha^2)^{\frac{1}{2}} = (\zeta + i\sqrt{i}\alpha)^{\frac{1}{2}}(\zeta - i\sqrt{i}\alpha)^{\frac{1}{2}}$ and note that $(\zeta + i\sqrt{i}\alpha)^{-\frac{1}{2}}_{+}$ is analytic for $\eta > -\alpha/\sqrt{2}$ and that $(\zeta - i\sqrt{i}\alpha)^{-\frac{1}{2}}_{-}$ is analytic for $\eta < 0$ then equation (3.10) will be transformed into

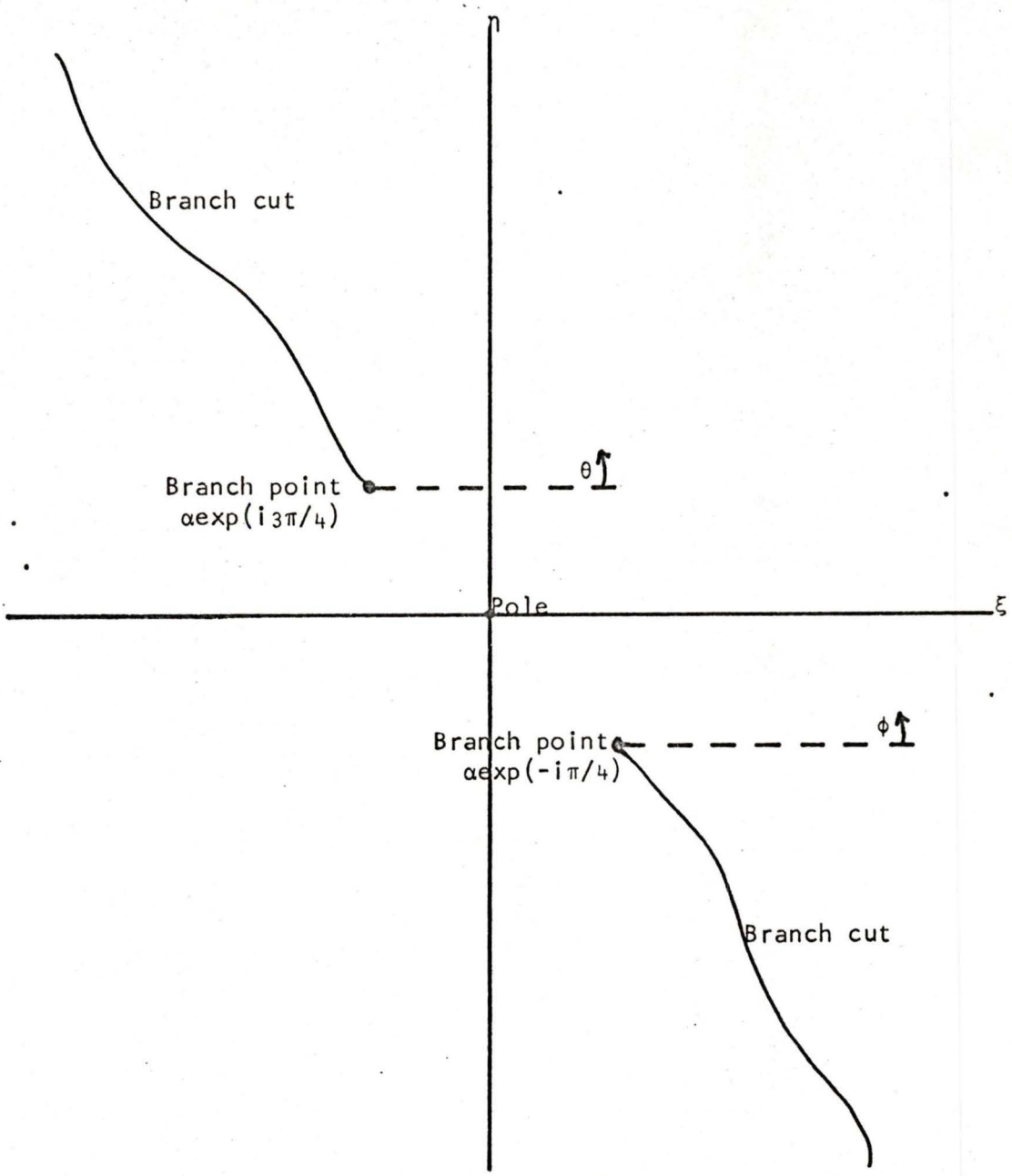

Fig. 3.1 The ζ Plane

$$(-\hat{F}/\{\zeta-i\sqrt{i\alpha}\}^{\frac{1}{2}})_- = B_0\{\zeta+i\sqrt{i\alpha}\}^{\frac{1}{2}}/i\sqrt{2\pi}\zeta + (\hat{U}\{\zeta+i\sqrt{i\alpha}\}^{\frac{1}{2}})_+ \qquad (3.14)$$

The first term on the right hand side cannot be classified as either a '+' function or a '-' function because of the pole at $\zeta=0$ and the branch point at $\zeta=-i\sqrt{i\alpha}$ .To overcome this difficulty we rearrange the term as follows

$$\frac{B_0(\zeta+i\sqrt{i\alpha})^{\frac{1}{2}}}{i\sqrt{2\pi}\ \zeta} = \left[\frac{B_0\{(\zeta+i\sqrt{i\alpha})^{\frac{1}{2}} - (i\sqrt{i\alpha})^{\frac{1}{2}}\}}{i\sqrt{2\pi}\ \zeta}\right]_+ + \left[\frac{B_0(i\sqrt{i\alpha})^{\frac{1}{2}}}{i\sqrt{2\pi}\ \zeta}\right]_- \qquad (3.15)$$

Hence equation (3.14) can be rewritten as

$$\left[\frac{-\hat{F}}{(\zeta-i\sqrt{i\alpha})^{\frac{1}{2}}} - \frac{B_0(i\sqrt{i\alpha})^{\frac{1}{2}}}{i\sqrt{2\pi}\ \zeta}\right]_- = \left[\frac{B_0\{(\zeta+i\sqrt{i\alpha})^{\frac{1}{2}} - (i\sqrt{i\alpha})^{\frac{1}{2}}\}}{i\sqrt{2\pi}\ \zeta} + \hat{U}(\zeta+i\sqrt{i\alpha})^{\frac{1}{2}}\right]_+ \qquad (3.16)$$

By noting the form of $\hat{F}$ in equation (3.13) it becomes apparent that the limit $\lim_{\substack{|\zeta|\to\infty \\ \eta<0}} |\hat{F}_-|=0$ .This fact along with an inspection of equation (3.16) reveals immediately that

$$\lim_{\substack{|\zeta|\to\infty \\ \eta<0}} \left[\frac{-\hat{F}}{(\zeta-i\sqrt{i\alpha})^{\frac{1}{2}}} - \frac{B_0(i\sqrt{i\alpha})^{\frac{1}{2}}}{i\sqrt{2\pi}\ \zeta}\right] = 0 \qquad (3.17)$$

Therefore by the extended form of Liouville's theorem (see appendix A) we can deduce that the complete left hand side of equation (3.16) is a polynomial of degree zero,or a constant,over the entire lower half plane. Furthermore since it has a value of zero at $|\zeta| = \infty$ it must be identically zero throughout the lower half plane.The same argument could be applied to the right hand side but is now unnecessary since we already know that both sides are equal .We now employ this result in eqution (3.16) to obtain

$$\hat{U}_+ = \frac{B_0\{(\zeta+i\sqrt{i\alpha})^{\frac{1}{2}} - (i\sqrt{i\alpha})^{\frac{1}{2}}\}}{i\sqrt{2\pi}\ \zeta(\zeta+i\sqrt{i\alpha})^{\frac{1}{2}}} \qquad (3.18)$$

This value combined with equations (3.6),(3.7) and (3.8) yields

$$\hat{B}(\zeta,z) = \frac{\sqrt{\alpha}B_0\exp(-i\pi/8)}{\sqrt{2\pi}}\left[\frac{\exp(-z\{\zeta^2+i\alpha^2\}^{\frac{1}{2}})}{\zeta|\zeta-\alpha\exp(-i\pi/4)|^{\frac{1}{2}}\exp(i\phi/2)}\right] \qquad (3.19)$$

By applying the inverse Fourier transform along the path discussed previously we aquire the solution

$$B(y,z) = (2\pi)^{-\frac{1}{2}} \int_{-\infty-i\varepsilon}^{\infty-i\varepsilon} \hat{B}(\zeta,z)\exp(-i\zeta y)\,d\zeta \qquad (3.20)$$

where $\hat{B}(\zeta,z)$ is defined in equation (3.19).

The above complex integral can be simplified to a real integral by the application of Cauchy's integral theorem.Thus we must find a closed contour which contains the inversion path,excludes the branch cut and ensures the convergence of the integral.The possibilities of divergence lie in the expontial term contained in the numerator of the integrand namely in

$$\exp\left[-\left(z\left|\zeta-\alpha\exp\{-i\pi/4\}\right|^{\frac{1}{2}}\left|\zeta-\alpha\exp\{i3\pi/4\}\right|^{\frac{1}{2}}\exp\{i\tfrac{1}{2}(\theta+\phi)\} + i\zeta y\right)\right]$$

Now $\exp(-i\zeta y) = \exp(-i\xi y)\cdot\exp(\eta y)$ which implies that we must have $\eta<0$ when $y>o$ and $\eta>0$ when $y<0$ to ensure convergence.Accordingly it will be necessary to derive two solutions for $B(y,z)$,one obtained by integrating around a contour in the lower half plane,for $y>0$,and the other from a contour in the upper half of the ζ plane,for $y<0$ .The only term of questionable sign left in the argument of the exponential is $\exp(i\frac{1}{2}\{\theta+\phi\})$. (Since both z and the square roots are positive)By inspection it is evident that the real part of the above term,$\cos\{\frac{1}{2}(\theta+\phi)\}$,must be positive which results in the restriction that

$$-\pi/2 \leq \tfrac{1}{2}(\theta+\phi) \leq \pi/2 \qquad (3.21)$$

Hence it will be necessary to position the branch cuts with considerable care.The only solution which was found to satisfy all of the above conditions was to position the branch cuts on the limiting case,ie. $\frac{1}{2}(\theta+\phi) = \pm\pi/2$,which implies $\sin(\theta+\phi) = 0$ .If we write $\zeta^2+i\alpha^2$ in the form $(\xi^2-\eta^2) + i(2\xi\eta + \alpha^2)$ it becomes apparent that $\sin(\theta+\phi) = 0$ is equivalent to writing

$$\frac{2\xi\eta+\alpha^2}{\left|(\xi^2 - \eta^2)^2 + (2\xi\eta + \alpha^2)^2\right|^{\frac{1}{2}}} = 0 \qquad (3.22)$$

This equation will be satisfied along the branch cuts if we position them along the hyperbola defined by

$$\xi\eta = -\alpha^2/2 \qquad (3.23)$$

The resulting contour for $y>0$ is illustrated in Fig.(3.2) where the inversion path in question is represented by C_1.The integrals along

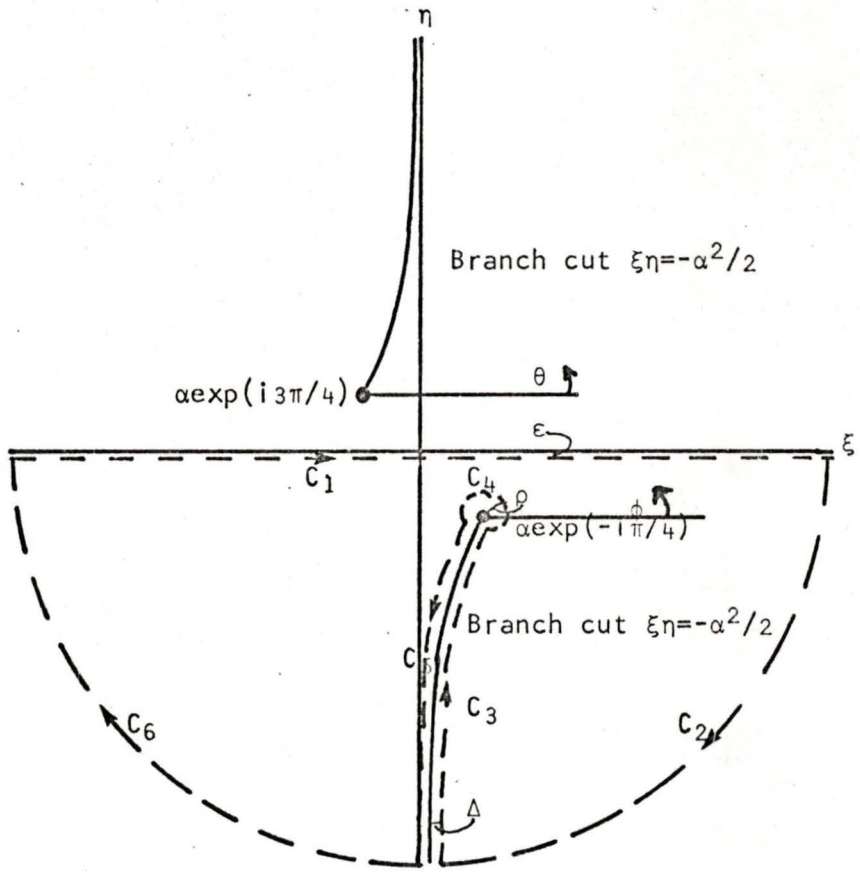

Contour	2	4 (as $\rho \to 0$)	6
θ initial	0	$-\pi/4$	$-\pi/2$
θ final	$-\pi/2$	$-\pi/4$	$-\pi$
ϕ initial	0	$-\pi/4$	$3\pi/2$
ϕ final	$-\pi/2$	$3\pi/4$	π
$(\theta+\phi)/2$ initial	0	$-\pi/4$	$\pi/2$
$(\theta+\phi)/2$ final	$-\pi/2$	$\pi/4$	0

Fig. 3.2 Contour of integration for y>0 with limits of θ and ϕ on selected contours

C_3 and C_5 are known to satisfy restriction (3.21)as $\Delta\to 0$.To see that C_2, C_4 and C_6 satisfy (3.21) we simply note the initial and final values of θ and ϕ for each case.(See Fig.(3.2))

Since there are no poles enclosed within the contour the application of Cauchy's integral formula yields

$$I_1 = -(I_2 + I_3 + I_4 + I_5 + I_6) \tag{3.24}$$

where we have defined I_j to be the integral along the j'th part of the contour.The integrand under consideration as obtained from equations (3.19) and (3.20) is

$$\frac{\exp\{-z(\zeta^2 + i\alpha^2)^{\frac{1}{2}} - i\zeta y\}}{\zeta|\zeta - \alpha\exp(-i\pi/4)|^{\frac{1}{2}}\exp(i\phi/2)} \tag{3.25}$$

As the above expression $\to 0$ as $|\zeta| \to \infty$,providing restriction (3.21) is satisfied,we can deduce that I_2 and I_6 give no contribution.I_4 can be shown to be zero by substituting $(\zeta-\alpha\exp\{-i\pi/4\}) = \rho\exp(i\phi)$ into the integrand then taking the limit as $\rho\to 0$.We now turn our attention to the evaluation of I_3 and I_5.The value of $(\theta+\phi)/2$ is equal to $-\pi/2$ on C_3 and $+\pi/2$ on C_5 while $\zeta = -\alpha^2/2\eta + i\eta$ on both contours.A particular point on C_3 has an associated value of ϕ_3 whereas the corresponding point on C_5 has a value of $\phi_5 = \phi_3 - 2\pi$ which implies

$$\exp(i\phi_5/2) = \exp(i\phi_3/2)\exp(-i\pi) = -\exp(i\phi_3/2)$$

From this we have that

$$(\zeta - \alpha\exp\{-i\pi/4\})\big|_{\text{on } C_3} = -(\zeta - \alpha\exp\{-i\pi/4\}\big|_{\text{on } C_5}$$

A substitution of the above results into equations (3.25) and (3.24)yields

$$I_1 = 2\int_{-\alpha/\sqrt{2}}^{-\infty} \frac{\exp\{(i\alpha^2/2\eta+\eta)y\}\cos(z|\alpha^4/4\eta^2-\eta^2|^{\frac{1}{2}})\ (\alpha^2/2\eta + i)d\eta}{(-\alpha^2/2\eta+i\eta)\ (-\alpha^2/2\eta-\alpha/\sqrt{2}+i\{\eta+\alpha/\sqrt{2}\})^{\frac{1}{2}}} \tag{3.26}$$

The form of this integral can be simplified substantially by making the following definitions

$$\begin{aligned} z' &= z\alpha/\sqrt{2} \\ y' &= y\alpha/\sqrt{2} \\ v^2 &= 2\eta/\alpha^2 - \alpha^2/2\eta \Rightarrow v\,dv = (2/\alpha^2 + \alpha^2/2\eta^2)d\eta \end{aligned} \tag{3.27}$$

(Note that z' and y' are simply the coordinates expressed in terms of skin depths,$\delta=\sqrt{2}/\alpha$)If we also recall the relationship between B(y,z)and I_1,(see equations (3.19)and(3.20),the solution will take the final form

$$B(y,z)_{y>0} = \frac{B_0\sqrt{2}\exp(i\pi/8)}{\pi}\int_0^\infty \frac{\{(v^2+2i)^{\frac{1}{2}}+(2i)^{\frac{1}{2}}\}^{\frac{1}{2}}\cos(z'v)\exp\{-y'(v^2+2i)\}dv}{(v^2+2i)} \quad (3.28)$$

The solution for $B(y,z)_{y<0}$ is obtained in a similar manner by using the contour illustrated in figure (3.3).As in the previous work it will be necessary for the entire contour to satisfy the restriction $-\pi/2 < \frac{1}{2}(\theta+\phi) < \pi/2$ for the inversion integral not to diverge.Contours 1,3 and 5 are known to satisfy the restriction and contours 2,4 and 6 can be shown to be acceptable by inspection.(See Fig.(3.3))By the form of the integrand (Eq.(3.25)) we can see that I_2 and $I_6 \to 0$ as $|\zeta| \to \infty$ and I_4 can be shown to be zero as $\rho \to 0$ by writing $(\zeta-\alpha\exp\{i3\pi/4\}) = \rho\exp(i\theta)$ and taking the limit.Hence by the application of Cauchy's integral theorem and by noting that this time the contour encloses a pole at $\zeta = 0$ we can deduce that

$$B(y,z)_{y<0} = \frac{\sqrt{\alpha}B_0\exp(-i\pi/8)}{2\pi} I_1 = \frac{\sqrt{\alpha}B_0\exp(-i\pi/8)}{2\pi}(-I_3-I_5+2\pi iR) \quad (3.29)$$

where R is the residue at the specified pole.Consider first the integrals along C_3 and C_5.The value of $(\theta+\phi)/2$ is equal to $\pi/2$ and $-\pi/2$ on C_3 and C_5 respectively while the value of $\phi/2$ is identical on both contours.As usual we shall abbreviate $|\zeta-\alpha\exp(-i\pi/4)|^{\frac{1}{2}}\exp(i\phi/2)$ to $(\zeta-\alpha\exp\{-i\pi/4\})^{\frac{1}{2}}$ and simply note that since $\phi/2$ has a range of $3\pi/8$ to $\pi/4$ the result will be positive .The above values along with the substitution $\zeta = -\alpha^2/2\eta + i\eta$ into the integrals yields

$$-(I_3+I_5) = -2i\int_{\alpha/\sqrt{2}}^\infty \frac{\exp(\{i\alpha^2/2\eta+\eta\}y)\ (\alpha^2/2\eta^2+i)\sin(z|\alpha^2/4\eta^2-\eta^2|^{\frac{1}{2}})d\eta}{(-\alpha^2/2\eta+i\eta)\ (-\alpha^2/2\eta-\alpha/\sqrt{2}+i\{\eta+\alpha/\sqrt{2}\})^{\frac{1}{2}}} \quad (3.30)$$

which can be simplified algebraically with definitions (3.27) to produce

$$-(I_3+I_5) = \frac{-2\exp(i\pi/4)\ (2)^{\frac{1}{4}}}{\sqrt{\alpha}}\int_0^\infty \frac{\exp(y'\{v^2+2i\}^{\frac{1}{2}})\sin(z'v)(\{v^2+2i\}^{\frac{1}{2}}-\sqrt{2i})^{\frac{1}{2}}dv}{(v^2+2i)} \quad (3.31)$$

From the integrand given in equation (3.25) we see that the residue can be obtained by setting $\zeta=0$ in the following expression

$$\frac{\exp(-z|\zeta-\alpha\exp\{i3\pi/4\}|^{\frac{1}{2}}|\zeta-\alpha\exp\{-i\pi/4\}|^{\frac{1}{2}}\exp(\frac{1}{2}i\{\theta+\phi\}) - i\zeta y)}{|\zeta-\alpha\exp(-i\pi/4)|^{\frac{1}{2}}\exp(i\phi/2)} \quad (3.32)$$

At $\zeta= 0$ $\theta = -\pi/4$ and $\phi= 3\pi/4$ which gives us the result that

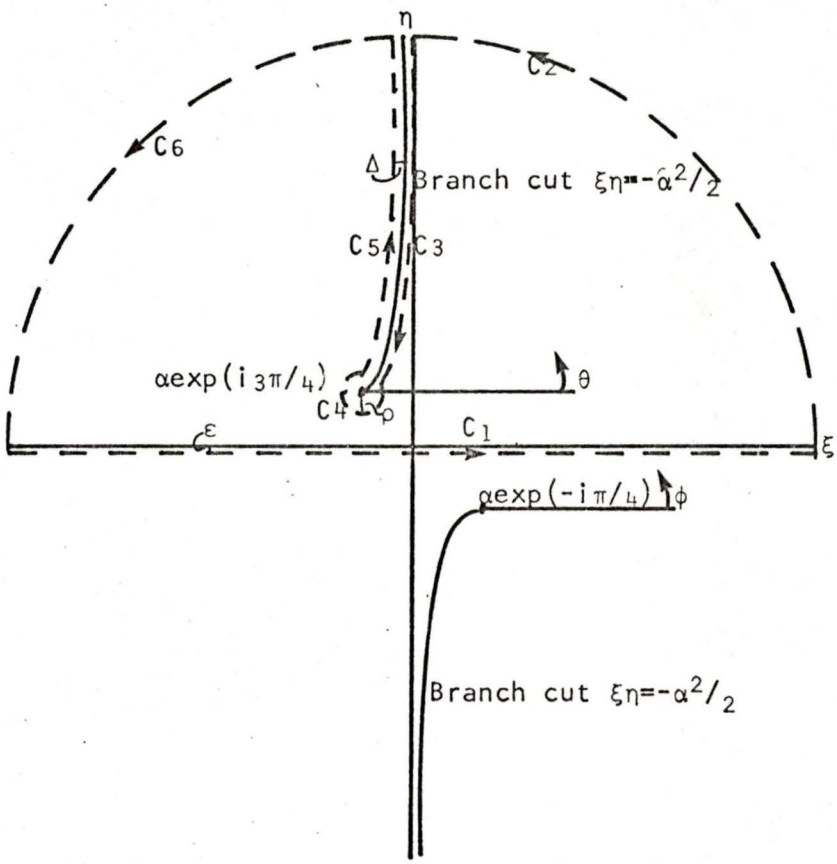

Contour	2	4(as $\rho \to 0$)	6
θ initial	0	$-\pi/4$	$-3\pi/4$
θ final	$\pi/2$	$-5\pi/4$	$-\pi$
ϕ initial	0	$3\pi/4$	$\pi/2$
ϕ final	$\pi/2$	$3\pi/4$	π
$(\theta+\phi)/2$ initial	0	$\pi/2$	$-\pi/2$
$(\theta+\phi)/2$ final	$\pi/2$	$-\pi/2$	0

Fig. 3.3 Contour of integration for $y<0$ with limits of θ and ϕ on selected contours

$$R = \frac{\exp(i\pi/8)\ \exp(-z\sqrt{i}\alpha)}{i\sqrt{\alpha}} \tag{3.33}$$

This value along with equation (3.31) defines all the unknowns in equation (3.29) to yield

$$B(y,z)_{y<0} = B_0\exp(-\sqrt{2i}\ z') -$$

$$\frac{\exp(i\pi/8)B_0(2)^{\frac{1}{4}}}{\pi}\int_0^{\infty}\frac{\exp(y'\{v^2+2i\}^{\frac{1}{2}})\sin(z'v)(\{v^2+2i\}^{\frac{1}{2}} - \{2i\}^{\frac{1}{2}})^{\frac{1}{2}}}{(v^2 + 2i)}\,dv \tag{3.34}$$

Thus we have two expressions which represent the complete solution for B(y,z) throughout the half space. That this solution does actually satisfy the original differential equation and boundary conditions is demonstrated in Appendix B.

CHAPTER 4

THE SOLUTION OF THE SECOND MODEL

The method of solving this second model is similar to the solution of the first model, so to avoid repetitions many of the steps in the Wiener-Hopf technique will be skimmed over.

By taking the Fourier transform of the diffusion equation with respect to y in the region illustrated in Fig.(2.2) we obtain the general solution

$$\hat{B}(\zeta,z) = F(\zeta)\exp(z\{\zeta^2+i\alpha^2\}^{\frac{1}{2}}) + C(\zeta)\exp[-(z\{\zeta^2+i\alpha^2\}^{\frac{1}{2}})] \quad (4.1)$$

In this model neither term can be set equal to zero since z is bounded. We now differentiate equation (4.1) and apply the z=D boundary condition to obtain

$$(\zeta^2+i\alpha^2)^{\frac{1}{2}}F(\zeta)\exp(D\{\zeta^2+i\alpha^2\}^{\frac{1}{2}}) - (\zeta^2+i\alpha^2)^{\frac{1}{2}}C(\zeta)\exp(-D\{\zeta^2+i\alpha^2\}^{\frac{1}{2}})=0 \quad (4.2)$$

which implies

$$C(\zeta) = F(\zeta)\exp(2D\{\zeta^2+i\alpha^2\}^{\frac{1}{2}}) \quad (4.3)$$

The combination of this result with equation (4.1) gives us

$$\hat{B}(\zeta,z) = \frac{F(\zeta)2\cosh(\{z-D\}\gamma)}{\exp(-D\gamma)} \quad (4.4)$$

where $\gamma \equiv \{\zeta^2+i\alpha^2\}^{\frac{1}{2}}$. If we now redifine $F(\zeta)$ in terms of the z=0 boundary value, $\hat{B}(\zeta,0)$, equation (4.4) becomes

$$\hat{B}(\zeta,z) = \frac{\hat{B}(\zeta,0)\cosh(\{z-D\}\gamma)}{\cosh(D\gamma)} \quad (4.5)$$

As in the previous section we can write

$$\hat{B}(\zeta,0) = B_0/(i\sqrt{2\pi}\,\zeta) + \hat{B}^+(\zeta,0) \quad (4.6)$$

where the second term is unknown. Combining the above equation with equation (4.5) then differentiating the result with respect to z and evaluating at z=0 will give

$$\hat{B}_z^-(\zeta,0) + 0 \equiv \left.\frac{\partial\hat{B}(\zeta,z)}{\partial z}\right|_{z=0} = -\left[\frac{B_0\gamma\tanh(\gamma D)}{i\sqrt{2\pi}\,\zeta} + \hat{B}^+(\zeta,0)\gamma\tanh(\gamma D)\right] \quad (4.7)$$

where $\hat{B}_z^-(\zeta,0)$ is the unknown boundary condition on $\partial\hat{B}/\partial z$ at z=0 and y<0.

Equation (4.7) can be rearranged to yield

$$\frac{B_0}{i\sqrt{2\pi}\zeta} + \hat{B}^+(\zeta,0) = \frac{\hat{B}_z^-(\zeta,0)(\gamma D\coth\{\gamma D\})}{\gamma D} \tag{4.8}$$

To obtain a solution for $\hat{B}^+(\zeta,0)$ it will be necessary to separate the terms of equation (4.8) into the '+' and '-' functions defined earlier. It can be shown by identical arguments as those used previously that $\hat{B}^+(\zeta,0)$ is analytic for $\eta>-\alpha/\sqrt{2}$ and that $\hat{B}_z^-(\zeta,0)$ is analytic for $\eta<0$. To separate the hyperbolic function in equation (4.8) we first express the function in terms of an infinite product. The outcome as demonstrated in Appendix C is

$$\gamma D\coth(\gamma D) = \prod_{n=1}^{\infty}\left[\frac{\{(1+i\alpha^2D_{n-\frac{1}{2}}^2) + \zeta^2D_{n-\frac{1}{2}}^2\}}{\{(1+i\alpha^2D_n^2) + \zeta^2D_n^2\}}\right] \tag{4.9}$$

where

$$D_n = D/(n\pi) \tag{4.10}$$

Factoring the right hand side of Eq. (4.9) into two infinite products and defining the left hand side as the product of two functions which are analytic in the required regions gives us

$$K_+(\zeta)K_-(\zeta) = \left[\prod_{n=1}^{\infty}\frac{\{(1+i\alpha^2D_{n-\frac{1}{2}}^2)^{\frac{1}{2}} + i\zeta D_{n-\frac{1}{2}}\}}{\{(1+i\alpha^2D_n^2)^{\frac{1}{2}} + i\zeta D_n\}}\right] \cdot \left[\prod_{n=1}^{\infty}\frac{\{(1+i\alpha^2D_{n-\frac{1}{2}}^2)^{\frac{1}{2}} - i\zeta D_{n-\frac{1}{2}}\}}{\{(1+i\alpha^2D_n^2)^{\frac{1}{2}} - i\zeta D_n\}}\right] \tag{4.11}$$

From this we can deduce that

$$K_+(\zeta) = \prod_{n=1}^{\infty}\left[\frac{\{(1+i\alpha^2D_{n-\frac{1}{2}}^2)^{\frac{1}{2}} - i\zeta D_{n-\frac{1}{2}}\}}{\{(1+i\alpha^2D_n^2)^{\frac{1}{2}} - i\zeta D_n\}}\right] \tag{4.12}$$

and

$$K_-(\zeta) = \prod_{n=1}^{\infty}\left[\frac{\{(1+i\alpha^2D_{n-\frac{1}{2}}^2)^{\frac{1}{2}} + i\zeta D_{n-\frac{1}{2}}\}}{\{(1+i\alpha^2D_n^2)^{\frac{1}{2}} + i\zeta D_n\}}\right] \tag{4.13}$$

Therefore equation (4.8) becomes

$$\frac{B_0(\zeta+i\sqrt{i}\alpha)}{i\sqrt{2\pi}\ \zeta K_+(\zeta)} + \left[\frac{\hat{B}^+(\zeta,0)(\zeta+i\sqrt{i}\alpha)}{K_+(\zeta)}\right]_+ = \left[\frac{\hat{B}_z^-(\zeta,0)\ K_-(\zeta)}{D(\zeta-i\sqrt{i}\alpha)}\right]_- \tag{4.14}$$

To complete the required seperation into '+' and '-' functions we can rewrite the first term on the left hand side of (4.14) as

$$\frac{B_0(\zeta+i\sqrt{i}\alpha)}{i\sqrt{2\pi}\zeta K_+(\zeta)} = \left[\frac{K_+(0)B_0(\zeta+i\sqrt{i}\alpha)-B_0 i\sqrt{i}\alpha K_+(\zeta)}{i\sqrt{2\pi}\ \zeta K_+(0)\ K_+(\zeta)}\right]_+ + \left[\frac{B_0 i\sqrt{i}\alpha}{i\sqrt{2\pi}\zeta K_+(0)}\right]_- \tag{4.15}$$

Substituting this result back into equation (4.14)gives us

$$\left[\frac{\hat{B}^+(\zeta,0)(\zeta+i\sqrt{i}\alpha)}{K_+(\zeta)} + \frac{K_+(0)B_0(\zeta+i\sqrt{i}\alpha)-B_0 i\sqrt{i}\alpha K_+(\zeta)}{i\sqrt{2\pi}\ \zeta\ K_+(0)\ K_+(\zeta)}\right]_+ =$$

$$\left[\frac{\hat{B}_z^-(\zeta,0)K_-(\zeta)}{D(\zeta-i\sqrt{i}\alpha)} - \frac{B_0 i\sqrt{i}\alpha}{i\sqrt{2\pi}\ \zeta\ K_+(0)}\right]_- \tag{4.16}$$

We can now apply Liouville's theorem to see that each side of the above equation is identically zero.(See Appendix A) Thus we can procure a solution for $\hat{B}^+(\zeta,0)$,namely

$$\hat{B}^+(\zeta,0) = \frac{B_0 i\sqrt{i}\alpha K_+(\zeta)-K_+(0)B_0(\zeta+i\sqrt{i}\alpha)}{(\zeta+i\sqrt{i}\alpha)i\sqrt{2\pi}\ \zeta\ K_+(0)} \tag{4.17}$$

This defines the only unknown in equation (4.5) with the outcome that

$$\hat{B}(\zeta,z) = \frac{\sqrt{i}\alpha B_0}{\sqrt{2}\pi K_+(0)}\left[\frac{K_+(\zeta)\cosh\{(z-D)\gamma\}}{(\zeta+i\sqrt{i}\alpha)\ \cosh(\gamma D)}\right] \tag{4.18}$$

It can be shown that a suitable inversion path is situated ε below the real axis in the ζ plane. Thus by applying the inverse Fourier transform to equation (4.18) we obtain

$$B(y,z) = \frac{B_0\alpha\exp(i\pi/4)}{2\pi K_+(0)}\int_{-\infty-i\varepsilon}^{\infty-i\varepsilon}\frac{K_+(\zeta)\cosh\{\gamma(z-D)\}\exp(-i\zeta y)}{(\zeta+i\sqrt{i}\alpha)\,\zeta\cosh(\gamma D)}\,d\zeta \tag{4.19}$$

It will be convenient to have available an alternate form of the solution which involves $K_-(\zeta)$ instead of $K_+(\zeta)$. This can be aquired by the utilization of equations (4.9) and (4.11),along with some algebraic manipulations,to yield

$$B(y,z) = \frac{B_0 K_-(0)}{2\pi\coth(D\sqrt{i}\alpha)}\int_{-\infty-i\varepsilon}^{\infty-i\varepsilon}\frac{(\zeta-\alpha\exp(i3\pi/4)\cosh\{\gamma(z-D)\}\exp(-i\zeta y)}{\gamma\zeta K_-(\zeta)\ \sinh(\gamma D)}\,d\zeta \tag{4.20}$$

We can now proceed to evaluate the complex integral via residue theory. Noting the similarity of the exponential argument involving y to that in Chapter 3 it becomes apparent that

$$\begin{aligned} y > 0 &\Rightarrow \eta < 0 \\ y < 0 &\Rightarrow \eta > 0 \end{aligned} \tag{4.21}$$

The contour chosen for y>0 is illustrated in Fig.(4.1).In this case there is no restriction on $(\theta+\phi)/2$ since z is bounded and the integrand will always go to zero as $|\zeta| \to \infty$ providing restriction (4.21) is satisfied. This is why the branch cut can be defined in a simpler manner than before.In fact the use of the same branch cut would give rise to complications since the poles of the hyperbolic function in the integrand would coincide with points on the branch cut. Since $K_-(\zeta)$ has no poles or zeroes for $\eta<0$ it will ease the evaluation of the residues if we use equation (4.20) rather than equation (4.19) to evaluate $B(y,z)_{y>0}$ .It will prove expedient to make the following definitions

$$b = \frac{B_0 K_-(0)}{2\pi \coth(D\sqrt{i\alpha})} \tag{4.22}$$

$$I_j = \int_{C_j} \frac{\cosh\{\gamma(z-D)\}\exp(-i\zeta y)(\zeta-\alpha\exp\{i3\pi/4\})}{\gamma\, K_-(\zeta)\, \zeta\, \sinh(\gamma D)}\, d\zeta \tag{4.23}$$

This implies equation (4.20) can be rewritten as

$$B(y,z) = bI_1 \tag{4.24}$$

We now apply Cauchy's theorem to obtain

$$B(y,z)_{y>0} = -b(I_2+I_3+I_4+I_5+I_6) - 2\pi i bR \tag{4.25}$$

where R is the residue and is preceeded by a minus sign since the direction of integration is clockwise.By considering the limit $|\zeta| \to \infty$ of the integrand we can deduce that I_2 and I_6 will give no contribution. Turning our attention to C_3 and C_5 we see that,as $\Delta \to 0, \zeta \to \alpha/\sqrt{2} + i\eta$ on both contours,ϕ has the value of $-\pi/2$ on C_3 and $3\pi/2$ on C_5 whereas $-\pi/4 > \theta > -\pi/2$ on both of them. By the same method used in Chapter 3 we can show that

$$\exp\{i\tfrac{1}{2}(\theta+\phi)\}\big|_{\text{on } C_3} = -\exp\{i\tfrac{1}{2}(\theta+\phi)\}\big|_{\text{on } C_5} \tag{4.26}$$

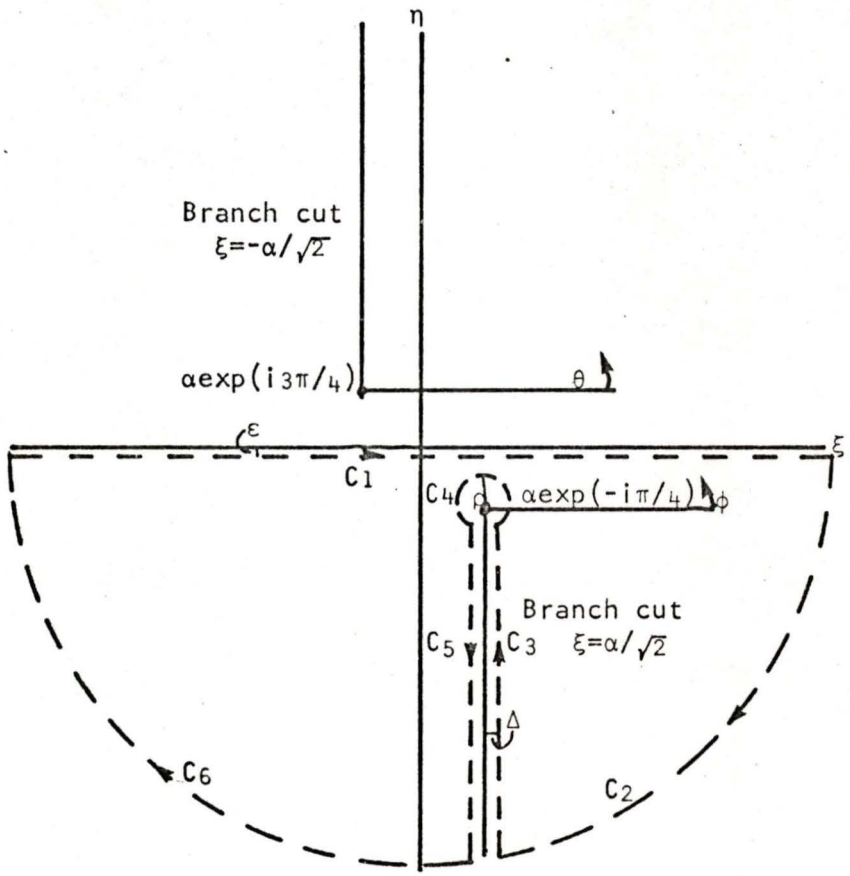

Fig. 4.1 Contour of integration for $y>0$

which implies $\gamma_3 = -\gamma_5$. (See the expression for γ as in equation (3.5)) By noting that cosh is an even function and that sinh is an odd function it becomes apparent that a replacement of γ by $-\gamma$ in the integrand under consideration produces no net change in sign. Thus we can conclude that I_3 and I_5 are of equal magnitude which will result in cancellation because of the reversed directions of integration.

An expression for I_4 can be obtained by setting $\zeta-\alpha\exp(-i\pi/4)=\rho\exp(i\phi)$ in equation (4.23) and integrating the result with respect to ϕ. The result is

$$I_4 = \int_{-\pi/2}^{3\pi/2} \frac{2\exp\{-i\gamma\alpha\exp(-i\pi/4)\}\ \sqrt{\rho}\exp(i\phi)\quad d\phi}{\sqrt{2\alpha}\exp(-\tfrac{1}{2}\theta+i\tfrac{1}{2}\phi)K_-\{\alpha\exp(-i\tfrac{1}{4}\pi)\ \sinh\left[D\sqrt{\rho}\exp(i\tfrac{1}{2}\phi)(2\alpha\exp\{-i\tfrac{1}{4}\pi\})^{\frac{1}{2}}\right]} \quad (4.27)$$

We now take the limit as $\rho\to 0$, by assuming the limit can be taken under the integral sign, and apply L'Hopital's rule to obtain

$$bI_4 = \frac{B_0\exp(i3\pi/4)K_-(0)\exp(-\gamma\alpha\sqrt{i})}{D\alpha\coth(D\sqrt{i}\alpha)K_-\{\alpha\exp(-i\pi/4)\}} \quad (4.28)$$

The poles of the integrand occur inside the closed contour when

$$\sinh\{D(\zeta^2+i\alpha^2)^{\frac{1}{2}}\} = 0 \quad (4.29)$$

or at the points

$$\zeta_m = -i(m^2\pi^2/D^2 + i\alpha^2)^{\frac{1}{2}} \quad (4.30)$$

where m is an integer from 1 to ∞. Thus by applying well known techniques[1] we can calculate the total residue as

$$2\pi i bR = \frac{-B_0K_-(0)}{D\coth(D\sqrt{i}\alpha)}\sum_{m=1}^{\infty}\left\{\frac{(u_m^2+i\alpha^2)^{\frac{1}{2}}+\alpha\exp(i\tfrac{1}{4}\pi)\}\cos(u_mz)\exp\{-\gamma(u_m^2+i\alpha^2)^{\frac{1}{2}}\}}{K_-\{-i(u_m^2+i\alpha^2)^{\frac{1}{2}}\}(u_m^2+i\alpha^2)}\right. \quad (4.31)$$

where u_m has been defined as $m\pi/D$ for convenience. This result along with equations (4.25) and (4.28) yield the solution

$$B(\gamma,z)_{\gamma>0} = \frac{-B_0\exp(i3\pi/4)K_-(0)\exp(-\gamma\alpha\sqrt{i})}{D\alpha\coth(D\alpha\sqrt{i})K_-(\alpha\exp\{-i\pi/4\})} +$$

$$\frac{B_0K_-(0)}{D\coth(D\alpha\sqrt{i})}\sum_{m=1}^{\infty}\left[\frac{\{(u_m^2+i\alpha^2)^{\frac{1}{2}}+\exp(i\tfrac{1}{4}\pi)\}\cos(u_mz)\exp\{-\gamma(u_m^2+i\alpha^2)^{\frac{1}{2}}\}}{K_-\{-i(u_m^2+\alpha^2)^{\frac{1}{2}}\}(u_m^2+i\alpha^2)}\right] \quad (4.32)$$

1. For example method 4, page 85, Mathematical Physics, Butkov (1968).

The form of this solution can be streamlined by making the definitions

$$\Delta u = \pi/D \tag{4.33}$$

$$a_m = \frac{K_-(0)\{(u_m^2+i\alpha^2)^{\frac{1}{2}}+\alpha\exp(i\pi/4)\}\exp\{-y(u_m^2+i\alpha^2)^{\frac{1}{2}}\}}{K_-\{-i(u_m^2+i\alpha^2)^{\frac{1}{2}}\}(u_m^2+i\alpha^2)} \tag{4.34}$$

which lead to

$$B(y,z)_{y>0} = \frac{B_0}{\pi\coth(D\alpha\sqrt{i})}\left[\frac{a_0\Delta u}{2} + \sum_{m=1}^{\infty} a_m\cos(u_m z)\Delta u\right] \tag{4.35}$$

This is easily recognized as a Fourier cosine series.

To obtain the solution for $y<0$ we shall utilize equation (4.19) and integrate around the contour illustrated in Fig.(4.2).By similar techniques to those already employed we can show that I_2, I_4, and I_6 are zero and that I_3 and I_5 cancel to give

$$B(y,z)_{y<0} = \frac{B_0\alpha\exp(i\pi/4)\ 2\pi i\ R}{2\pi K_+(0)} \tag{4.36}$$

where R is the total residue.The pole at $\zeta=0$ produces a net contribution to R of

$$R_0 = \frac{K_+(0)\ \cosh\{(z-D)\alpha\sqrt{i}\}}{i\sqrt{i}\ \alpha\cosh(D\alpha\sqrt{i})} \tag{4.37}$$

Further poles exist when $\cosh\{D(\zeta^2+i\alpha^2)^{\frac{1}{2}}\} = 0$ which is satisfied if

$$\zeta \equiv \zeta_{m-\frac{1}{2}} = i(u_{m-\frac{1}{2}}^2 + i\alpha^2)^{\frac{1}{2}} \tag{4.38}$$

where $u_{m-\frac{1}{2}} = (m-\frac{1}{2})\pi/D$ .Since $\zeta_{m-\frac{1}{2}} = \zeta_{(-m+1)-\frac{1}{2}}$ we can deduce that it is sufficient to sum from m=1 to ∞.Thus we can write

$$R = R_0 + \sum_{m=1}^{\infty} R_m \tag{4.39}$$

where it can be shown that

$$R_m = \frac{(m-\frac{1}{2})\ K_+(\zeta_{m-\frac{1}{2}})\sin(u_{m-\frac{1}{2}}z)\exp(-iy\zeta_{m-\frac{1}{2}})}{(\zeta_{m-\frac{1}{2}} + i\sqrt{i}\alpha)\zeta_{m-\frac{1}{2}}^2\ D^2} \tag{4.40}$$

The combination of equations (4.36) through (4.40) yields the final solution

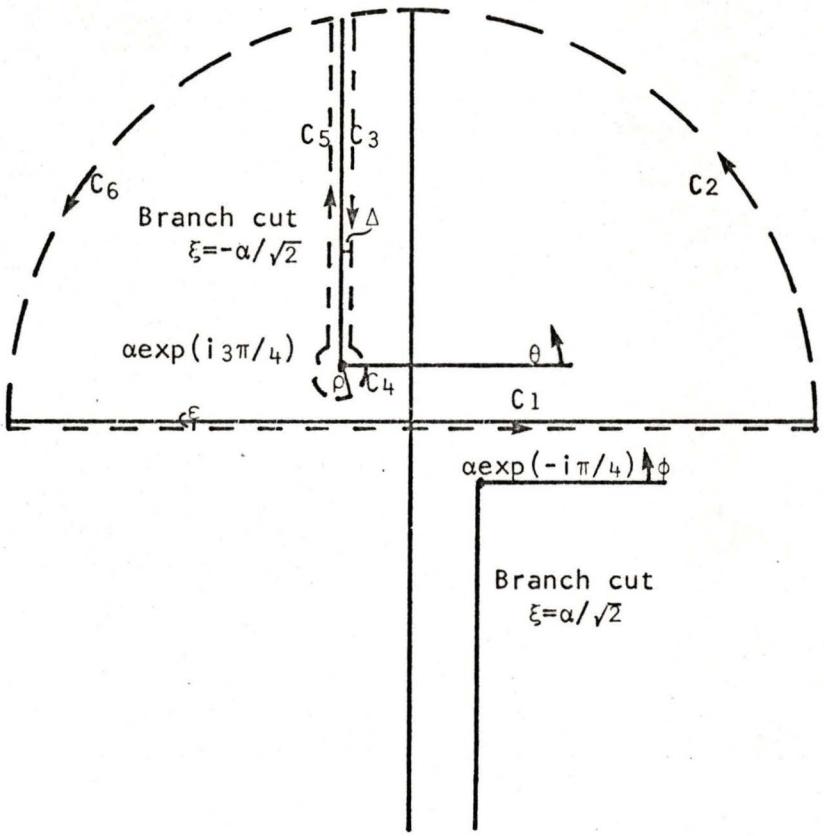

Fig. 4.2 Contour of integration for y<0

$$B(y,z)_{y<0} = \frac{B_0 \cosh\{(z-D)\alpha\sqrt{i}\}}{\cosh(D\alpha\sqrt{i})} + \frac{\alpha B_0 \exp(i3\pi/4)}{\pi} \sum_{m=1}^{\infty} b_{m-\frac{1}{2}} \sin(u_{m-\frac{1}{2}} z)\Delta u \quad (4.41)$$

where

$$b_{m-\frac{1}{2}} = \frac{u_{m-\frac{1}{2}} K_+(\zeta_{m-\frac{1}{2}}) \exp(-iy\zeta_{m-\frac{1}{2}})}{(\zeta_{m-\frac{1}{2}} + i\sqrt{i}\alpha)\zeta^2_{m-\frac{1}{2}} K_+(0)} \quad (4.42)$$

Equations (4.35) and (4.41) represent the complete analytic solution for the magnetic field throughout the crust. Appendix D demonstrates that this is a correct and reasonable solution of the model.

CHAPTER 5

NUMERICAL RESULTS

The solution for the magnetic field obtained in the last chapter is sufficiently complex to eliminate any possibility of being able to visualize the form the magnetic field lines would take within the earth. This chapter presents three sets of graphical output corresponding to different values of the input parameters.

For convenience we make the familiar definitions $D'=D\alpha/\sqrt{2}$, $y'=y\alpha/\sqrt{2}$ and $z'=z\alpha/\sqrt{2}$. Then to simplify computation and presentation we employ the ratios y'/D' and z'/D' as coordinates and B/B_0 to represent the magnetic field. The application of these definitions to equations (4.37) and (4.46) modifies the solution into a suitable form for computation, namely

$$\frac{B(y_-,z)}{B_0} = \frac{\cos\{(1-i)(z'-D')\}}{\cos(1-i)D'} + \frac{i\sqrt{2}\exp(i3\pi/4)\pi(D'\sin\{(1-i)D'\})^{\frac{1}{2}}}{\{(1-i)\cos[D'(1-i)]\}^{\frac{1}{2}}} \cdot \sum_{m=1}^{\infty} \frac{(m-\frac{1}{2})K^+(i\sqrt{A}/D)\exp(\sqrt{A}y'/D')\sin\{(m-\frac{1}{2})z'/D'\}}{(\sqrt{A} + \sqrt{2}iD')A} \qquad (5.1)$$

where $A=(\{m-\frac{1}{2}\}^2\pi^2 + 2iD'^2)$, and

$$\frac{B(y_+,z)}{B_0} = \left[\frac{(i-1)D'\sin\{(1-i)D'\}}{\cos\{(1-i)D'\}}\right]^{\frac{1}{2}} \cdot \left[\frac{-\exp(i3\pi/4 - \sqrt{2i}y')}{\sqrt{2}D'K^-(-i\sqrt{2iD'^2}/D)} + \sum_{m=1}^{\infty} \frac{(\sqrt{E} + \sqrt{2i}D')\exp(-\sqrt{E}y'/D')\cos(m\pi z'/D')}{EK^-(-i\sqrt{E}/D)}\right] \qquad (5.2)$$

where $E = (m^2\pi^2 + 2iD'^2)$

The expressions for K^+ and K^- (equations (4.13) and (4.14) respectively) where algebraicly modified to obtain the fastest possible convergence. The final forms used were

$$K^+(iA^{\frac{1}{2}}/D) = \prod_{n=1}^{\infty}\left[1 + \frac{i2D'^2(n-\frac{1}{4})\{\pi^2 n(n-\frac{1}{2})(G+F)\}^{-1} + A^{\frac{1}{2}}/2\pi}{n(n-\frac{1}{2})(G+A^{\frac{1}{2}}/n\pi)}\right] \qquad (5.3)$$

and

$$K^-(-iE^{\frac{1}{2}}/D) = \prod_{n=1}^{\infty}\left[1 + \frac{i2D'^2(n-\frac{1}{4})\{\pi^2 n(n-\frac{1}{2})(G+F)\}^{-1} + E^{\frac{1}{2}}/2\pi}{n(n-\frac{1}{2})(G+E^{\frac{1}{2}}/n\pi)}\right] \qquad (5.4)$$

where $G = (1 + i2D'^2/n^2\pi^2)^{\frac{1}{2}}$ and $F = (1 + i2D'^2/(n-\frac{1}{2})^2\pi^2)^{\frac{1}{2}}$.

The electric field components can be expressed in terms of derivatives of B(y,z) by the use of Maxwell's equations to give

$$E_y = \frac{1}{\mu_0\sigma}\frac{\partial B(y,z)}{\partial z}$$
$$E_z = \frac{-1}{\mu_0\sigma}\frac{\partial B(y,z)}{\partial z} \qquad (5.5)$$

Therefore actual values for E_y and E_z can be evaluated by simply differentiating equations (5.1) and (5.2) before computation. (This will affect the rate of convergence of the series since the power of m in the numerator of each term is increased by 1 when the series is differentiated. However this is only noticeable when the exponential is not dominating the convergence, ie for very small values of y'/D'.) The value of the current density follows immediately since $\vec{J} = \sigma\vec{E}$. It follows from Maxwells equations that the current will flow in the direction defined by curl $\vec{B}$, which in turn is tangential to the lines of constant magnetic field. (See Appendix E). This suggests that the results be presented as lines of constant $|B/B_0|$ followed by a table of current density values $|J/B_0|$. To complete the solution it is necessary to have results for values of t throughout the period of the oscillating source field. Recall that we defined $B(y, z, t) = \mathrm{Re}\{B(y,z)\exp(i\omega t)\}$ and since $B(y, z)$ is of the form

$$B(y, z) = B_R(y, z) + iB_I(y, z) \qquad (5.6)$$

the net result is

$$B(y, z, t) = B_R(y, z)\cos(\omega t) - B_I(y, z)\sin(\omega t) \qquad (5.7)$$

where the subscripts R and I signifies the real and imaginary parts respectively. Values of ωt were chosen from 0 to $7\pi/8$ in steps of $\pi/8$ since the results of the second half of the cycle will be the negative of those already obtained.

The magnitude of the current density as a function of time can be obtained by considering

$$E_y(y, z, t) = E_{yR}\cos(\omega t) - E_{yI}\sin(\omega t)$$
$$E_z(y, z, t) = E_{zR}\cos(\omega t) - E_{zI}\sin(\omega t) \qquad (5.8)$$

implying that

$$|J(t)| = \sigma|E(t)| = \sigma|E_y(y, z, t)^2 + E_z(y, z, t)^2|^{\frac{1}{2}} \qquad (5.9)$$

It is still necessary to define values for y/D, z/D, and D' before values

of B/B_0 and J/B_0 can be computed. A value of 1.08×10^{-5} mho/m was chosen for the conductivity of the crust, which is within the range of 10^{-4} to 10^{-5} mho/m suggested by Chapman and Bartels (1940). Garland (1971) gives D, the depth of the crust, as 650 km. leaving the choice of the period of oscillation to define D'. (Recall the defination of D' and α to obtain $D' = D(\frac{1}{2}\mu_0\sigma\omega)^{\frac{1}{2}}$.) The periods chosen were 18 seconds, 1 hour and $\frac{1}{2}$ day which correspond to D' values of 1, .0705 and .0204 respectively. The values of z/D will naturally range from 0 to 1 and y/D was chosen to range from -2 to +2. (In other words 1300 km. inland to 1300 km. at sea) A grid of values was established within these limits with finer spacing near the crucial boundaries. The actual values chosen are shown in the current tables.

The series can now be computed with the various parameters producing the results illustrated in figures 5.1 to 5.24 and tables 5.1 to 5.3 .

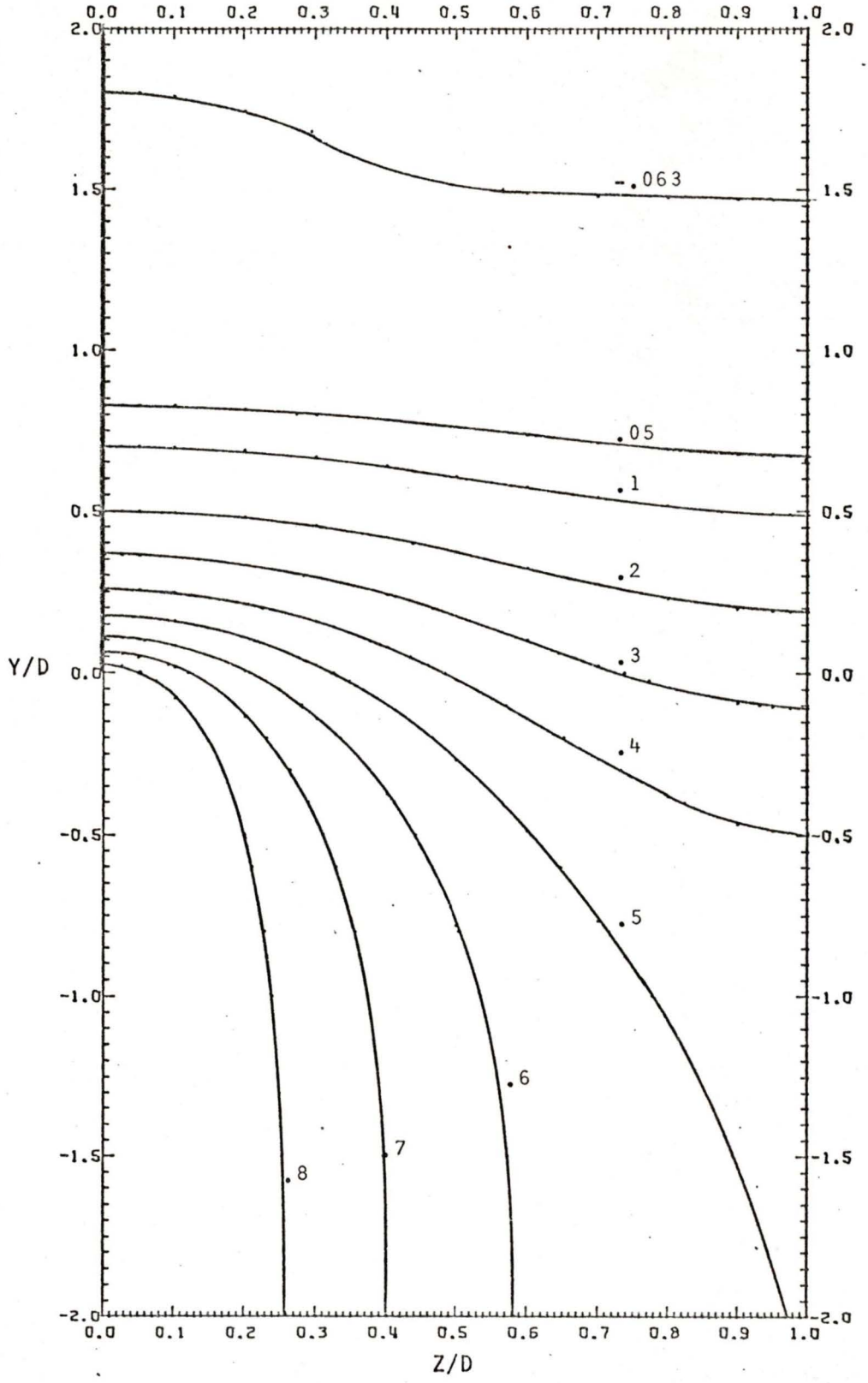

FIG. 5.1 Contours of constant B/B_0 for τ=18 seconds and ωt=0

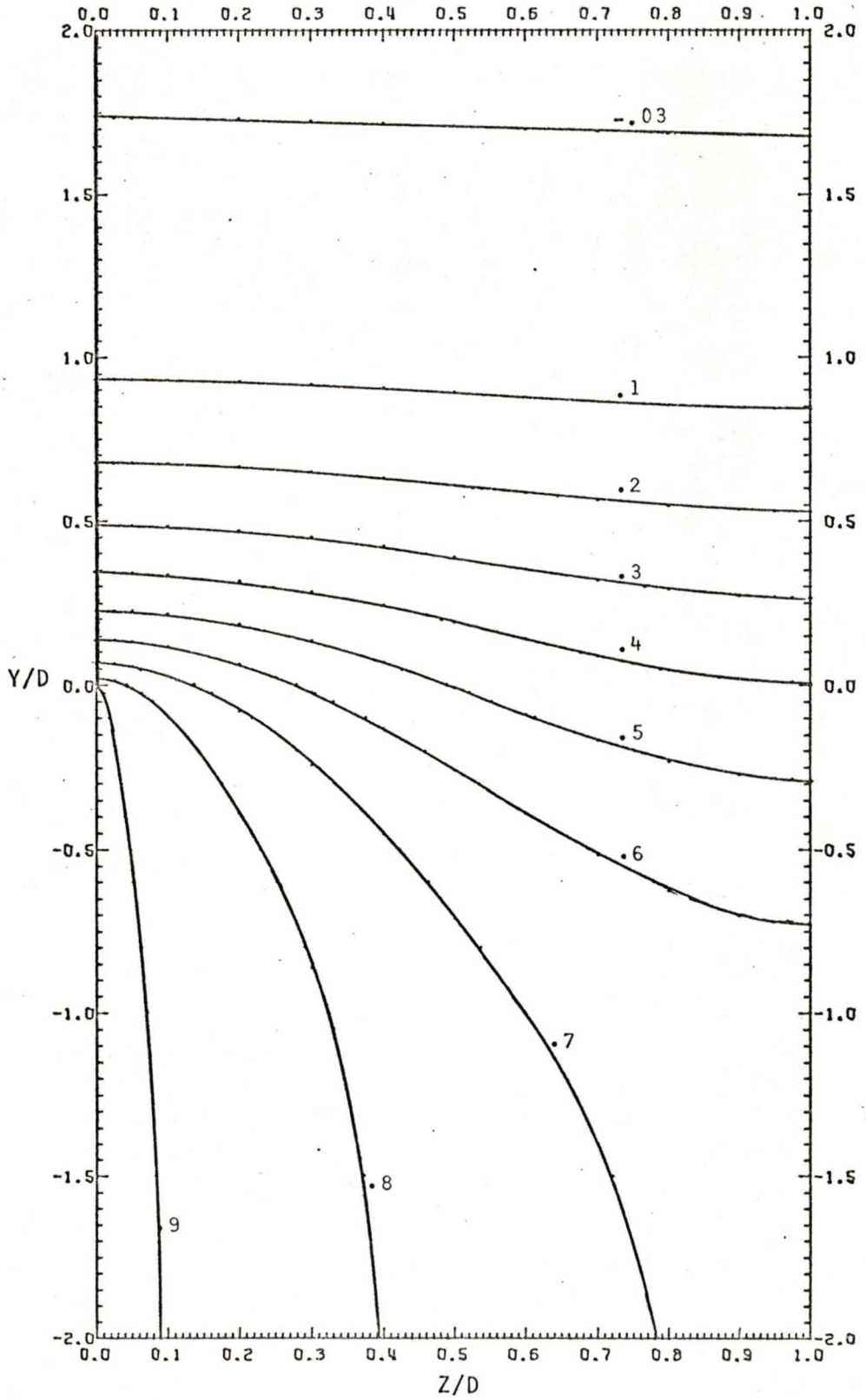

FIG. 5.2 Contours of constant B/B_0 for τ=18 seconds and $\omega t=\pi/8$

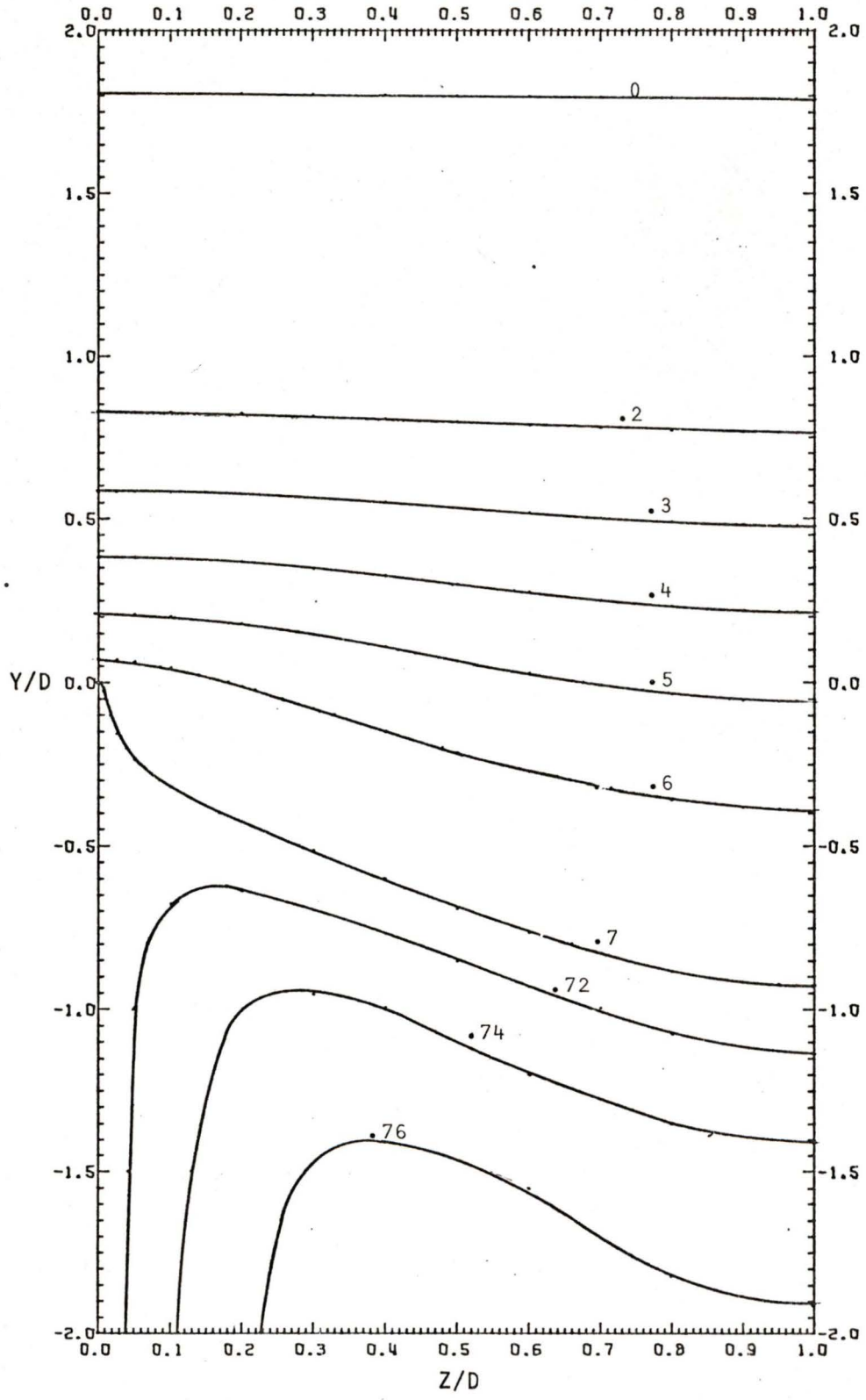

FIG. 5.3 Contours of constant B/B_0 for τ=18 seconds and $\omega t=\pi/4$

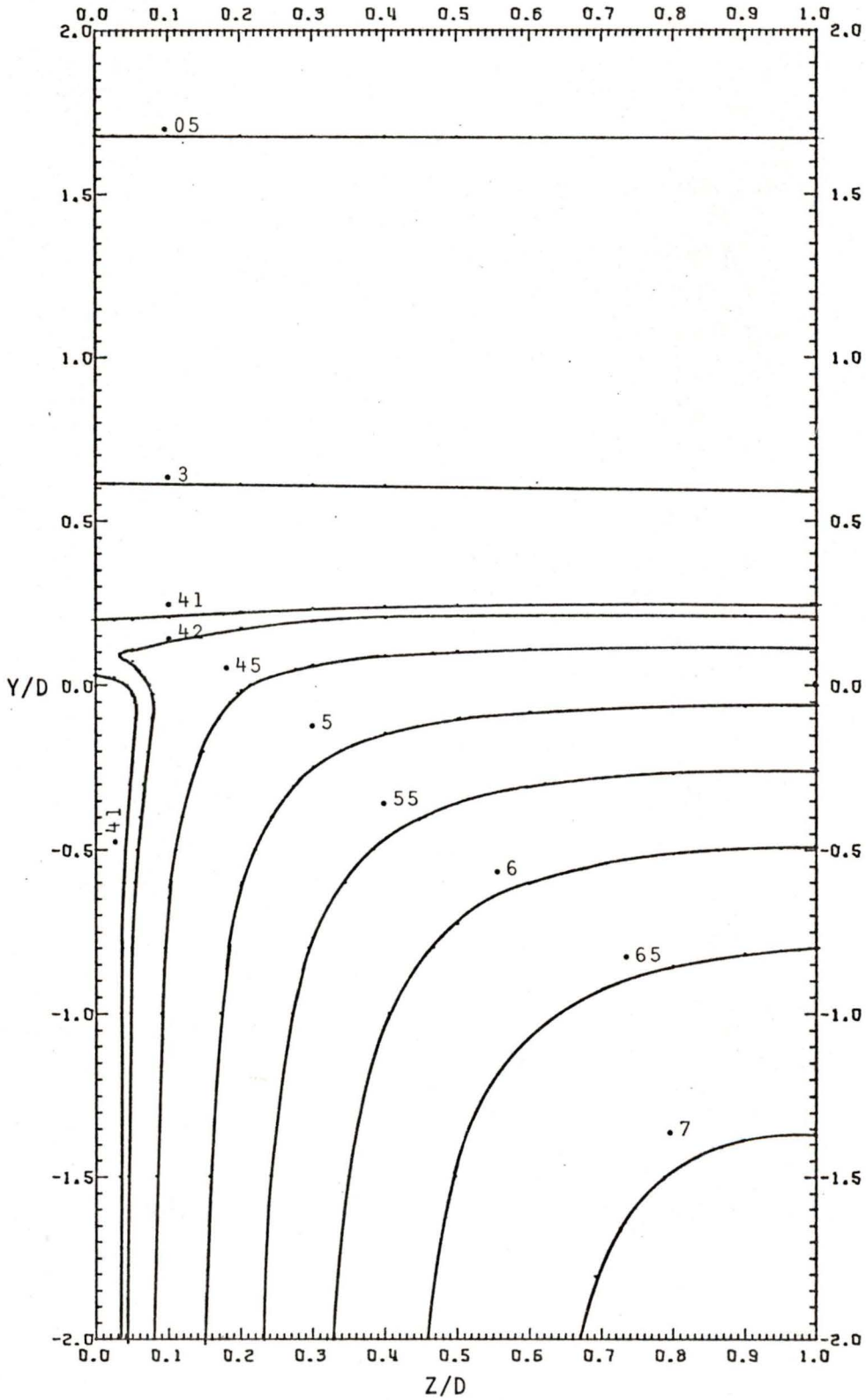

FIG. 5.4 Contours of constant B/B_0 for τ=18 seconds and $\omega t=3\pi/8$

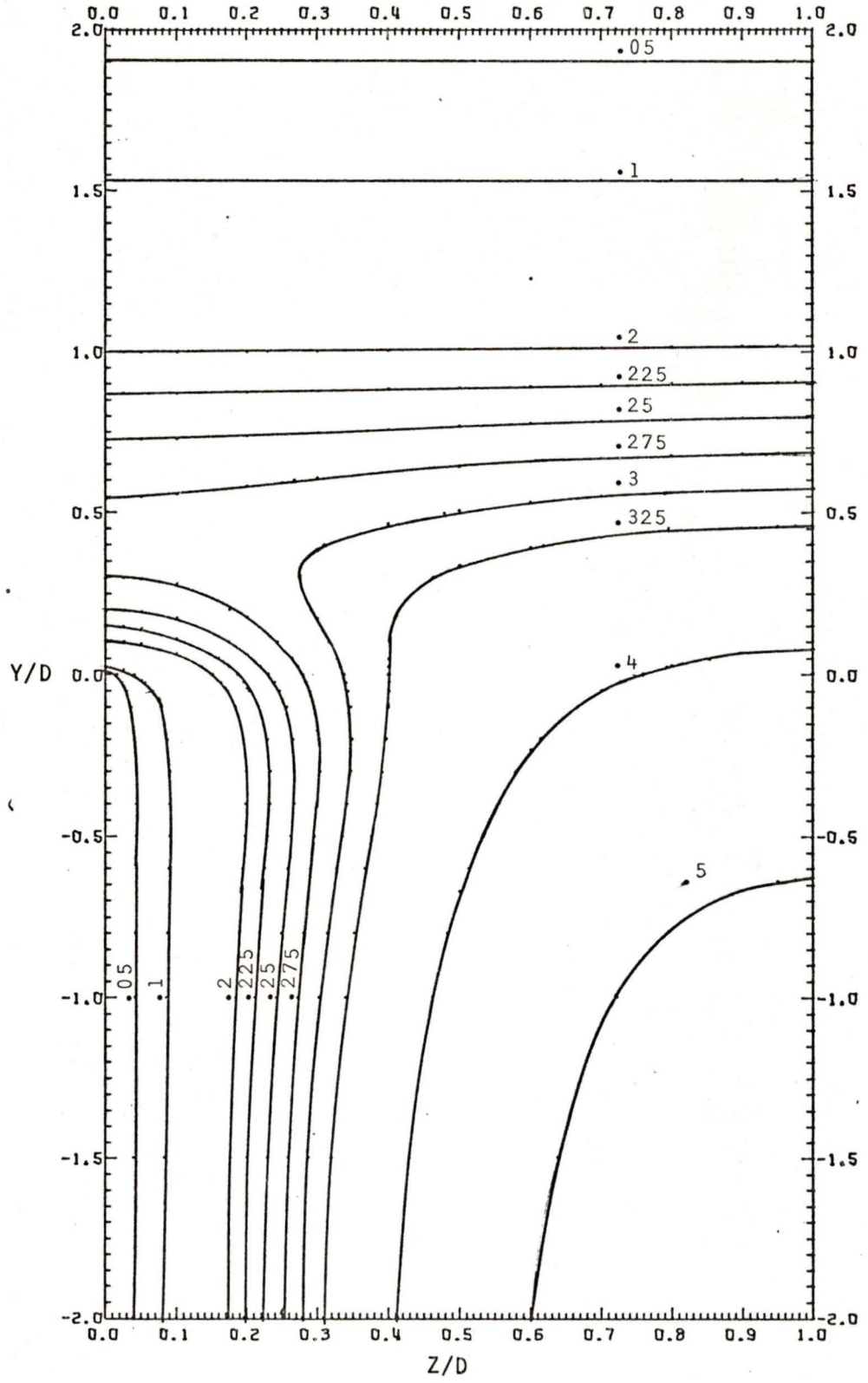

FIG. 5.5 Contours of constant B/B_0 for τ=18 seconds and $\omega t=\pi/2$

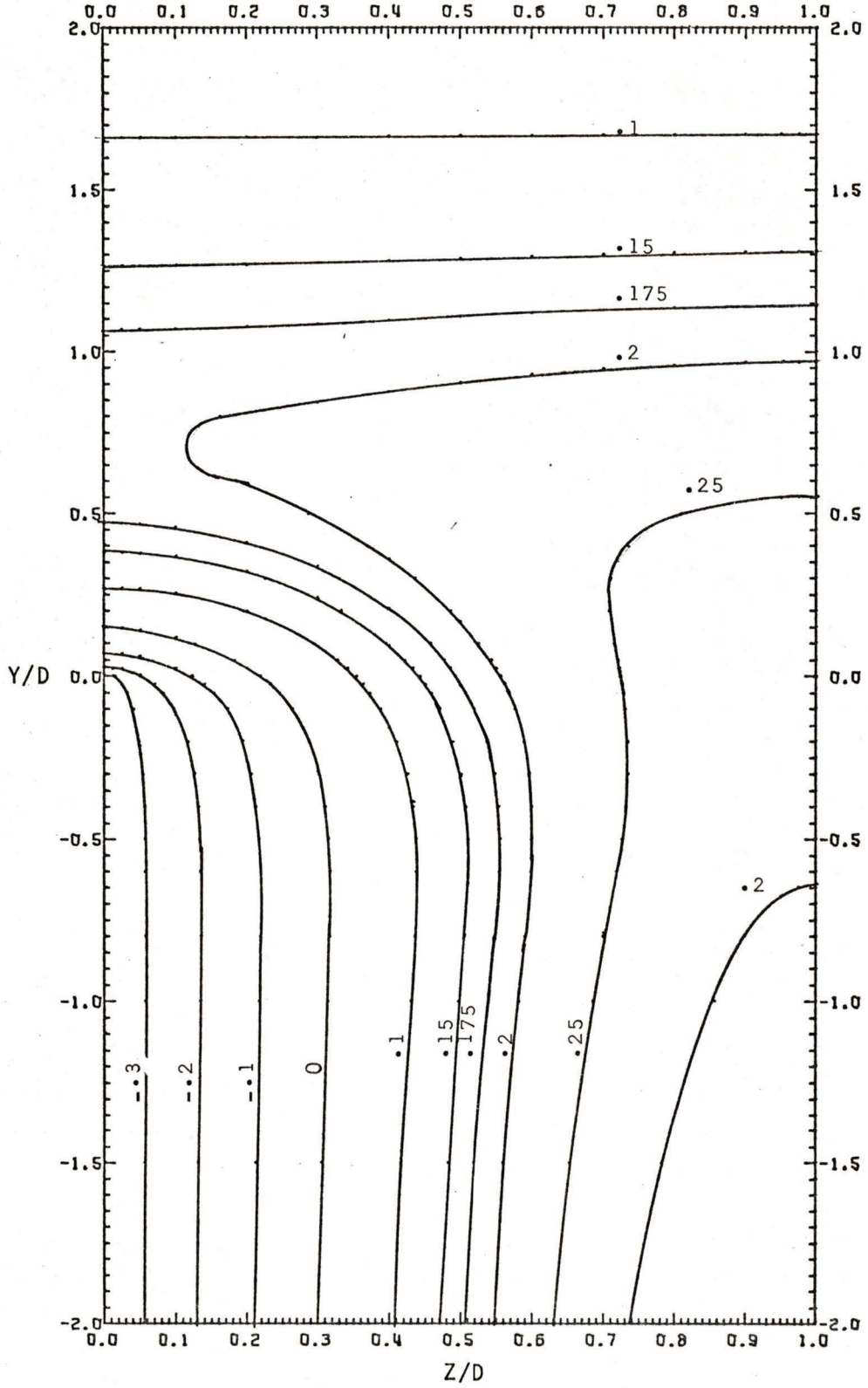

FIG. 5.6 Contours of constant B/B_0 for τ=18 seconds and $\omega t = 5\pi/8$

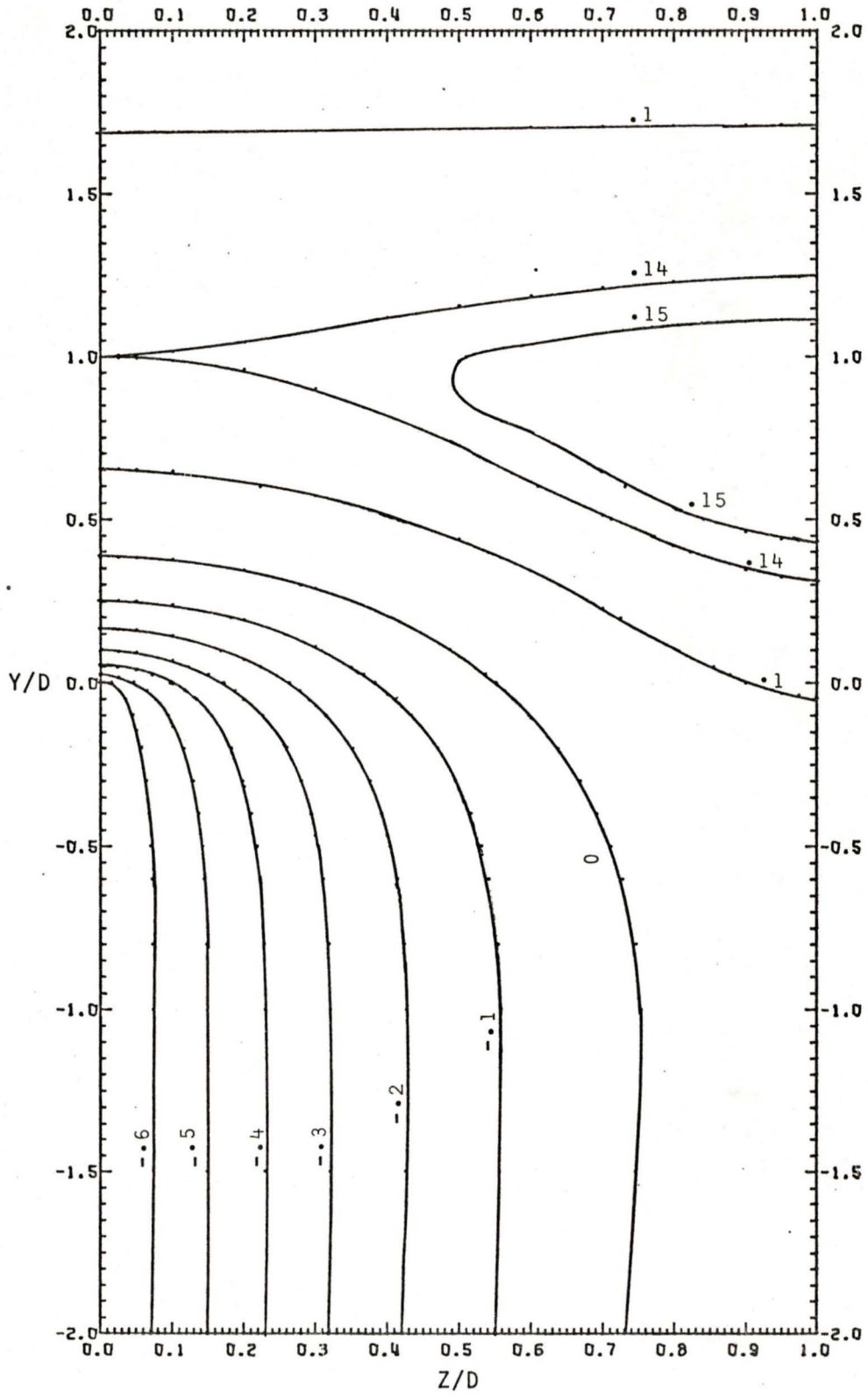

FIG. 5.7 Contours of constant B/B_0 for τ=18 seconds and $\omega t = 3\pi/4$

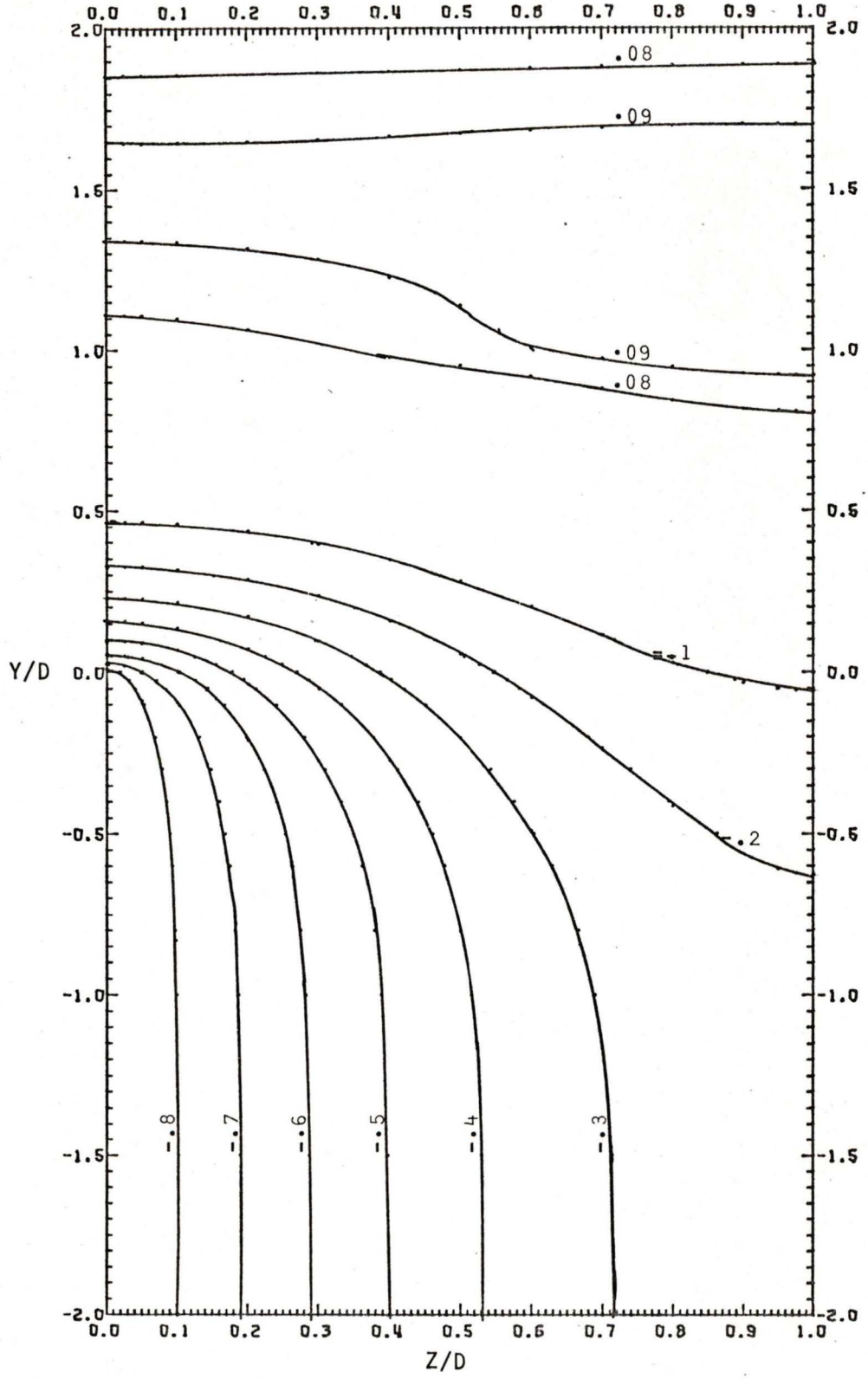

FIG. 5.8 Contours of constant B/B_0 for τ=18 seconds and $\omega t = 7\pi/8$

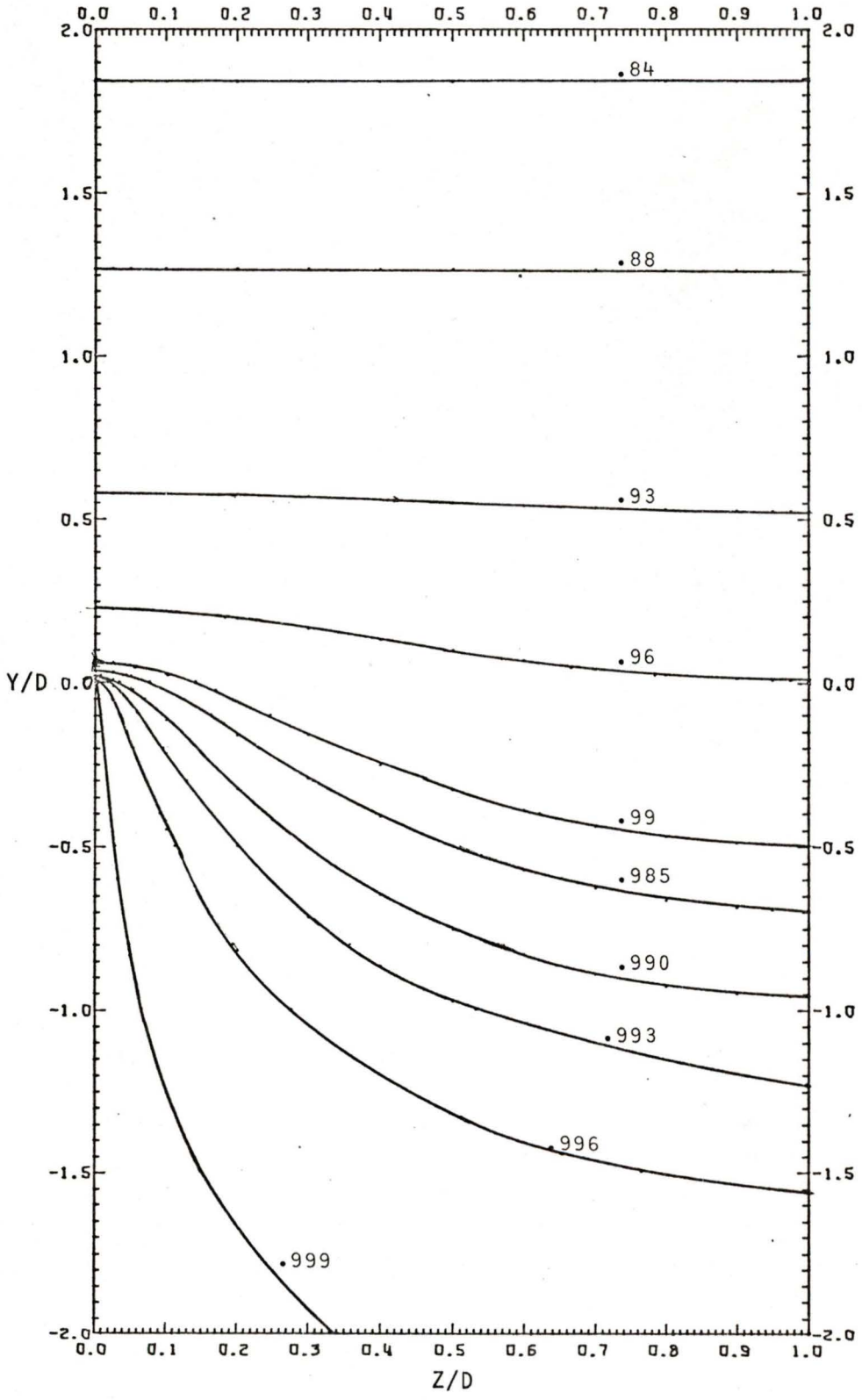

FIG. 5.9 Contours of constant B/B_0 for τ=1 hour and ωt=0

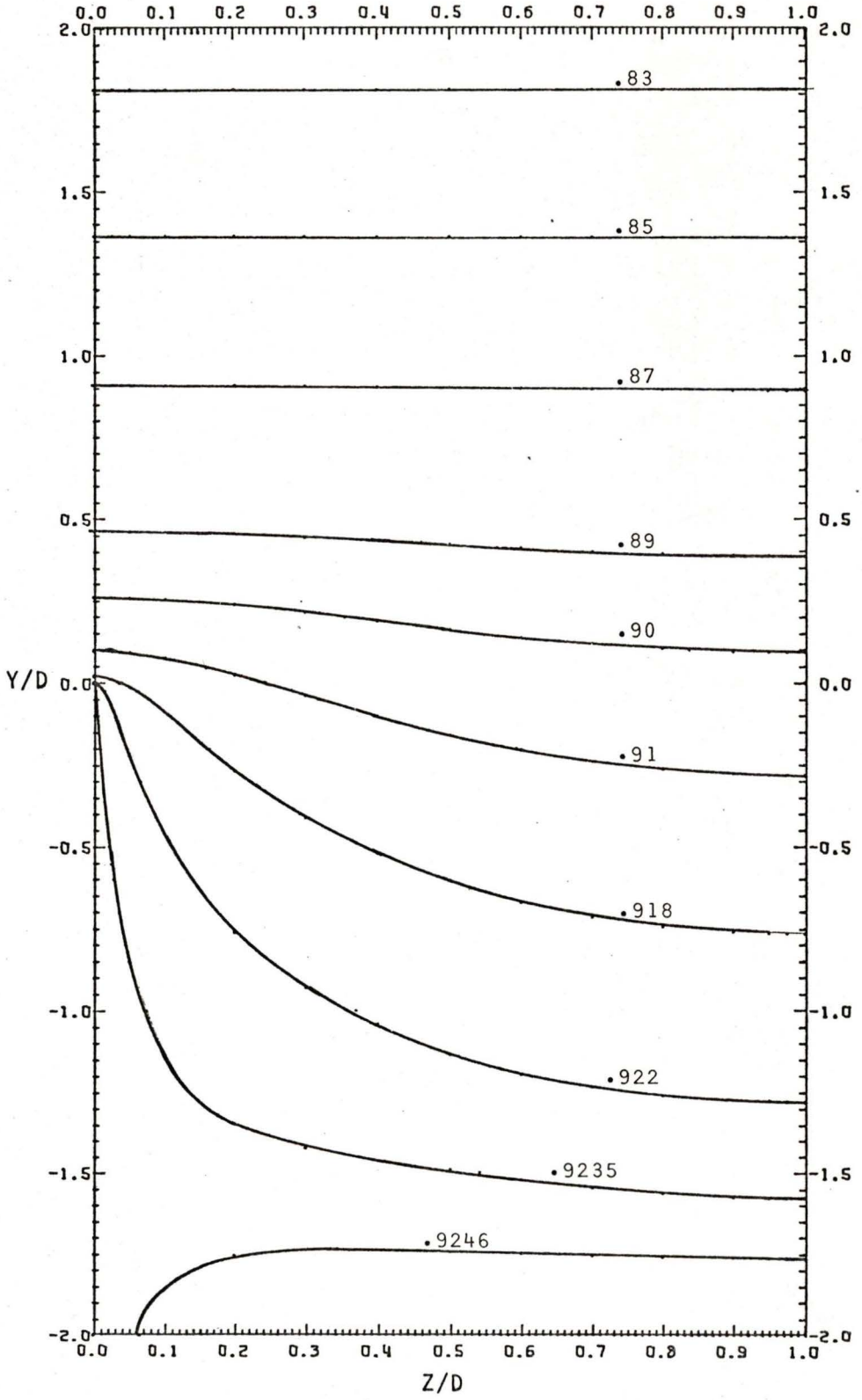

FIG. 5.10 Contours of constant B/B_0 for τ=1 hour and $\omega t=\pi/8$

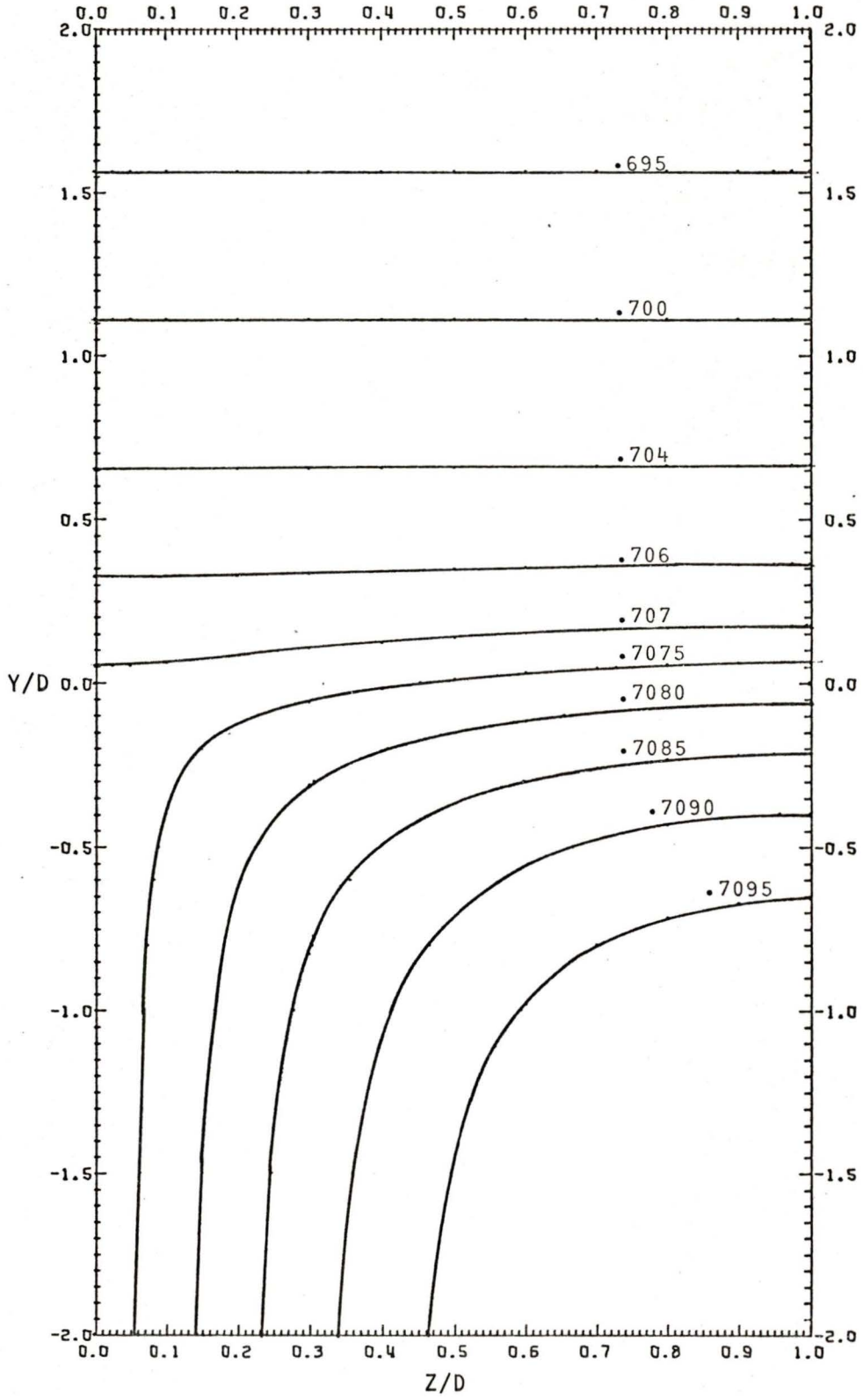

FIG. 5.11 Contours of constant B/B_0 for τ=1hour and $\omega t=\pi/4$

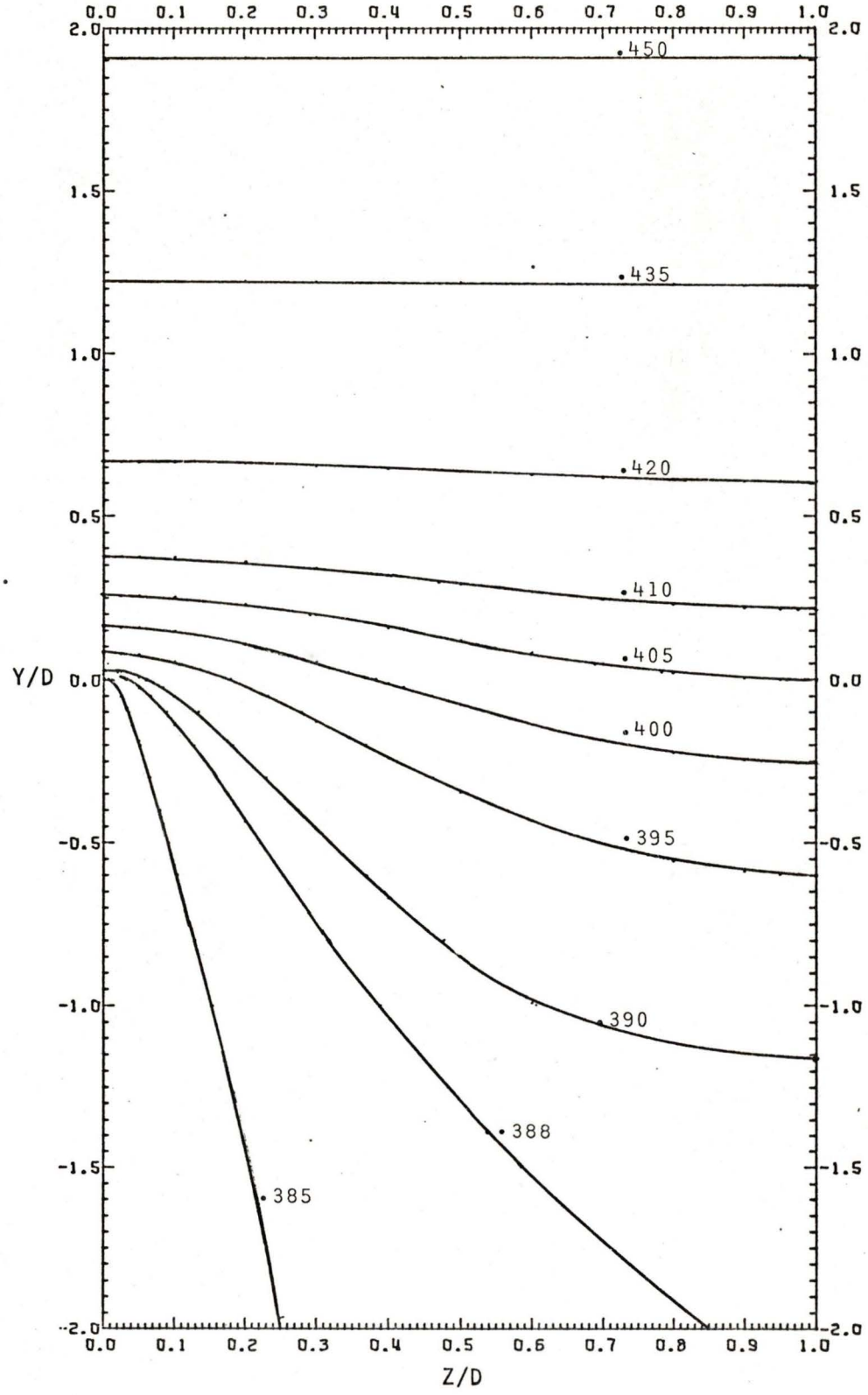

FIG. 5.12 Contours of constant B/B_0 for τ=1 hour and $\omega t=3\pi/8$

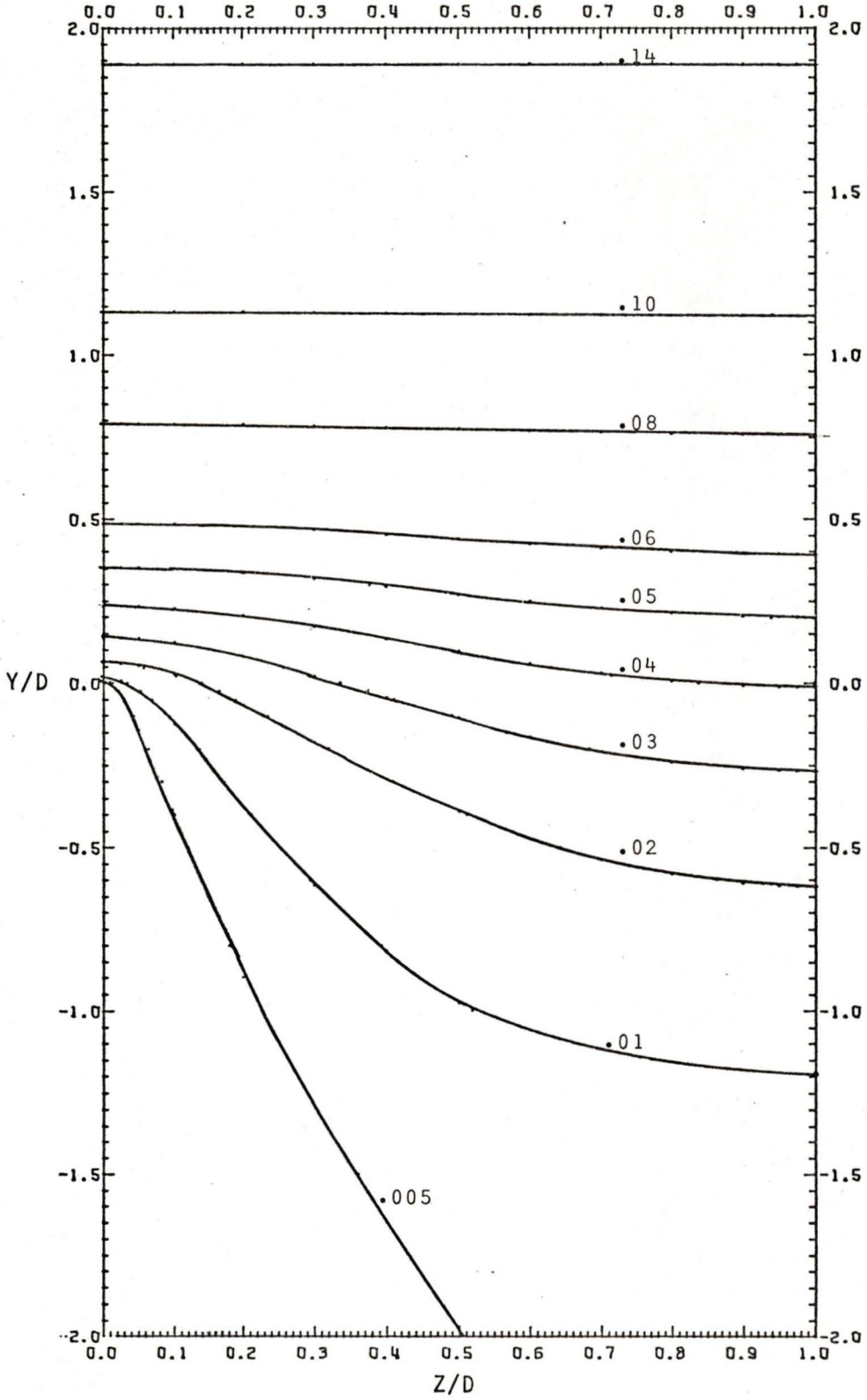

FIG. 5.13 Contours of constant B/B_0 for τ=1 hour and $\omega t=\pi/2$

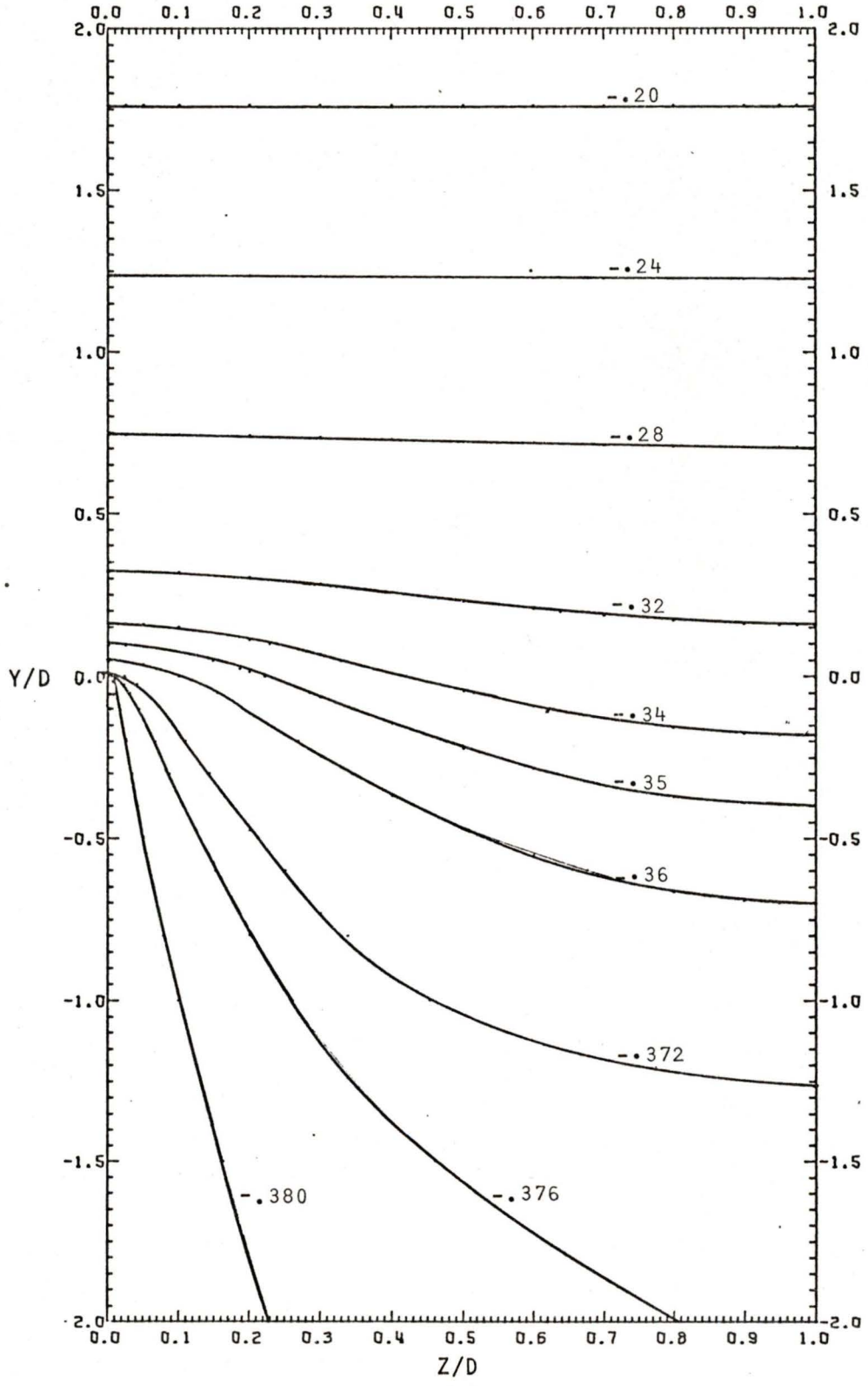

FIG. 5.14 Contours of constant B/B_0 for τ=1 hour and $\omega t=5\pi/8$

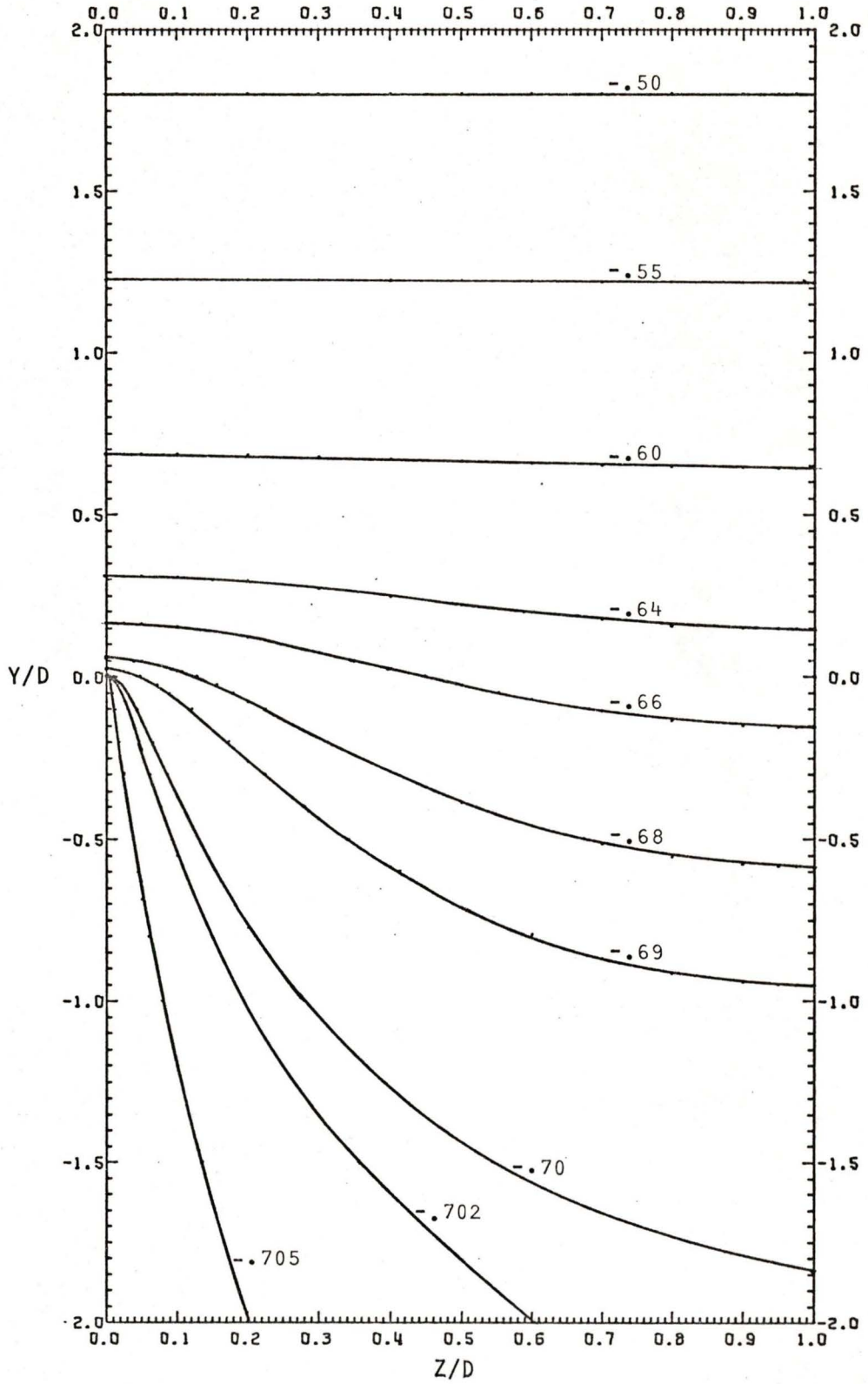

FIG.5.15 Contours of constant B/B_0 for τ=1 hour and $\omega t = 3\pi/4$

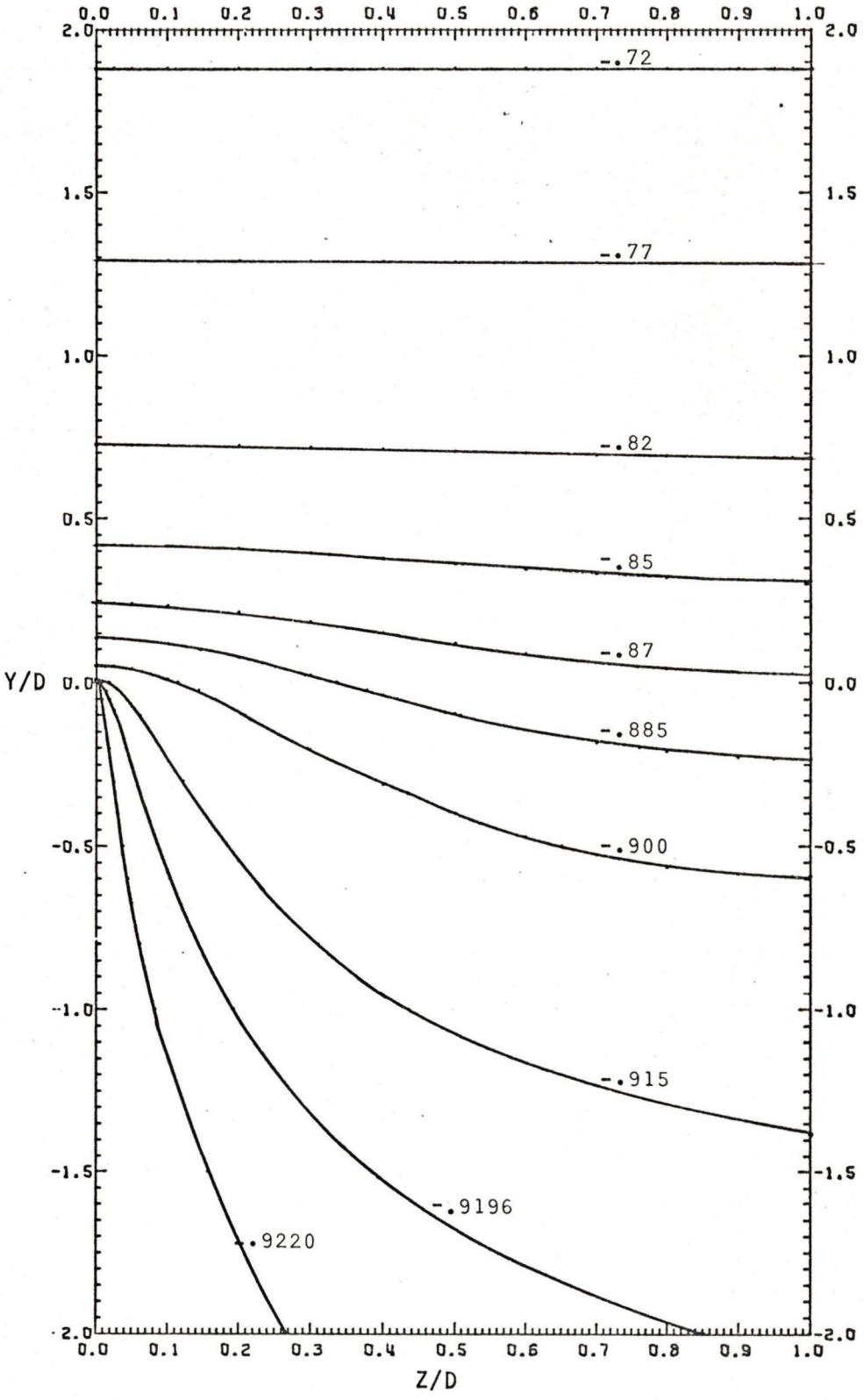

FIG. 5.16 Contours of constant B/B_0 for τ=1 hour and $\omega t = 7\pi/8$

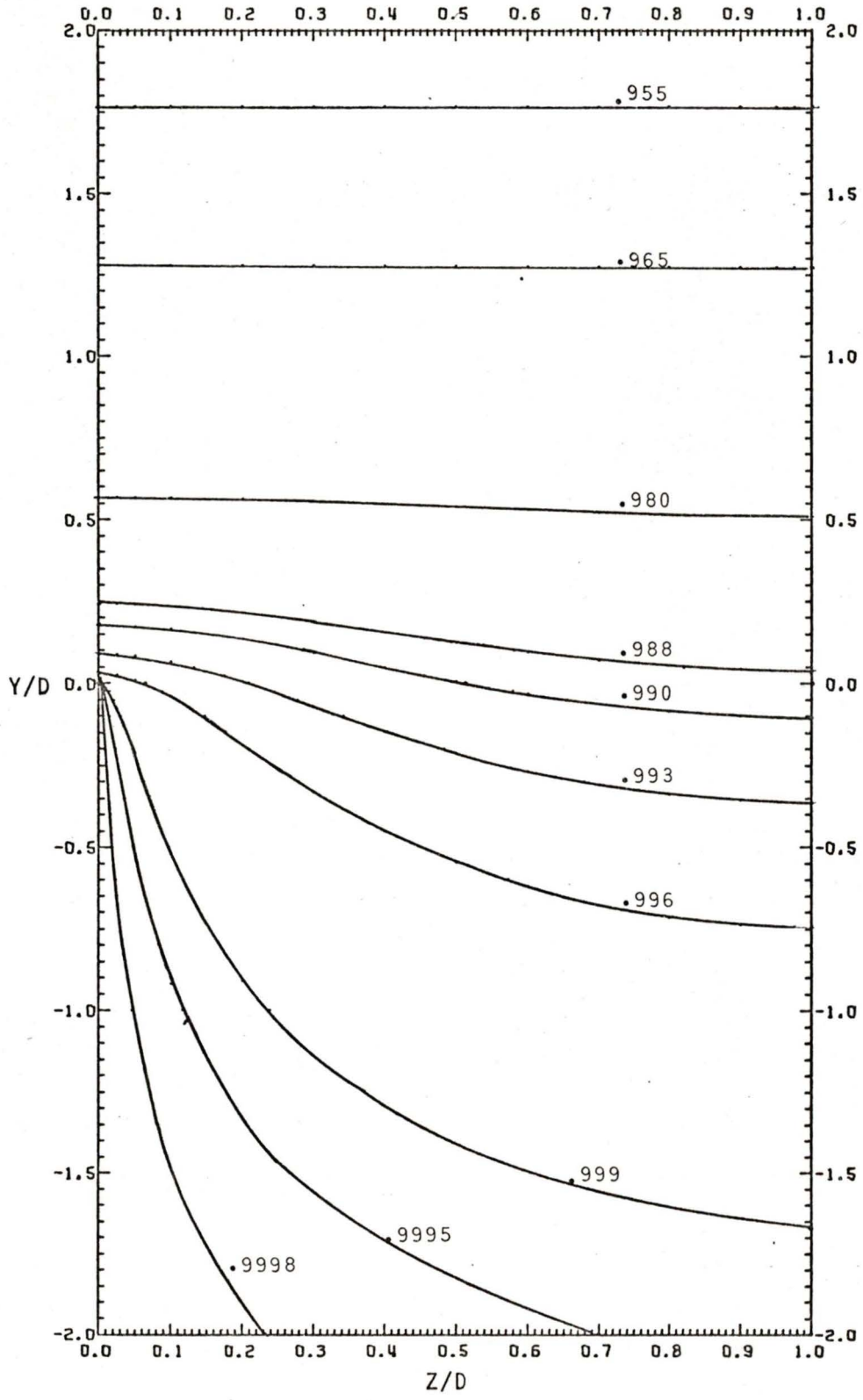

FIG. 5.17 Contours of constant B/B_0 for $\tau=\frac{1}{2}$ day and $\omega t=0$

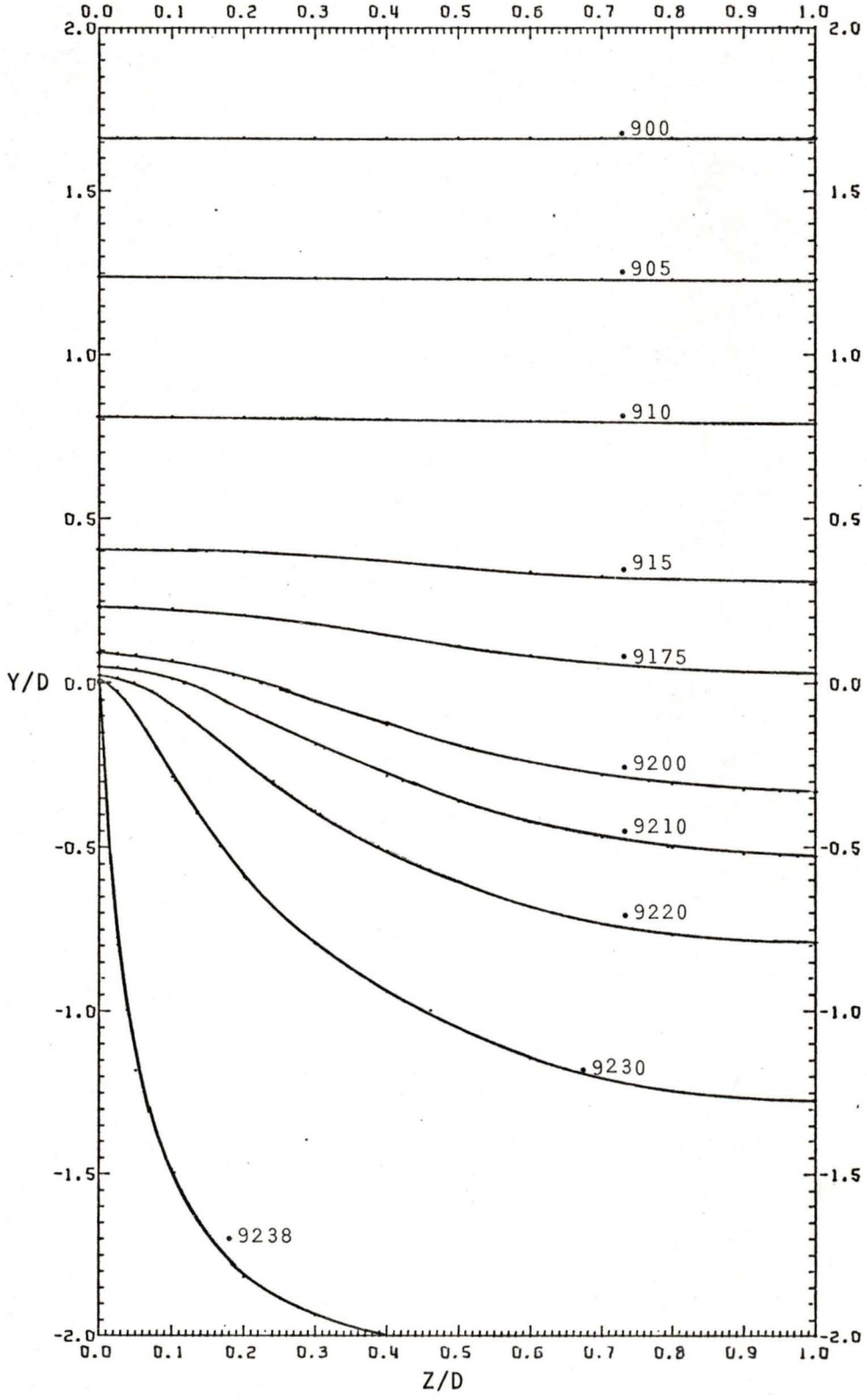

FIG. 5.18 Contours of constant B/B_0 for $\tau=\frac{1}{2}$ day and $\omega t=\pi/8$

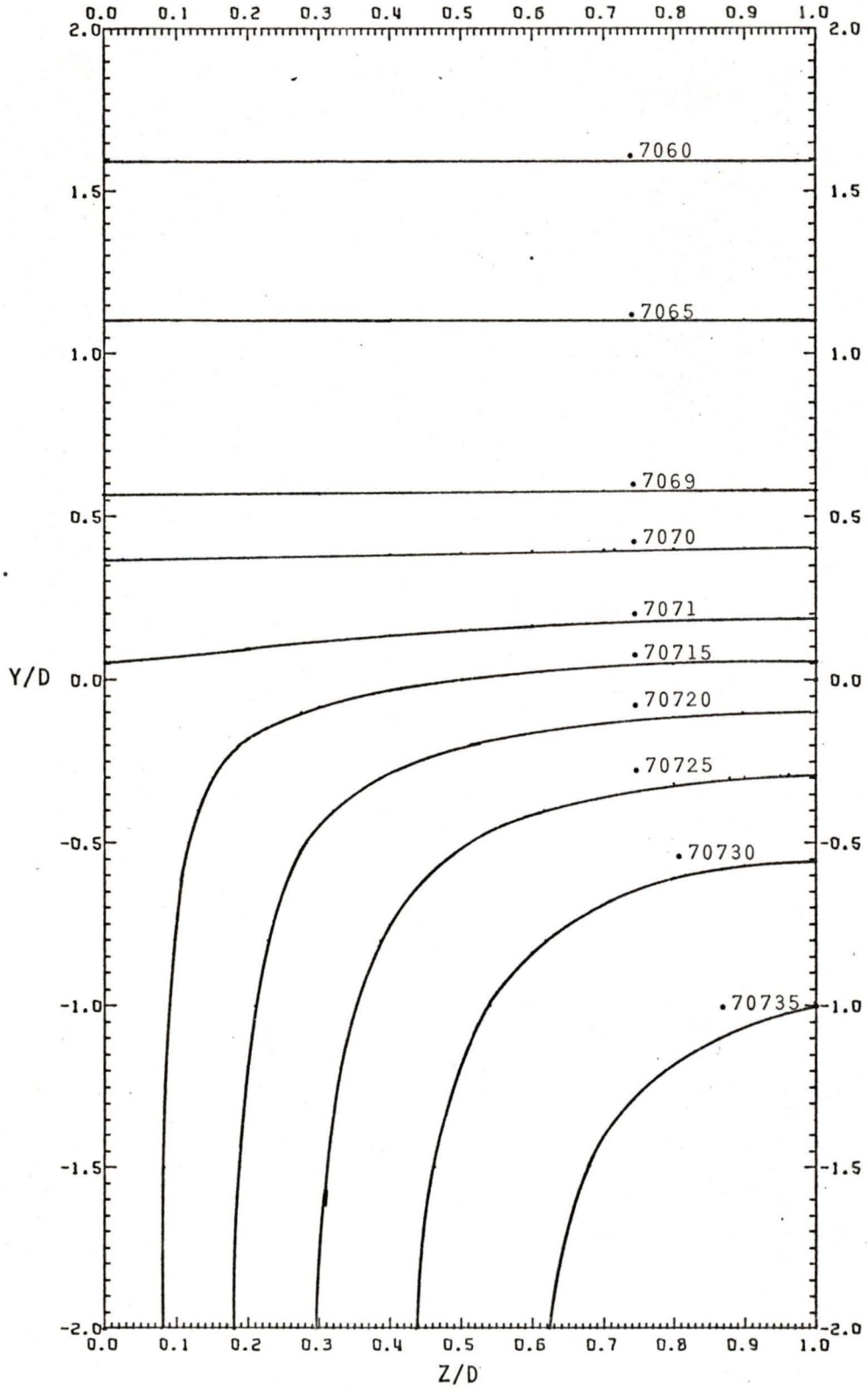

FIG. 5.19 Contours of constant B/B_0 for $\tau=\frac{1}{2}$ day and $\omega t=\pi/4$

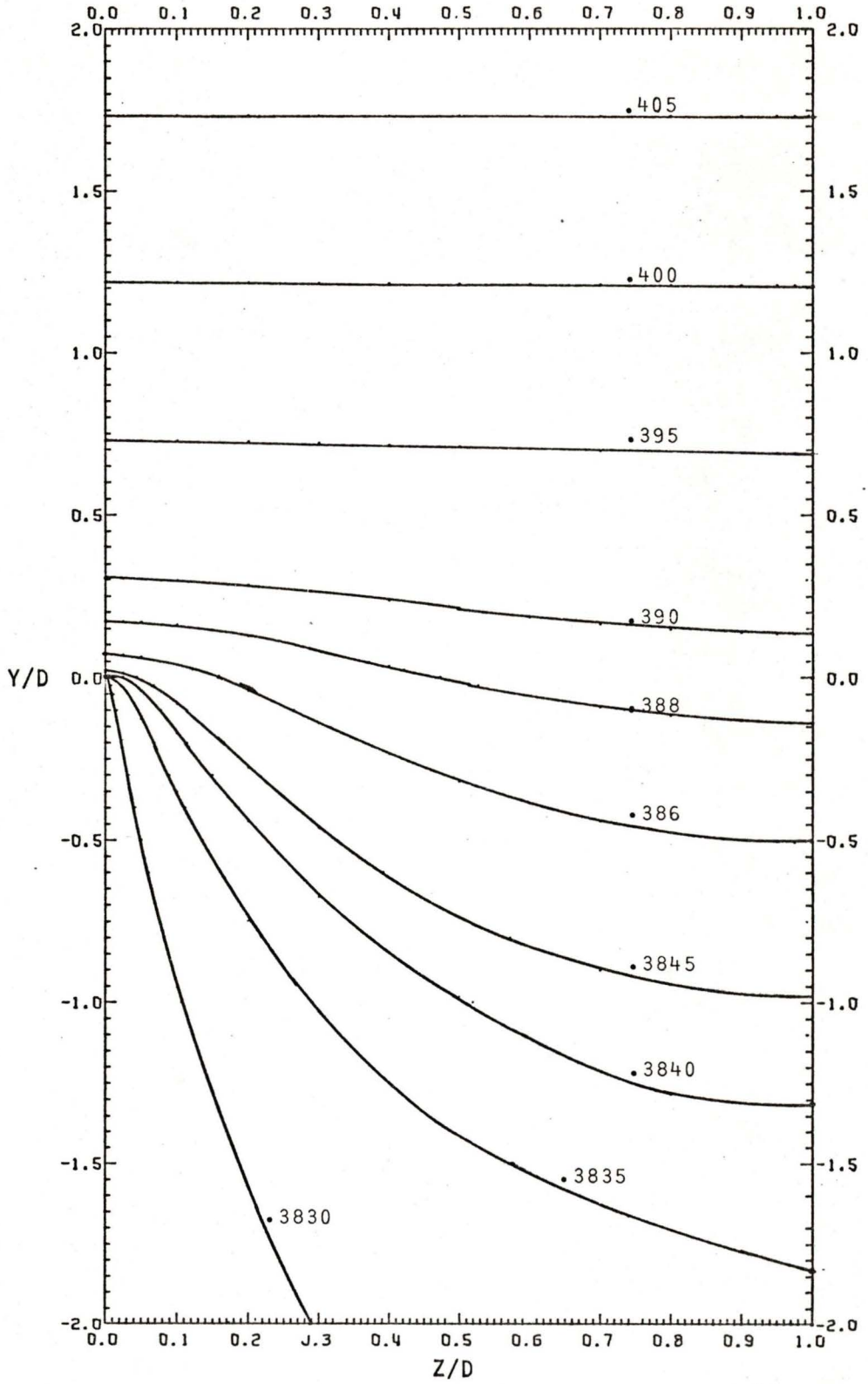

FIG. 5.20 Contours of constant B/B_0 for $\tau=\frac{1}{2}$ day and $\omega t=3\pi/8$

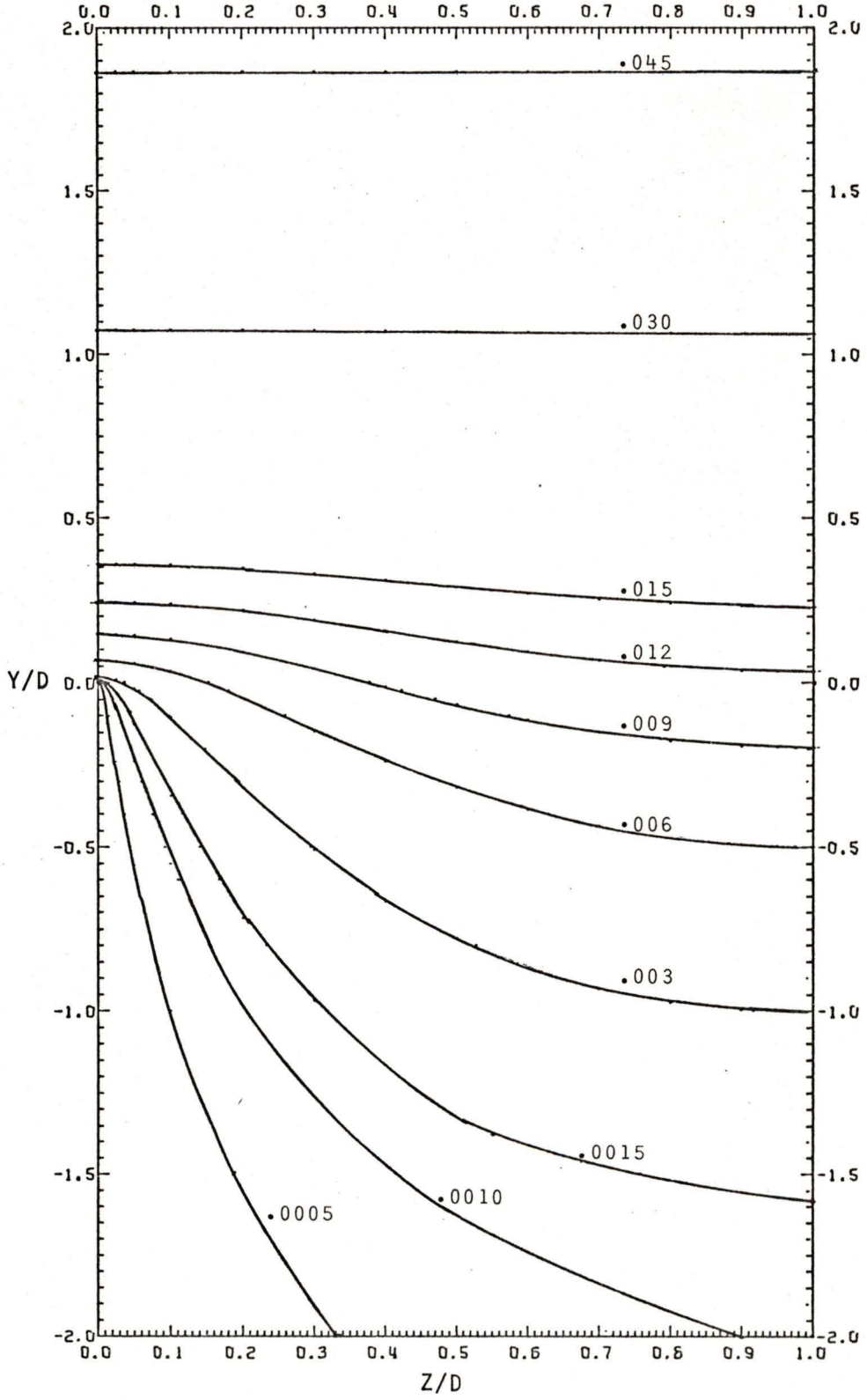

FIG. 5.21 Contours of constant B/B_0 for $\tau=\frac{1}{2}$ day and $\omega t=\pi/2$

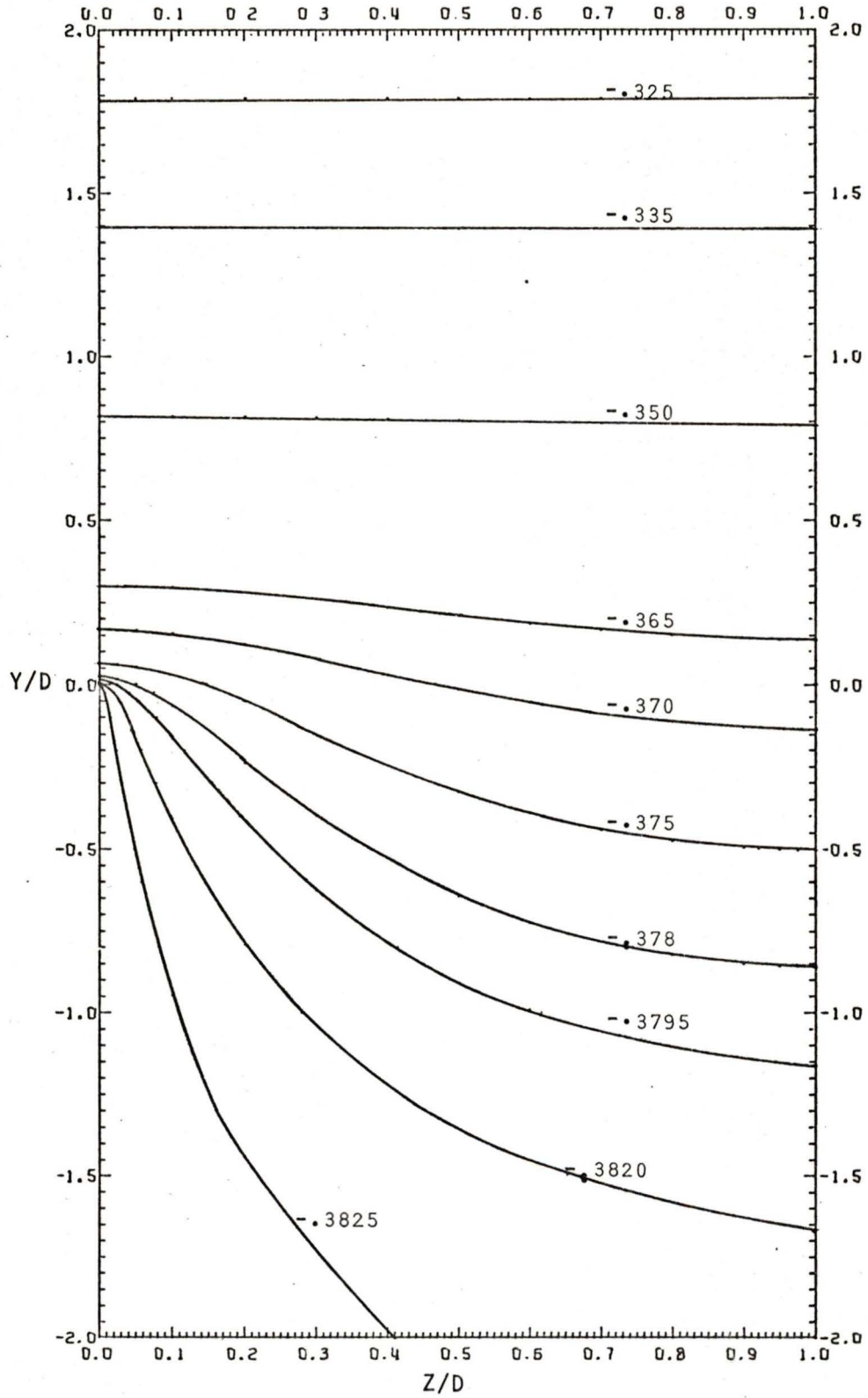

FIG. 5.22 Contours of constant B/B_0 for $\tau=\frac{1}{2}$ day and $\omega t=5\pi/8$

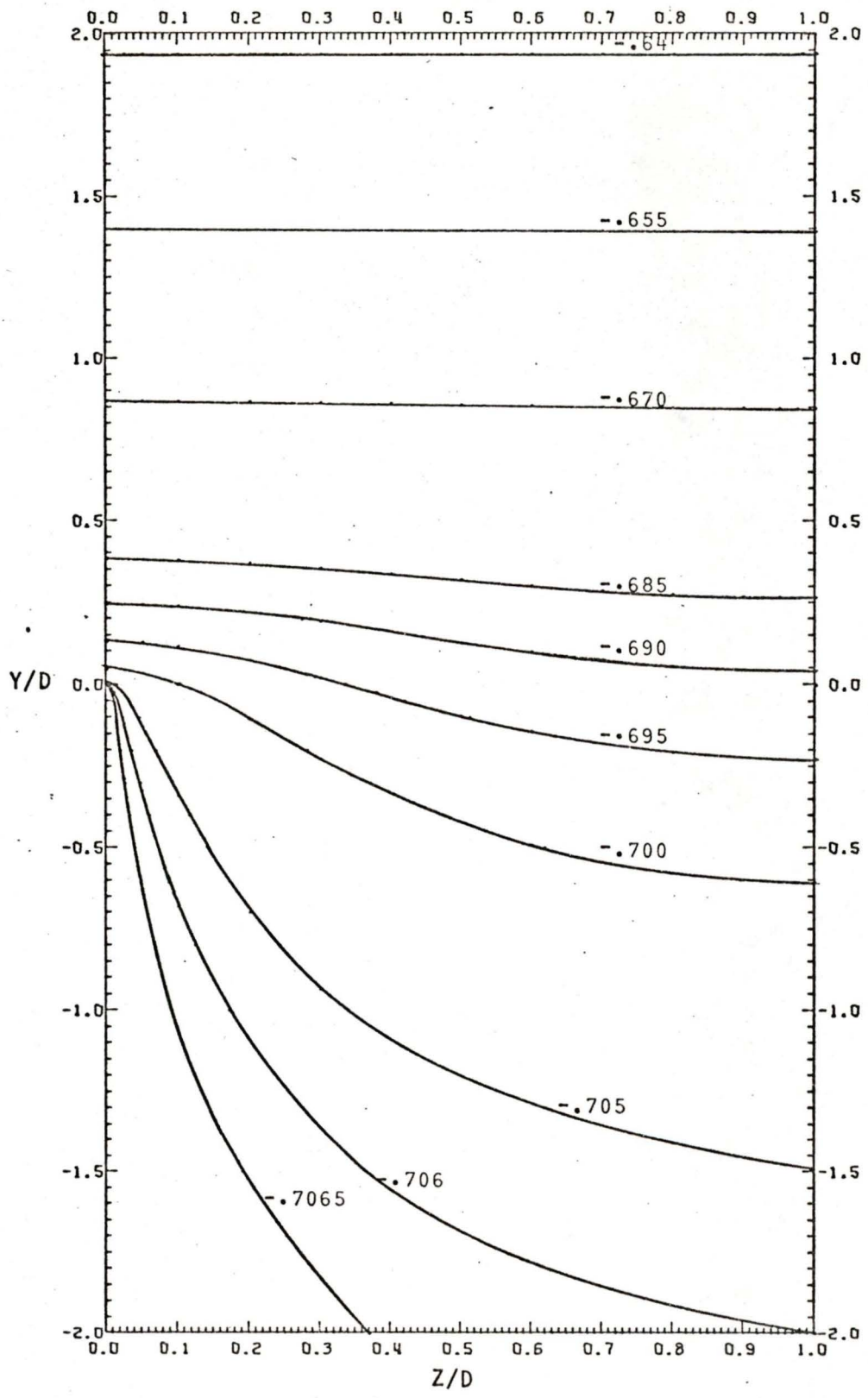

FIG. 5.23 Contours of constant B/B_0 for $\tau=\frac{1}{2}$ day and $\omega t=3\pi/4$

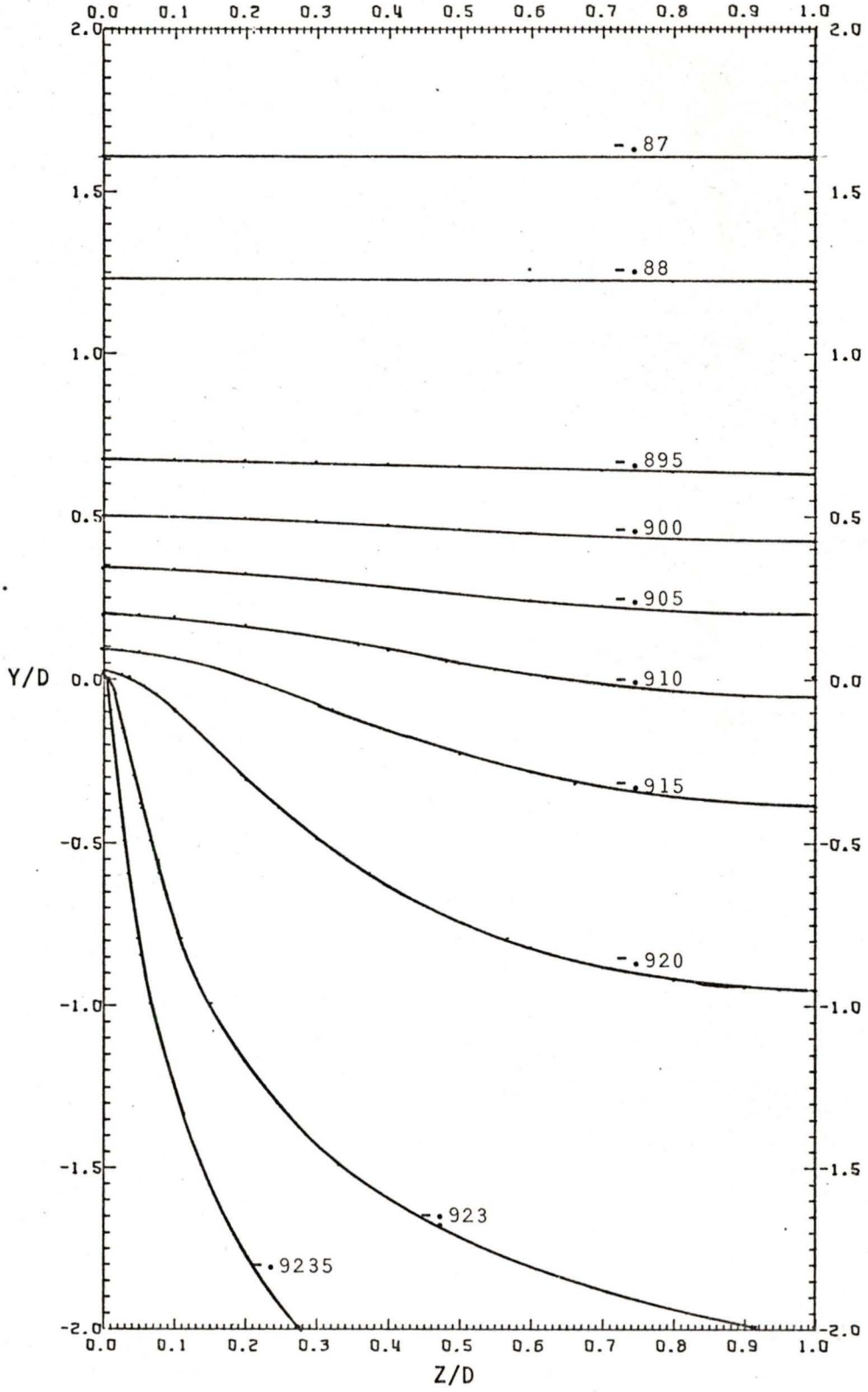

FIG. 5.24 Contours of constant B/B_0 for $\tau=\frac{1}{2}$ day and $\omega t=7\pi/8$

TABLE 5.1

Ratio of Current Density to B_0 (in amp/m^2tesla)
for τ=18 seconds and ωt=0

Y/D \ Z/D	0.00	.025	.050	.100	.200	.300	.400	.500	.600	.700	.800	.900	.950	.975	1.00
2.0	.031	.031	.031	.032	.032	.033	.033	.034	.035	.035	.036	.036	.036	.036	.036
1.5	.058	.058	.058	.058	.057	.055	.052	.051	.048	.045	.043	.041	.041	.041	.041
1.0	.278	.278	.276	.275	.270	.261	.249	.238	.217	.213	.203	.197	.194	.194	.193
.8	.424	.424	.423	.421	.410	.393	.371	.349	.325	.303	.286	.274	.271	.271	.270
.6	.629	.628	.627	.621	.598	.565	.525	.482	.439	.401	.370	.351	.346	.344	.344
.5	.764	.764	.761	.753	.718	.669	.612	.554	.498	.449	.409	.384	.378	.376	.376
.4	.937	.936	.932	.917	.863	.788	.708	.629	.556	.493	.444	.411	.403	.401	.401
.3	1.18	1.17	1.16	1.13	1.04	.922	.808	.704	.611	.533	.471	.431	.421	.418	.417
.2	1.54	1.53	1.51	1.44	1.25	1.06	.906	.772	.658	.564	.490	.442	.429	.425	.424
.1	2.29	2.26	2.16	1.91	1.48	1.20	.990	.828	.695	.584	.498	.441	.425	.422	.421
.05	3.32	3.13	2.78	2.20	1.58	1.25	1.02	.849	.708	.591	.499	.437	.421	.417	.415
.025	4.74	3.98	3.16	2.31	1.61	1.27	1.04	.858	.713	.593	.498	.434	.417	.413	.412
0.0		5.5	3.7	2.2	1.6	1.2	1.0	0.8	0.7	0.6	0.5	0.4	0.3	0.3	0.3
-.025	4.82	4.05	3.22	2.36	1.64	1.29	1.05	.870	.720	.595	.495	.427	.409	.404	.402
-.05	3.44	3.25	2.89	2.28	1.64	1.30	1.06	.875	.723	.595	.492	.422	.403	.398	.397
-.1	2.47	2.43	2.34	2.06	1.60	1.29	1.06	.879	.725	.593	.486	.414	.391	.386	.384
-.2	1.81	1.80	1.78	1.70	1.47	1.25	1.05	.875	.720	.583	.468	.386	.362	.356	.354
-.3	1.53	1.53	1.52	1.48	1.35	1.18	1.02	.857	.706	.567	.446	.355	.329	.322	.319
-.4	1.37	1.37	1.36	1.34	1.25	1.12	.980	.833	.687	.547	.421	.323	.293	.285	.282
-.5	1.27	1.27	1.26	1.24	1.17	1.07	.943	.807	.667	.528	.397	.291	.257	.248	.245
-.6	1.20	1.20	1.19	1.18	1.12	1.02	.910	.783	.647	.508	.376	.261	.224	.213	.210
-.8	1.11	1.11	1.11	1.09	1.04	.961	.860	.742	.613	.476	.339	.213	.166	.152	.147
-1.0	1.06	1.06	1.06	1.04	.995	.921	.826	.714	.588	.454	.315	.181	.125	.106	.099
-1.5	1.01	1.01	1.00	.990	.945	.876	.786	.679	.559	.428	.291	.149	.079	.048	.031
-2.0	.992	.991	.988	.977	.932	.864	.775	.670	.551	.422	.286	.144	.072	.037	.006

TABLE 5.2

Ratio of Current Density to B_0 (in amp/m^2tesla)
for τ=1 hour and ωt=0

Y/D \ Z/D	0.00	.025	.050	.100	.200	.300	.400	.500	.600	.700	.800	.900	.950	.975	1.00
2.0	.084	.084	.084	.084	.084	.084	.084	.084	.084	.084	.084	.084	.084	.084	.084
1.5	.086	.086	.086	.086	.086	.085	.085	.085	.085	.085	.085	.085	.085	.085	.085
1.0	.088	.088	.088	.088	.087	.087	.086	.086	.085	.085	.084	.084	.084	.084	.084
.8	.090	.090	.090	.090	.089	.088	.087	.086	.085	.084	.083	.083	.083	.083	.083
.6	.094	.094	.094	.093	.092	.090	.088	.086	.084	.082	.081	.081	.080	.080	.080
.5	.097	.097	.097	.096	.094	.091	.088	.085	.083	.081	.080	.079	.079	.079	.079
.4	.102	.102	.102	.101	.097	.093	.090	.085	.082	.079	.078	.077	.076	.076	.076
.3	.111	.111	.110	.108	.102	.095	.089	.083	.080	.077	.075	.074	.073	.073	.073
.2	.127	.126	.125	.120	.107	.096	.088	.081	.077	.074	.071	.070	.070	.070	.070
.1	.167	.164	.158	.141	.113	.096	.085	.078	.076	.070	.067	.066	.066	.066	.066
.05	.227	.215	.191	.152	.113	.094	.083	.076	.071	.067	.065	.064	.064	.064	.064
.025	.316	.265	.211	.156	.112	.093	.081	.074	.069	.066	.064	.064	.063	.062	.062
0.0		.4	.2	.1	.1	.09	.08	.07	.07	.06	.06	.06	.06	.06	.06
-.025	.303	.255	.203	.150	.108	.089	.078	.071	.067	.064	.062	.060	.060	.060	.060
-.05	.210	.199	.177	.141	.104	.087	.077	.070	.065	.062	.060	.059	.059	.059	.059
-.1	.143	.141	.135	.120	.096	.082	.073	.067	.062	.060	.058	.057	.056	.056	.056
-.2	.093	.092	.091	.088	.079	.070	.064	.059	.056	.054	.052	.051	.051	.051	.051
-.3	.069	.069	.069	.068	.064	.059	.055	.052	.050	.048	.047	.046	.046	.046	.046
-.4	.055	.055	.055	.054	.052	.050	.047	.045	.044	.042	.042	.041	.041	.041	.041
-.5	.045	.045	.045	.044	.043	.042	.040	.039	.038	.037	.036	.036	.036	.036	.036
-.6	.037	.037	.037	.037	.036	.035	.034	.034	.033	.032	.032	.032	.032	.031	.031
-.8	.026	.026	.026	.026	.026	.025	.025	.025	.024	.024	.024	.024	.024	.024	.024
-1.0	.019	.019	.019	.019	.019	.018	.018	.018	.018	.018	.018	.018	.018	.018	.018
-1.5	.008	.008	.008	.008	.008	.008	.008	.008	.008	.008	.008	.008	.008	.008	.008
-2.0	.004	.004	.004	.004	.004	.004	.004	.004	.004	.004	.004	.004	.004	.004	.004

TABLE 5.3

Ratio of Current Density to B_0 (in amp/m^2tesla)
for $\tau=\frac{1}{2}$ day and $\omega t=0$

Y/D \ Z/D	0.00	.025	.050	.100	.200	.300	.400	.500	.600	.700	.800	.900	.950	.975	1.00
2.0	.025	.025	.025	.025	.025	.025	.025	.025	.025	.025	.025	.025	.025	.025	.025
1.5	.025	.025	.025	.025	.025	.025	.025	.025	.025	.025	.025	.025	.025	.025	.025
1.0	.026	.026	.026	.026	.025	.025	.025	.025	.025	.025	.025	.024	.024	.024	.024
.8	.026	.026	.026	.026	.026	.026	.025	.025	.025	.024	.024	.024	.024	.024	.024
.6	.027	.027	.027	.027	.027	.026	.025	.025	.024	.024	.024	.023	.023	.023	.023
.5	.028	.028	.028	.028	.027	.026	.026	.025	.024	.023	.023	.023	.023	.023	.023
.4	.030	.030	.029	.029	.028	.027	.026	.025	.024	.023	.022	.022	.022	.022	.022
.3	.032	.032	.032	.031	.029	.027	.026	.024	.023	.022	.022	.021	.021	.012	.021
.2	.037	.036	.036	.035	.031	.028	.025	.023	.022	.021	.021	.020	.020	.020	.020
.1	.048	.047	.046	.041	.032	.028	.025	.022	.021	.020	.019	.019	.019	.019	.019
.05	.066	.062	.055	.044	.033	.027	.024	.022	.020	.019	.019	.018	.018	.018	.018
.025	.091	.077	.061	.045	.032	.027	.023	.021	.020	.019	.018	.018	.018	.018	.018
0.0		.1	.07	.04	.03	.03	.02	.02	.02	.02	.02	.02	.02	.02	.02
-.025	.087	.074	.059	.043	.031	.026	.023	.021	.019	.018	.018	.017	.017	.017	.017
-.05	.061	.057	.051	.041	.030	.025	.022	.020	.019	.018	.017	.017	.017	.017	.017
-.1	.041	.041	.039	.035	.028	.024	.021	.019	.018	.017	.017	.016	.016	.016	.016
-.2	.027	.027	.026	.025	.023	.020	.018	.017	.016	.016	.015	.015	.015	.015	.015
-.3	.020	.020	.020	.019	.018	.017	.016	.015	.014	.014	.014	.013	.013	.013	.013
-.4	.016	.016	.016	.016	.015	.014	.014	.013	.013	.012	.012	.012	.012	.012	.012
-.5	.013	.013	.013	.013	.012	.012	.012	.011	.011	.011	.011	.010	.010	.010	.010
-.6	.011	.011	.011	.011	.010	.010	.010	.010	.009	.009	.009	.009	.009	.009	.009
-.8	.007	.007	.007	.007	.007	.007	.007	.007	.007	.007	.007	.007	.007	.007	.007
-1.0	.005	.005	.005	.005	.005	.005	.005	.005	.005	.005	.005	.005	.005	.005	.005
-1.5	.002	.002	.002	.002	.002	.002	.002	.002	.002	.002	.002	.002	.002	.002	.002
-2.0	.001	.001	.001	.001	.001	.001	.001	.001	.001	.001	.001	.001	.001	.001	.001

CHAPTER 6

DISCUSSION AND CONCLUSIONS

The first point to discuss is the reliability of the results. For the reasons discussed earlier the only case where the computation of more terms in the series would have been effective is when $y/D = 0$ for the current. (Hence the one significant figure accuracy in the tables for $y/D = 0$). It was not considered worthwhile to do the extra computing for these few values. The convergence obtained for the magnetic field results is supported by the continuity of the constant B/B_0 lines across $y = 0$. (Recall that the solution was computed from a separate series for y positive or negative.) This continuity, however, only demonstrates the consistency of the results, so for a final check the magnetic field values were compared to those calculated numerically by Brewitt-Taylor (1976, private communication). The values were the same to within 2% for the real part and 3% for the imaginary. The validity of the analytic solutions is demonstrated in Appendices B and D. In Appendix D it is also shown that as the depth of the mantle approaches ∞ in the solution of the second model, the solution of the first model is obtained.

The computer time required to calculate the series for one particular D' value is fifty minutes on an IBM System/370, Model 145 computer. This time would not increase significantly if the grid contained more points, since the infinite products which account for a large part of the computing time are not dependent on y or z. This could be a definite advantage of the analytic solution over a numerical one.

The accessible region, as far as observational data would be concerned, is at the surface of the land and at the bottom of the sea. At the surface of the land the important parameter is the y component of the electric field, since the magnetic field is constant and the z component of the electric field is proportional to $\partial B/\partial y$, which is zero. From the tabulated current values, (tables 5.1 through 5.4), it can be deduced that E_y increases sharply as the coastline is approached. Under the sea the parameters of interest are the z component of the electric field and the magnetic field since $\partial B/\partial z$,

and hence E_y, is zero. From the tables and graphs of the previous chapter we can conclude that both E_z and the magnetic field increase as the coastline is approached from the seaward side. Thus there exists a peak in the current values at the coastline. This result is encouraging because if such a peak occurs in the field components arising in a three-dimensional model, it could create the coast-effect. Unfortunately there are no existing observational or analogue model data available for comparison with these theoretical results. Obtaining such values would be an excellent project for future work.

The graphs in figures (5.1) through (5.24) clearly indicate the existence of current loops linking the ocean and the mantle. (Recall from Chapter 5 that the current will follow along the lines of constant magnetic field.) Whether the current is flowing away or towards the sea can be established by the sign of E_z, or equivalently the sign of $-\partial B/\partial y$. For example in figure (5.1) the current is flowing away from the sea along all the lines. Figure (5.7) is one of the graphs which illustrates the return currents of the loop since at $y/D \simeq 1$ $\partial B/\partial y$ changes from positive to negative implying that for $y/D<1$ the current is flowing from the crust into the sea and for $y/D>1$ it is flowing from the sea into the crust. To demonstrate that the loops exist out to infinity we differentiate equation (4.35) and note that $\partial B_{y>0}/\partial y$, and hence E_z, has an $\exp(y'\sqrt{i})$ dependence which has an oscillating sign for increasing y. An impression of the current flow can be obtained by realizing that the product of current density and the distance between constant B lines is simply proportional to the change in B. This implies that there is equal current flow between any two constant B lines which differ by the same amount

One must be careful when comparing the graphs with different periods since we have chosen to present graphs representing the same physical size . To illustrate this point consider graphs plotted out to a number of skin depths instead. The first case of $D'=1$ would go out to a y' value of 2 but when $D'=.0705$ and $.0204$ the graphs would only illustrate results out to y' values of .1411 and .0408 respectively. Similar reasoning explains why smaller periods could be said to have a larger effect whereas larger D values do not, even though the same D' values may result. Tables (5.1) to(5.3) indicate that the current values near the coastline decrease in magnitude as the frequency decreases for the

periods calculated. The precise frequency dependence of the magnetic field can be seen from equations(4.35)and (4.41) to be extremely complex.(Recall that α is proportional to the square root of the frequency.) Thus care should be taken in extrapolating any frequency dependence noticed from the few calculated values in Chapter (5). It is interesting to note that because the magnetic field has an $\exp(z\sqrt{f})$ and $\exp(y\sqrt{f})$ dependence the electric field, and hence the current, will be proportional to $\sqrt{f}B$. Hence any decrease in magnetic field with a decrease in frequency will be amplified in the electric field and current values. Owing to the lack of observational data available for comparison it is impossible to decide whether the induced currents are of a reasonable magnitude or not. However the fact that the ratio of current to B_0 can increase by a factor of two from its value 130 km from the coastline,(see table 5.1), definitely supports the possibilty.

Since the model chosen allows only one varying magnetic field component it is impossible to conclude whether or not current loops flowing through the crust do contribute to the coast effect. What has been proven is that vertical current loops can exist in the earth, and this suggests that further work in solving a more complex three-dimensional model might lead to the demonstration of a coast effect. The E polarization case,(E field parallel and B field perpendicular to the coastline), is required to create currents parallel to the coast which can then induce the necessary vertical magnetic fields. A three dimensional model with a coastline of finite length is necessary since a two-dimensional E polarization case would not have vertical currents. The frequency dependence of the currents obtained seems to indicate that the three-dimensional case may only be able to explain the coast effect for a certain frequency range. It would then be necessary to compare this frequency range to the range of other induction models,(see Introduction), to see whether the observed result could be obtained by a combination of induction schemes. It is important to note that an upwelling of the mantle at the coastline would enhance the electrical coupling of the sea to the mantle.

The rather inconclusive results obtained above are as expected since the main objective of this thesis was to provide an analytic solution which could serve as a check on numerical methods which can then be applied to the more complex models. The selection of results in

Chapter 5 are not presented to illustrate dramatic trends but merely to provide a variety of results for reference purposes.

The Wiener-Hopf technique could naturally be applied to different models possessing mixed boundary conditions. However, it would become much more complex for models of a more sophisticated character than those presented here. The main problem that arises is that the separation of the basic equation into terms which are analytic in the prescribed regions can become very different. This is verified by noting the simplicity with which the solution was obtained for the first model with that for the second model.

REFERENCES

Ahlfors, L.V., 1953. Complex Analysis, McGraw-Hill, New York.

Apostal, T.M., 1957. Mathematical Analysis, Addison and Wesley, Palo Alto.

Bailey, R.C., 1974. H-Polarization induction over an ocean edge in contact with a conducting substratum. Paper presented at the 2nd Workshop on Electromagnetic Induction in the Earth, Ottawa.

Brewitt-Taylor, C. R., 1974. A model for the coast-effect. Paper presented at the 2nd Workshop on Electromagnetic Induction in the Earth, Ottawa.

Brewitt-Taylor, C.R., 1975. A model for the coast-effect, Phys. Earth Planet. Int., 10, 151-158.

Brewitt-Taylor, C.R., 1976. A model for the coast-effect - further results, Phys. Earth Planet. Int., submitted for publication.

Brewitt-Taylor, C.R., 1976. Private Communication.

Bullard, E.C. and Parker, R.L., 1970. Electromagnetic induction in the oceans, in *The Sea*, A.E. Maxwell (ed.), Vol. 4, 695-730, Wiley, New York.

Butkov, E., 1968. Mathematical Physics, Addison-Wesley, California.

Chapman, S.C. and Bartels, J., 1940. Geomagnetism, Oxford, London.

Dosso, H.W., 1966. Analogue model measurements for electromagnetic variations near a coast line. Canad. J. Earth Sci., 3, 917-936.

Everett, J.E. and Hyndman, R.D., 1967. Phys. Earth Planet. Int., 1, 24.

Garland, G.D., 1971. Introduction to Geophysics, Saunders, Philadelphia.

Lambert, A., and C. Caner, 1965. Geomagnetic "depth-sounding" and the coast effect in Western Canada. Canad. J. Earth Sci., 2, 485-509.

Noble, B., 1958. Methods based on the Wiener-Hopf technique for the solution of partial differential equations, Pergamon, London.

Parkinson, W.D., 1959. Directions of rapid geomagnetic fluctuations. Geophys. J., 2, 1-13.

Parkinson, W.D., 1962. The influence of continents and oceans on geomagnetic variations. Geophys. J., 6, 441-449.

Parkinson, W.D., 1964. Conductivity anomalies in Australia and the ocean effect. J. Geomagn. Geoelectr., 15, 222-226.

Titchmarsh, E.C., 1939. The Theory of Functions, Oxford, London.

APPENDIX A

LIOUVILLE'S THEOREM

Liouville's theorem as stated by Noble (1958) is as follows;"If $f(\zeta)$ is an integral function, in an arbitrary region Ω, such that $|f(\zeta)| \leq M$ for all ζ, M being a constant, then $f(\zeta)$ is a constant." This result can be extended to obtain:"If $f(\zeta)$ is an integral function in an arbitrary region Ω, such that $|f(\zeta)| < M|\zeta|^p$ as $|\zeta| \to \infty$, where p is a constant, then $f(\zeta)$ is a polynomial of degree $\leq [p]$, where $[p]$ is the integral part of p."

It is sufficient to prove the extended form since the simpler form can be considered a special case. The following proof is from Ahlfors (1953). Consider a function $f(z)$ analytic in Ω, for a point a in Ω we assign a neighborhood Δ contained in Ω and in Δ a circle c around a. Cauchy's integral formula applied to c yields

$$f(z) = \frac{1}{2\pi i}\int_c \frac{f(\zeta)\, d\zeta}{(\zeta - z)}$$

This equation can be differentiated n times to give

$$f^n(z) = \frac{n!}{2\pi i}\int_c \frac{f(\zeta)\, d\zeta}{(\zeta - z)^{n+1}}$$

Now we let the radius of c be r, substitute the initial condition that $|f(\zeta)| < M|\zeta|^p$, let $z = a$ and replace $(\zeta - a)$ with r to obtain

$$|f^n(a)| < \frac{Mn!}{2\pi i}\int_c \frac{|r+a|^p\, dr}{r^{n+1}}$$

which, by the application of the M.L. theorem, becomes

$$|f^n(a)| \leq \frac{n!M|r+a|^p}{ir^n}$$

Since the initial conditions are valid for arbitrary Ω and a, we can take the limit as $r \to \infty$ to conclude that $|f^n(\zeta)| \leq 0$ providing we choose $n > p$. By integration of the last inequality we can deduce that $f(\zeta)$ is a polynomial of degree less than or equal to $(n-1)$, and by choosing the minimum allowable n we can write $(n-1) = [p]$ which is the required result.

For the first model the required limits were demonstrated in the text. For the second model the expression under consideration, as in equation (4.16), is

$$\lim_{\substack{|\zeta|\to\infty \\ \eta\to-\infty}} \left[\frac{\hat{B}_z^-(\zeta,0)K_-(\zeta)}{D(\zeta - i\sqrt{i}\alpha)} - \frac{B_0 i\sqrt{i}\,\alpha}{i\sqrt{2\pi}\zeta K_+(0)} \right] \tag{A.1}$$

By inspection we can deduce that the second term goes to zero when the limit is taken. From Chapter 4 we have that $\hat{B}_z^-(\zeta,0)$ will give rise to an $\exp(-|\eta||y|)$ which will force the first term to zero as long as $\lim|\zeta|\to\infty$ of $K_-(\zeta)$ does not diverge. We have from equation (4.13) that

$$\lim_{|\zeta|\to\infty} K_-(\zeta) = \lim_{|\zeta|\to\infty} \left[\prod_{n=1}^{\infty} \frac{(1+i\alpha^2 D_{n-\frac{1}{2}}^2)^{\frac{1}{2}} + i\zeta D_{n-\frac{1}{2}}}{(1+i\alpha^2 D_n^2)^{\frac{1}{2}} + i\zeta D_n} \right]$$

$$\to \prod_{n=1}^{\infty} \frac{1}{1-1/2n}$$

which does not diverge. Hence expression (A.1) has a limit of zero as $|\zeta|\to\infty$ and therefore must be identically zero by Liouville's theorem.

APPENDIX B

VERIFICATION OF THE FIRST SOLUTION

It is a necessary precaution to check that the solution obtained does satisfy the required differential equation and boundary conditions.

The differential equation (2.11) can be expressed in terms of y' and z'as

$$\frac{\partial^2 B}{\partial y'^2} + \frac{\partial^2 B}{\partial z'^2} = 2iB$$

The solution for y<0 ,equation(3.34),can be put in the form

$$B(y,z)_{y<0} = B_0 \exp(-\sqrt{2i}z') - h\int_0^\infty f(v)\exp(y'\{v^2+2i\}^{\frac{1}{2}})\sin(z'v)\,dv \qquad (B.1)$$

where

$$h = \frac{\exp(i\pi/8)B_0(2)^{\frac{1}{4}}}{\pi}$$

and

$$f(v) = \frac{(\{v^2+2i\}^{\frac{1}{2}} - \{2i\}^{\frac{1}{2}})^{\frac{1}{2}}}{v^2+2i}$$

By differentiating equation (B.1) we can obtain

$$\frac{\partial^2 B}{\partial y'^2} = -h\int_0^\infty f(v)(v^2+2i)\sin(z'v)\exp(y'\{v^2+2i\}^{\frac{1}{2}})\,dv$$

and

$$\frac{\partial^2 B}{\partial z'^2} = 2iB_0\exp(-\sqrt{2i}z') + h\int_0^\infty v^2 f(v)\sin(z'v)\exp(y'\{v^2+2i\}^{\frac{1}{2}})\,dv$$

The addition of the above two equations yields the required result.

Similarily if we write

$$B(y,z)_{y>0} = h\int_0^\infty g(v)\cos(z'v)\exp(-y'\{v^2+2i\}^{\frac{1}{2}})\,dv$$

it becomes apparent that

$$\frac{\partial^2 B}{\partial y'^2} = h\int_0^\infty (v^2+2i)g(v)\cos(z'v)\exp(-y'\{v^2+2i\}^{\frac{1}{2}})\,dv$$

and

$$\frac{\partial^2 B}{\partial y'^2} = -h\int_0^\infty v^2 g(v)\cos(z'v)\exp(-y'\{v^2+2i\}^{\frac{1}{2}})\,dv$$

which, upon substitution, demonstrates that the differential equation is satisfied.

A substitution of $z'=0$ into equation (3.34) yields immediately the necessary result that $B(y,0)_{y<0} = B_0$.

The imposed condition on $B(y,0)_{y>0}$ was that $\partial B/\partial z = 0$. From equation (3.28) we can deduce that $\partial B_{y>0}/\partial z$ is proportional to $\sin(z'v)$ which vanishes at $z=0$.

By noting the prevalence of y in the exponential arguments in the two solutions it follows immediately that $B(-\infty,z) = B_0\exp(-z\alpha\sqrt{i})$ and that $B(\infty,z) = 0$ as required.

We now consider the limits of the two solutions as $z\to\infty$. The first term in equation (3.34) contains an $\exp(-z'\sqrt{2i})$ which obviously tends to zero. The remaining terms in the two solutions are both integrals and can be shown to approach zero by the well known theorem in calculus[2]

$$\text{limit}_{z\to\infty} \int_0^\infty f(v) \begin{Bmatrix} \sin(zv) \\ \cos(zv) \end{Bmatrix} dv = 0$$

The final condition that must be checked is to verify that the two solutions are equivalent at $y=0$, i.e. that

$$B(0_-,z) = B(0_+,z) \tag{B.2}$$

To simplify the argument we note that the two solutions can be abbreviated to the form

$$B(y,z)_{y>0} = +cI_a \tag{B.3}$$

$$B(y,z)_{y<0} = -cI_b + 2\pi i cR \tag{B.4}$$

where c is a constant, I_a and I_b are defined as the integrand (2.36) evaluated along the contours A and B respectively, (see Fig.B.1), and R is the residue at $\zeta=0$. (It is important to note that the plus sign in equation (B.3) results from contour A being defined in the reverse direction to that used to obtain the solution.) Equation (B.2) can now be restated in the form

$$I_a\Big|_{y=0} = -I_b\Big|_{y=0} + 2\pi i R \tag{B.5}$$

2. For example see theorem 15-9 in Mathematical Analysis by Apostal (1964)

We now consider the integral evaluated along the closed path A-C-B-D . In Chapter 3 it was necessary to restrict ourselves to the lower half of the ζ plane for positive y and the upper half plane for y negative, but if y is set equal to zero the contours will not be burdened with the above restrictions. It was shown in the text that the integrand goes to zero as $|\zeta| \to \infty$, from which we can conclude that the integrals evaluated along C and D are both zero. Hence the application of Cauchy's theorem gives the result

$$I_a + I_b = 2\pi i R$$

This expression proves that equation (B.5), and hence equation (B.2) are satisfied.

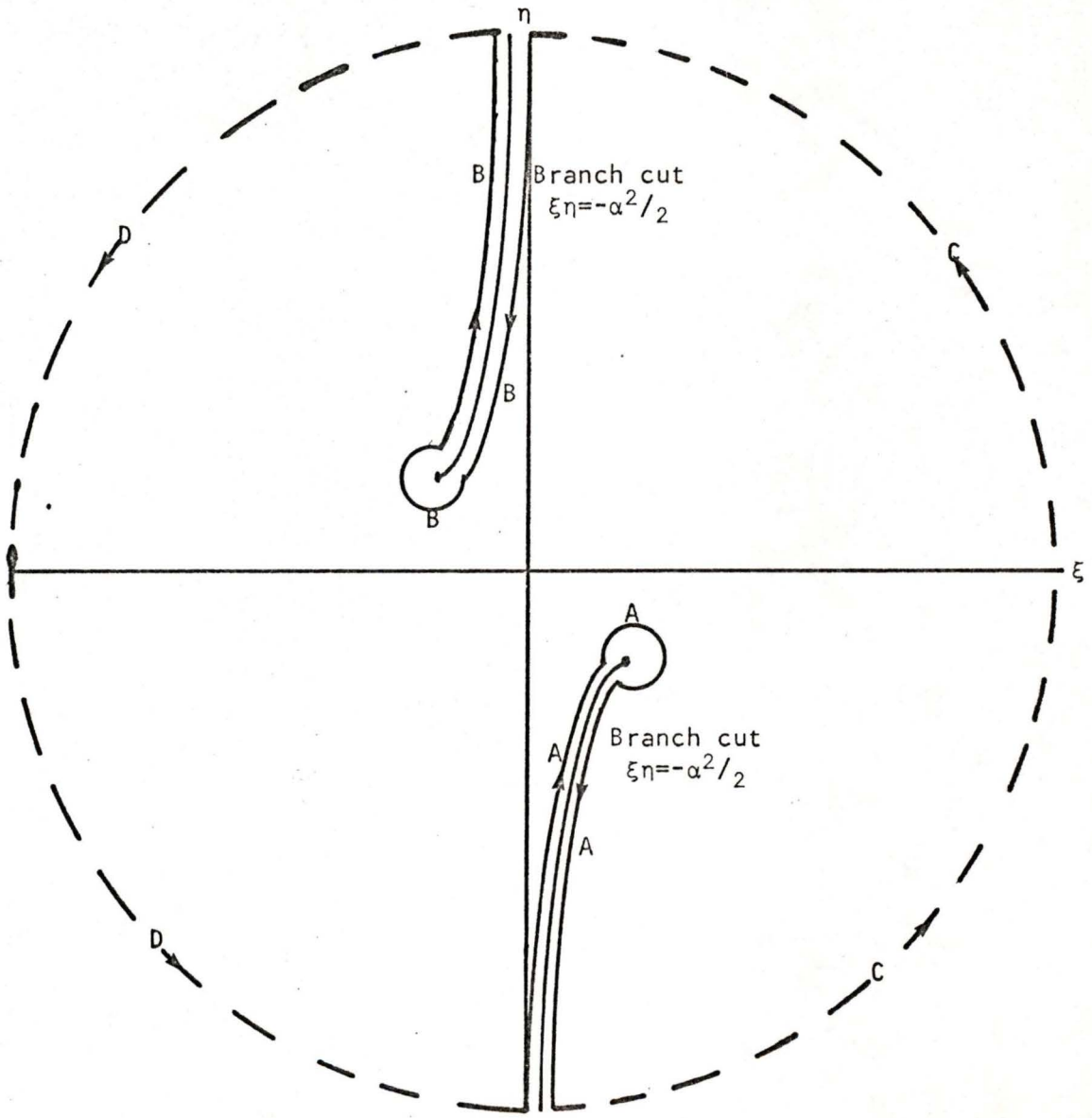

Fig. B.1 The contour of integration used to verify that the two solutions are equivalent at y=0 (for the first model)

APPENDIX C

INFINITE PRODUCTS

The following theorem and proof is taken from Titchmarsh (1939). Consider a function $f(\zeta)$ which is meromorphic everywhere in the ζ plane. Let the poles of $f(\zeta)$ be $a_1, a_2, a_3, \ldots$, where $0<|a_1|<|a_2|$ etc., and let the residues be $b_1, b_2, b_3, \ldots$. We now define a series of closed contours C_n, with maximum radius R_n, such that C_n encloses a_1 up to a_n and impose the condition that $f(\zeta)/R_n \to 0$ as $R_n \to \infty$. (See Titchmarsh (1939) for the case $f(\zeta)$ proportional to R_n^P.) Consider the integral

$$I = \frac{1}{2\pi i} \int_{C_n} \frac{f(w)}{(w-\zeta)w} \, dw \tag{C.1}$$

where ζ is inside C_n. By the application of residue theory we have

$$I = \sum_{m=1}^{n} \frac{b_m}{a_m(a_m-\zeta)} - \frac{f(0)}{\zeta} + \frac{f(\zeta)}{\zeta} \tag{C.2}$$

Alternately we can apply the M.L. theorem to obtain

$$|I| \leq \frac{L_n}{2\pi R_n(R_n-|\zeta|)} \text{ (maximum } |f(w)| \text{ on } C_n) \tag{C.3}$$

where L_n is the length of C_n and hence will be proportional to R_n. The limit of equation (C.3) as $n \to \infty$ gives

$$\text{limit}_{n\to\infty} |I| = 0 \tag{C.4}$$

since $R_n \to \infty$ as $n \to \infty$ and $f(w)/R_n \to 0$ as $R_n \to \infty$ by initial conditions. From equations (C.2) and (C.4) we can deduce that

$$f(\zeta) = f(0) + \sum_{n=1}^{\infty} b_n \left[\frac{1}{\zeta-a_n} + \frac{1}{a_n}\right] \tag{C.5}$$

Now let $h(\zeta)$ be an integral function of ζ in the ζ plane with simple zeroes at $a_1, a_2, a_3 \cdots\cdots$. In the neighborhood of a_n we can define a function $g(\zeta)$ such that

$$h(\zeta) = (\zeta-a_n)\, g(\zeta) \tag{C.6}$$

which implies

$$h'(\zeta)/h(\zeta) = 1/(\zeta-a_n) + g'(\zeta)/g(\zeta) \tag{C.7}$$

The last term in equation (C.7) is analytic at a_n which implies $h'(\zeta)/h(\zeta)$ has a simple pole at $\zeta = a_n$ with residue 1 . Since $h'(\zeta)/h(\zeta)$ satisfies the conditions imposed on $f(\zeta)$ we can apply equation (C.5) to obtain

$$\frac{h'(\zeta)}{h(\zeta)} = \frac{h'(0)}{h(0)} + \prod_{n=1}^{\infty}{}' \left[\frac{1}{(\zeta-a_n)} + \frac{1}{a_n}\right] \tag{C.8}$$

If this equation is integrated along a path from 0 to ζ and the resulting expression is exponentiated the outcome will be

$$h(\zeta) = h(0)\exp\{\zeta h'(0)/h(0)\} \prod_{n=1}^{\infty}{}' (1-\zeta/a_n)\exp(\zeta/a_n) \tag{C.9}$$

If $h(\zeta)$ is an even function the poles will occur in pairs which will simplify equation (C.9) to

$$h(\zeta) = h(0) \prod_{n=1}^{\infty}{}' (1-\zeta^2/a_n^2) \tag{C.10}$$

This formula can be applied to $\cosh(D\gamma)$ and $\sinh(D\gamma)/\gamma$ since they are both continuos across the branch cut of γ, which implies they are integral, and they both have simple zeroes. First we consider $h(\zeta)=\cosh(D\gamma)$ so that

$$f(\zeta) \equiv h'(\zeta)/h(\zeta) = D\zeta\tanh(D\gamma)/\gamma \tag{C.11}$$

from which we can deduce that $f(\zeta)/R_n \to 0$ as $R_n \to \infty$ as required. Thus equation (C.10) gives

$$\cosh(D\gamma) = \cosh(D\alpha\sqrt{i}) \prod_{n=1}^{\infty}{}' \left[1+ \frac{\zeta^2 D^2_{n-\frac{1}{2}}}{(1+iD^2_{n-\frac{1}{2}}\alpha^2)}\right] \tag{C.12}$$

since the zeroes of $\cosh(D\gamma)$ are $a_n = \pm\,(1/D^2_{n-\frac{1}{2}} + i\alpha^2)^{\frac{1}{2}}$. (Recall $D_{n-\frac{1}{2}}$ is defined in Chapter 4 as $D/(n-\frac{1}{2})\pi$.) We now re-apply equation (C.10) to $\cosh(D\sqrt{i}\alpha)$, which has zeroes at $a_n = \sqrt{i}/D_{n-\frac{1}{2}}$, to obtain

$$\cosh(D\alpha\sqrt{i}) = \prod_{n=1}^{\infty}{}' (1 + i\alpha^2 D^2_{n-\frac{1}{2}}) \tag{C.13}$$

The combination of equations (C.12) and (C.13) yields the result that

$$\cosh(D\gamma) = \prod_{n=1}^{\infty}{}' (1+i\alpha^2 D^2_{n-\frac{1}{2}}) + \zeta^2 D^2_{n-\frac{1}{2}} \tag{C.14}$$

For $\sinh(D\gamma)/D\gamma$ the only difference was that the algebra was more complex. The outcome was

$$\sinh(D\gamma)/D\gamma = \prod_{n=1}^{\infty}{}' (1+i\alpha^2 D_n^2) + \zeta^2 D_n^2 \tag{C.15}$$

which when divided into the previous result yields

$$D\gamma\coth(D\gamma) = \prod_{n=1}^{\infty} \frac{(1+i\alpha^2 D_{n-\frac{1}{2}}^2) + \zeta^2 D_{n-\frac{1}{2}}^2}{(1+i\alpha^2 D_n^2) + \zeta^2 D_n^2} \qquad (C.16)$$

as required.

APPENDIX D

VERIFICATION OF THE SECOND SOLUTION

By simply substituting z=0 into equation (4.41) we produce the first boundary that $B=B_0$ for negative y and z=0 .

If we differentiate equations (4.35) and (4.41) with respect to z the results are

$$\frac{\partial B(y,z)_{y\geq 0}}{\partial z} = \frac{-B_0}{\coth(D\alpha\sqrt{i})} \sum_{m=1}^{\infty} a_m u_m \sin(m\pi z/D)\ \Delta u \qquad (D.1)$$

and

$$\frac{\partial B(y,z)_{y<0}}{\partial z} = \frac{B_0\alpha\sqrt{i}\sinh\{(z-D)\alpha\sqrt{i}\}}{\cosh(D\alpha\sqrt{i})} + \frac{\alpha B_0 \exp(i3\pi/4)}{\pi} \sum_{m=1}^{\infty} u_{m-\frac{1}{2}} b_{m-\frac{1}{2}} \cos\{(m-\tfrac{1}{2})\pi z/D\}\Delta u \qquad (D.2)$$

It is apparent by inspection that equation (D.1) will vanish for z=0 or z=D and that equation (D.2) will be zero for z=D as required.

If we let $y\to-\infty$ in equation (4.41) it follows that $b_{m-\frac{1}{2}}=0$ which implies

$$B(-\infty,z) = \frac{B_0\cosh\{(z-D)\alpha\sqrt{i}\}}{\cosh(D\alpha\sqrt{i})} \qquad (D.3)$$

as called for.

The boundary condition at $y\to+\infty$, i.e. $B(\infty,z)\to 0$, is easily verified by the inspection of equation (4.31) .

To demonstrate that the two solutions are equivalent along the y=0 boundary we consider Fig.(D.1) and the following argument. To arrive at the two solutions required the use of two equivalent expressions of the same integral. It will be convenient if we label the one used for B(y,z) $y<0$ as I_1 , the other as I_2 and define the residues in the upper and lower half planes as R_u and R_L respectively. The solutions for B(y,z) can now be expressed in the form

$$B(y,z)_{y>0} = I_{2A} - 2\pi i R_{2L} \qquad (D.4)$$

$$B(y,z)_{y<0} = 2\pi i R_{1u} \qquad (D.5)$$

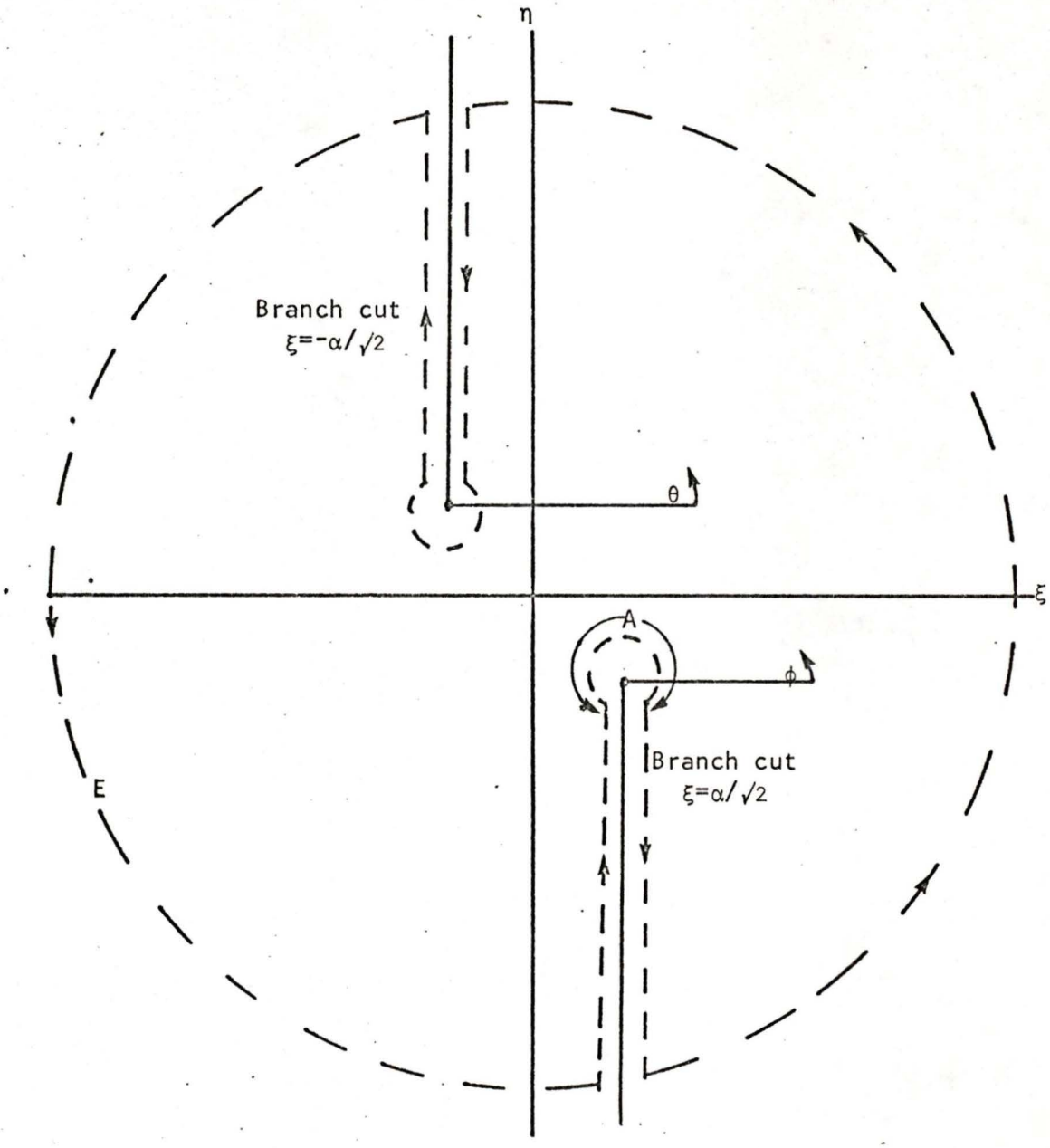

Fig. D.1 The contour of integration used to verify that the two solutions are equivalent at y=0(for the second model) Note that E is the complete dotted line

where A is the contour illustrated in Fig.(D.1). It can be shown that I_2, like I_1, gives no net contribution along all contours in the upper half plane which implies if we had used integral I_2 to obtain $B(y,z)_{y<0}$ the result would have been

$$B(y,z)_{y<0} = 2\pi i R_{2u} \tag{D.6}$$

By comparing this to equation (D.5) we can conclude that $R_{1u}=R_{2u}$ since the solution for B must be unique. Therefore to prove that $B(0_+,z)= B(0_-,z)$ it is sufficient to show

$$I_{2A} - 2\pi i R_{2L} = 2\pi i R_{2u} \tag{D.7}$$

at y=0 . This is accomplished by evaluating I_2 around the closed contour E.(See Fig.(D.1)) This contour is acceptable since at y=0 it is not necessary to restrict ourselves to the upper or lower half planes. Hence by the application of Cauchy's theorem we obtain equation (D.7) as required.

It is necessary to show that the two solutions do actually satisfy the required differential equation. Differentiating the two solutions gives the following results

$$\frac{\partial^2 B(y,z)_{y<0}}{\partial y^2} = \sum_{m=1}^{\infty} \frac{\alpha B_0 \exp(i3\pi/4)}{\pi}(i\alpha^2+u_{m-\frac{1}{2}}^2) b_{m-\frac{1}{2}} \sin(u_{m-\frac{1}{2}} z)\Delta u \tag{D.8}$$

$$\frac{\partial^2 B(y,z)_{y<0}}{\partial z^2} = \frac{\alpha^2 B_0 \cosh\{(z-D)\alpha\sqrt{i}\}}{\cosh(D\alpha\sqrt{i})} - \frac{\alpha B_0 \exp(i3\pi/4)}{\pi} \sum_{m=1}^{\infty} u_{m-\frac{1}{2}}^2 b_{m-\frac{1}{2}} \sin(u_{m-\frac{1}{2}} z)\Delta u \tag{D.9}$$

$$\frac{\partial^2 B(y,z)_{y>0}}{\partial y^2} = \frac{B_0}{\pi \coth(D\alpha\sqrt{i})}\left[i\alpha^2 a_0 \tfrac{1}{2}\Delta u + \sum_{m=1}^{\infty}(u_m^2+i\alpha^2) a_m \cos(u_m z)\Delta u\right] \tag{D.10}$$

$$\frac{\partial^2 B(y,z)_{y>0}}{\partial z^2} = \frac{-B_0}{\pi \coth(D\alpha\sqrt{i})}\left[\sum_{m=1}^{\infty} u_m^2\, a_m \cos(u_m z)\Delta u\right] \tag{D.11}$$

By combining equation (D.8) with (D.9) and (D.10) with (D.11) we obtain

$$\frac{\partial^2 B(y,z)_{y<0}}{\partial y^2} + \frac{\partial^2 B(y,z)_{y<0}}{\partial z^2} = i\alpha^2\left[\frac{B_0 \cosh\{(z-D)\alpha\sqrt{i}\}}{\cosh(D\alpha\sqrt{i})} + \frac{\alpha B_0 \exp(i3\pi/4)}{\pi} \sum_{m=1}^{\infty} b_{m-\frac{1}{2}} \sin(u_{m-\frac{1}{2}} z)\Delta u\right]$$

and

$$\frac{\partial^2 B(y,z)_{y>0}}{\partial y^2} + \frac{B(y,z)_{y>0}}{\partial z^2} = i\alpha^2\left[\frac{B_0}{\pi\coth(D\alpha\sqrt{i})}\{\tfrac{1}{2}a_0\Delta u + \sum_{m=1}^{\infty} a_m\cos(u_m z)\Delta u\}\right]$$

By comparing the right hand sides of these equations to the two solutions (equations (4.35) and (4.41)),it is apparent that the diffusion equation is satisfied.

It is interesting to note that the two models could be considered equivalent if the value of D in the second model is set equal to infinity. Thus if we take the limit as $D\to\infty$ of the second model solutions we should obtain the first model solutions. We consider first the limit $D\to\infty$ of $B(y,z)_{y>0}$ in equation (4.36). From the form of u_m and Δu we can deduce that as $D\to\infty$, $u_m\to u$, $\Delta u\to du$ and the Fourier series will become a Fourier integral to yield

$$\lim_{D\to\infty} B(y,z)_{y>0} = \frac{B_0}{\pi \lim_{D\to\infty}\coth(D\alpha\sqrt{i})}\int_0^{\infty}\{\lim_{D\to\infty} a(u)\}\cos(uz)\,du \quad \cdot(D.12)$$

From the definition of a_m,(Eq.4.34), it becomes apparent that to obtain an expression for limit $D\to\infty(a\{u\})$ it will be necessary to evaluate limit $D\to\infty\left[K_-(0)/K_-\{-i(u^2+\alpha^2)^{\frac{1}{2}}\}\right]$. It can be shown that the infinite product representing this function is uniformly convergent which allows us to consider the product of the limit rather than the limit of the product. As D becomes very large the expression for $K_-(\zeta)$,equation (4.13), can be modified to give us

$$\lim_{D\to\infty}\frac{K_-(\zeta)}{K_-(0)} \simeq \lim_{D\to\infty}\prod_{n=1}^{\infty}\frac{\{1+[iD/(n-\frac{1}{2})\pi][\zeta-\alpha\exp(i3\pi/4)]\}\{1-i\alpha D\exp(i3\pi/4)/n\pi\}}{\{1+[iD/n\pi][\zeta-\alpha\exp(i3\pi/4)]\}\{1-\alpha iD\exp(i3\pi/4)/n\pi\}} \qquad (D.13)$$

For convenience we define $\beta=iD(\zeta-\alpha\exp\{i3\pi/4\})/\pi$ and $\beta_0=-iD\alpha\exp(i3\pi/4)/\pi$ so that equation (D.13) becomes

$$\lim_{D\to\infty}\frac{K_-(\zeta)}{K_-(0)} \simeq \lim_{D\to\infty}\prod_{n=1}^{\infty}\frac{(1+\beta/\{n-\frac{1}{2}\})(1+\beta_0/n)}{(1+\beta/n)(1+\beta_0/\{n-\frac{1}{2}\})} \qquad (D.14)$$

By comparing this expression to the expression for Γ functions given in Noble (1958,p.41) we can deduce that if each term in the product is multiplied by $\exp\{-(\beta+\beta_0)/n\}/\exp\{-(\beta+\beta_0)/n\}$ the result will be

$$\lim_{D\to\infty}\frac{K_-(\zeta)}{K_-(0)} \simeq \lim_{D\to\infty}\left[\frac{\beta\Gamma(\beta)\Gamma(\beta_0+\frac{1}{2})}{\beta_0\Gamma(\beta_0)\Gamma(\beta+\frac{1}{2})}\right] \qquad (D.15)$$

Since $\beta \propto D$ the asymptotic behaviour of the gamma functions can be found by the use of Stirlings formula to give

$$\lim_{D\to\infty} \frac{K_-(\zeta)}{K_-(0)} \simeq \frac{(\zeta-\alpha\exp\{i3\pi/4\})^{\frac{1}{2}}}{(\alpha\exp\{-i\pi/4\})^{\frac{1}{2}}} \qquad (D.16)$$

We can now substitute $\zeta = -i(u^2+i\alpha^2)^{\frac{1}{2}}$ to aquire the final result

$$\lim_{D\to\infty} \frac{K_-(\zeta)}{K_-(0)} \simeq \frac{\{(u^2+i\alpha^2)^{\frac{1}{2}} + (i\alpha^2)^{\frac{1}{2}}\}^{\frac{1}{2}}}{\sqrt{\alpha}\ \exp(i\pi/8)} \qquad (D.17)$$

We now make the familiar definitions $y'=y\alpha/\sqrt{2}$, $z'=z\alpha/\sqrt{2}$ and $v=u\sqrt{2}/\alpha$, note that the limit $D\to\infty(\coth\{D\alpha\sqrt{i}\}) = 1$, obtain the limit $D\to\infty(a_m)$ from equations (4.34) and (D.17) and substitute the results into equation (D.12) to produce

$$\lim_{D\to\infty} B(y,z)_{y>0} =$$

$$\frac{B_0\exp(i\pi/8)(2)^{\frac{1}{4}}}{\pi} \int_0^\infty \frac{\{(v^2+2i)^{\frac{1}{2}}+(2i)^{\frac{1}{2}}\}^{\frac{1}{2}}\exp\{-y'(v^2+2i)^{\frac{1}{2}}\}\cos(z'v)dv}{v^2+2i} \qquad (D.18)$$

which is identical to the solution of the first model, (equation (3.28).

The same techniques were employed to demonstrate that the two $y<0$ solutions are equivalent in the limiting case.

APPENDIX E

DIRECTION OF CURL $\vec{B}$

It is required that we show curl $\vec{B}$, at a particular point, is tangential to the line of constant magnetic field passing through that point. The direction of curl $\vec{B}$ is shown in Fig.(E.1) to be defined by θ'. Since $\vec{B}=B(y,z)\hat{x}$, curl $\vec{B}$ can be expressed as $(\partial B/\partial z\ \hat{y} - \partial B/\partial y\ \hat{z})$ which implies

$$\tan(\theta') = \left.\frac{\partial B/\partial z}{\partial B/\partial y}\right| \text{evaluated at p}$$

The direction of the tangential line at p is demonstrated in Fig.(E.2) to be defined by θ. Because the line is of constant magnitude we can write

$$\left.\frac{\partial B}{\partial z}\right|_p \Delta s \cos\theta + \left.\frac{\partial B}{\partial y}\right|_p \Delta s \sin\theta = 0$$

Hence we can conclude

$$\tan\theta = \left.\frac{\partial B/\partial z}{\partial B/\partial y}\right| \text{ evaluated at p}$$

which implies $\theta= \theta'$ or $\theta'+\pi$ as required.

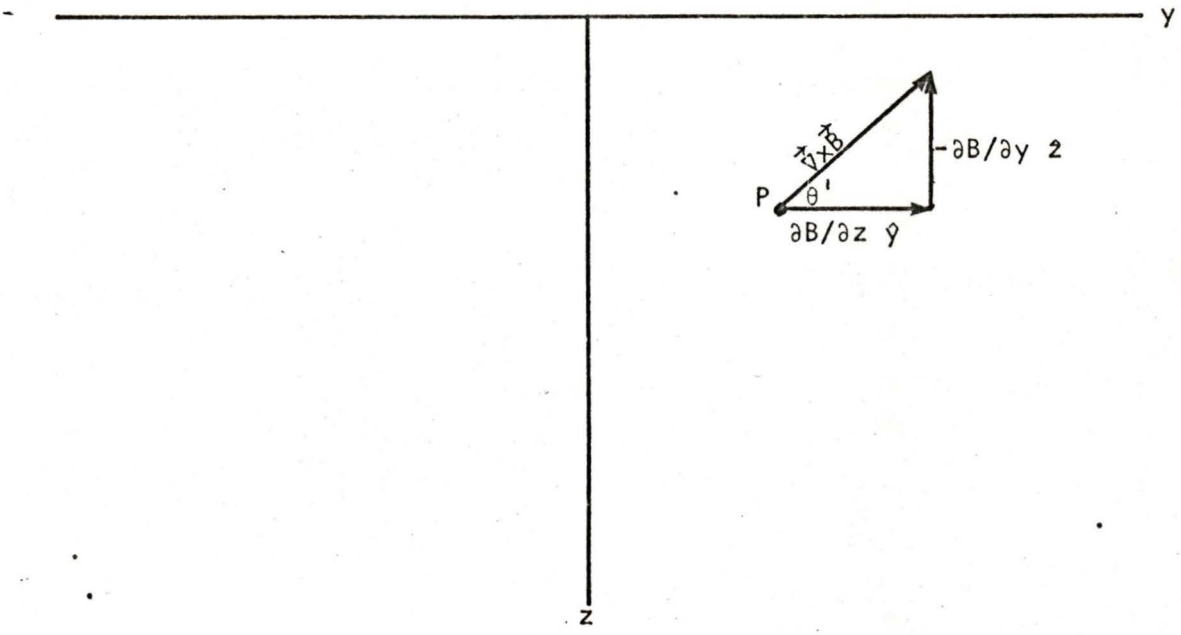

Fig. E.1 Direction of curl $\vec{B}$

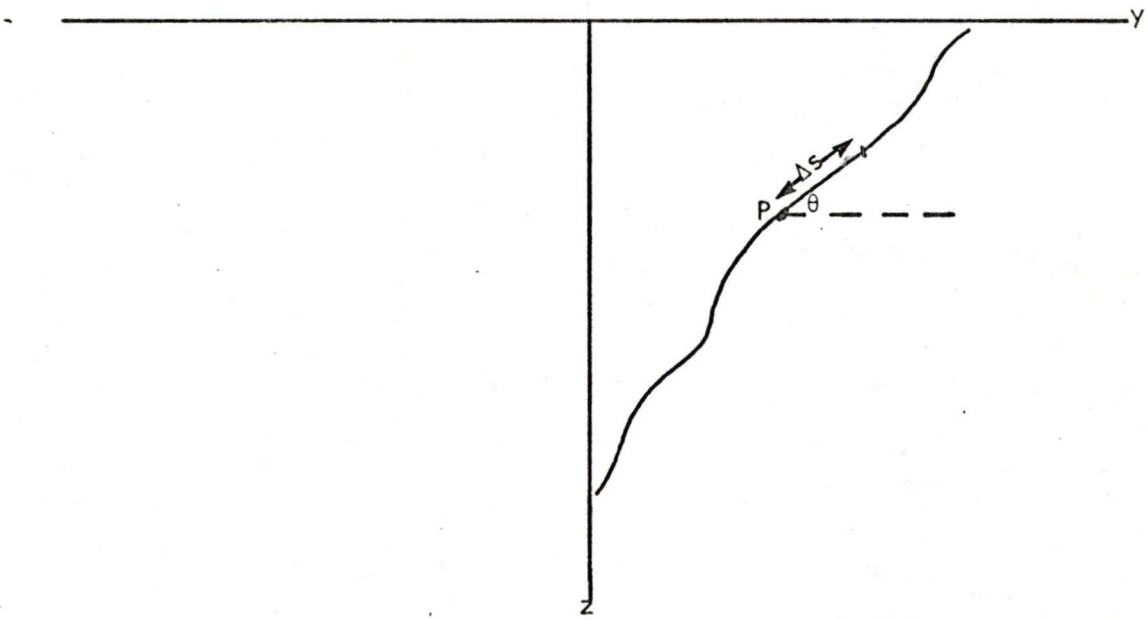

Fig. E.2 Direction of constant B/B_0 lines

VITA

Surname: NICOLL Given Names: MARTIN ADRIAN

Place of Birth: LONDON, ENGLAND

Date of Birth: JUNE 21, 1952

Educational Institutions Attended, with Dates of Entering and Leaving:

UNIVERSITY OF VICTORIA 1969 to 1976

Degrees, Diplomas, Etc., Awarded, with Dates and Names of Institutions:

B.Sc. (Honours) 1973 UNIVERSITY OF VICTORIA

Honours and Awards:

Government of British Columbia Scholarships 1969,1971,1972,and 1973.

University of Victoria Graduate Fellowship 1974

National Research of Canada Scholarship 1975

PARTIAL COPYRIGHT LICENSE

I hereby grant the right to lend my thesis (the title of which is shown below) to users of the University of Victoria Library, and to make *single copies only* for such users or in response to a request from the library of any other university, or similar institution, on its behalf or for one of its users. I further agree that permission for extensive copying of this thesis for scholarly purposes may be granted by me or a member of the University designated by me. It is understood that copying or publication of this thesis for financial gain shall not be allowed without my written permission.

AN APPLICATION OF THE WIENER-HOPF TECHNIQUE TO THE SOLUTION OF H-POLARIZATION INDUCTION OVER A COASTLINE

Author [redacted]

MARTIN ADRIAN NICOLL

JUNE, 1976